MSC-E Technical Report 6/2002

June 2002

MODELLING OF MERCURY HEMISPHERIC TRANSPORT AND DEPOSITIONS

Oleg Travnikov and Alexey Ryaboshapko

METEOROLOGICAL SYNTHESIZING CENTRE-EAST
Leningradsky prospekt, 16/2, 125040 Moscow, Russia
tel./fax: +7 095 214 39 93
e-mail: msce@msceast.org
home page: www.msceast.org

EXECUTIVE SUMMARY

Mercury is a global pollutant cycling in the environment for long periods. Therefore a correct assessment of mercury pollution requires the consideration on the hemispheric or global scale and needs to be based on the multi-compartment approach. In accordance with the EMEP work-plan for 2002 (ECE/EB.AIR/75, Annex VI) Meteorological Synthesizing Centre East of EMEP (MSC-E) is developing the hemispheric multi-compartment model of mercury transport (MSCE-Hem-Hg). At the current stage of the model development the atmospheric module of mercury airborne transport and deposition has been elaborated and verified. This report describes the progress in the model elaboration and preliminary results of mercury transport modelling over the Northern Hemisphere.

Motivation of the hemispheric modelling activity is given in **Introduction** of the report. It is pointed out that the model is to be used for multi-year computations of mercury cycling in the environment in order to evaluate its accumulation in the compartments and inter-compartmental fluxes, for the evaluation of the correct boundary conditions for the regional modelling (for the EMEP region), for the contamination assessment of remote regions (e.g. the Arctic), and finally, for the evaluation of future mercury contamination levels.

Literature survey of physical and chemical properties of mercury in the atmosphere is presented in **Chapter 1**. New scientific researches devoted to mercury atmospheric speciation and its transformations both in the gaseous and aqueous phase are considered in order to bring the model chemical scheme into conformity with contemporary knowledge of mercury behaviour in the atmosphere.

Description of the developed atmospheric module of the hemispheric model is presented in **Chapter 2**. It describes mercury emissions from anthropogenic and natural sources, transport in the atmosphere, chemical transformations both in gaseous and aqueous phase, and deposition to the surface. The model domain covers the whole Northern Hemisphere with resolution 2.5°×2.5°. The three-dimensional atmospheric transport is based on the flux-form Bott advection scheme.

Input information collected and adjusted to the hemispheric modeling is described in **Chapter 3**. It includes mercury emission data, meteorological and geophysical information, data on the atmospheric content of chemical reactants. Peculiar attention is paid to natural emission of mercury to the atmosphere. According to expert estimates up to 70% of the entire mercury input to the atmosphere can be contributed by natural sources.

Preliminary results of mercury transport and depositions modelling over the Northern Hemisphere are presented and described in **Chapter 4**. Mercury concentration levels in the ambient air and deposition fluxes over the Northern Hemisphere are assessed. The modelling results are verified against available monitoring data and calculated values obtained by the regional mercury transport model (MSCE-HM). The inter-continental transport of mercury in the Northern Hemisphere is estimated. According to the preliminary results more than 40% of mercury deposition to Europe is from external anthropogenic and global natural sources. The influence of different regions and continents on the Arctic mercury contamination is also investigated.

Basic principles of the multi-compartment model of mercury cycling in the environment are formulated in **Chapter 5** basing on the literature survey. The main environmental compartments are distinguished and qualified according to their capacity and mercury residence time. The most important inter-compartmental fluxes are pointed out. General steps of future model development are outlined.

CONTENTS

INTRODUCTION 5

Chapter 1. PHYSICAL AND CHEMICAL PROPERTIES OF MERCURY IN THE ATMOSPHERE 7

1.1. Mercury forms in the atmosphere 7

1.2. Physical and chemical transformations 8

1.3. Arctic mercury depletion 15

Chapter 2. MODEL DESCRIPTION 18

2.1. Overview of the model and computation domain 18

2.2. Atmospheric transport 19

2.3. Atmospheric chemistry 22

2.4. Removal processes 25

Chapter 3. INPUT INFORMATION 29

3.1. Natural emission of mercury to the atmosphere: a review 29

3.2. Emission data 36

3.3. Meteorological and geophysical input 40

3.4. Reactants 41

Chapter 4. ATMOSPHERIC TRANSPORT OF MERCURY IN THE NORTHERN HEMISPHERE (preliminary results for 1996) 43

4.1. Concentrations in the ambient air and deposition fluxes 43

4.2. Verification of the modelling results 45

4.3. Inter-continental mercury transport 47

4.4. Atmospheric mercury input to the Arctic 49

Chapter 5. MULTI-COMPARTMENT MODEL OF MERCURY CYCLING IN THE ENVIRONMENT: BASIC TENETS 51

CONCLUSIONS 58

ACKNOWLEDGMENTS 59

REFERENCES 60

INTRODUCTION

Mercury and its compounds are toxic substances negatively affecting both human health and the environment. One of the main pathways of mercury dispersion in the environment is the atmospheric transport. Due to properties of the prevailing mercury species (namely, elemental mercury vapour), its residence time in the atmosphere amounts to one year or even more. It makes possible mercury airborne transport over long distances from emission sources to remote regions all over the world.

The mercury long-range transport over the European region was assessed during the last decade by Meteorological Synthesizing Centre East (MSC-E) of EMEP under the UN/ECE Convention on Long-Range Transboundary Air Pollution (CLRTAP). However, global character of mercury pollution demands the development of more extended (hemispheric or global) approach to the pollution assessment. Indeed, mercury transport across the boundaries of the EMEP domain can make a significant contribution to the whole pollutant content within the region. Therefore, the regional modelling of mercury long-range transport requires adequately prescribed boundary conditions for evaluation of the pollutant incoming fluxes. Besides, mercury contamination of such remote regions as the Arctic is a separate problem deserving attention, which could be considered only on the hemispheric or global scale.

Another feature of the mercury pollution assessment is ability of mercury to cycling and accumulation in the environment. Mercury is a chemical element naturally occurring in the Earth's geosphere. It has been involved into the global circulation in the biosphere since the pre-industrial period up to now. Human activity leads to redistribution and accumulation of mercury in some environmental compartments (soil, seawater, bottom sediments etc.). Mercury transported in the atmosphere far from emission sources and deposited to the ground can be accumulated in soil and re-emitted to the atmosphere again. The accumulation for long periods can lead to significant mercury re-emissions from the polluted areas. Thus, a correct assessment of mercury pollution requires multi-compartment approach to the problem.

The problem of global mercury pollution is of a permanent concern within the environmental community. In 2002 the United Nations Environment Programme (UNEP) launched a global assessment of mercury and its compounds. Development of the hemispheric/global approach to the atmospheric pollution assessment was initiated under CLRTAP in 2000 according to "Strategy for EMEP 2000-2009" (EB.AIR/GE.1/2000/5). The Task Force on Measurements and Modelling of the EMEP programme recommended to MSC-E to extend the mercury modelling to the hemispheric and, eventually, global scales (EB.AIR/GE.1/2001/4). In accordance with the agreement between EMEP and the Arctic Monitoring and Assessment Programme (AMAP), within the framework of UNEP/GEF project "Persistent toxic substances, food security and indigenous people of the Russian North" MSC-E is developing the hemispheric multi-compartment model of mercury transport (MSCE-Hem-Hg).

At the current stage of the model development the atmospheric module of mercury airborne transport and deposition on a hemispheric scale has been elaborated and verified. For this purpose the chemical scheme of mercury transformations in the atmosphere of the regional model MSCE-HM was adjusted and incorporated to the hemispheric module of the pollutants airborne transport [*Travnikov*, 2001]. Besides, a survey of mercury physical and chemical properties in the atmosphere was accomplished. The chemical scheme of mercury transformations has been brought into conformity with the contemporary scientific researches.

Pilot calculations of mercury transport and depositions in the Northern Hemisphere were carried out for 1996. Mercury concentration levels in the ambient air as well as deposition fluxes were assessed and discussed. The modelling results were compared with available monitoring data and with modelling results obtained by the regional model. The comparison conducted has shown satisfactory agreement between the modelled and observed values as well as between both models. The inter-continental transport of mercury in the Northern Hemisphere has been assessed. Particular emphasis has been placed on the consideration of mercury depositions to the Arctic region. The effect of the mercury depletion phenomenon to the Arctic contamination has been illustrated. Basic principles of the multi-compartment model of mercury dispersion and cycling in the environment have been formulated.

Future activity in the field of the multi-compartment model development is elaboration of the modules describing other environmental compartments (ocean, soil, vegetation etc.) and transition of the model to the global scale. The model is intended to be used for multi-year computations of mercury cycling in the environment in order to evaluate its accumulation in environmental compartments and to estimate inter-compartmental fluxes (particularly, natural mercury emission to the atmosphere). Besides, it is to be applied for the evaluation of correct boundary conditions for the regional modelling (for the EMEP region) and the contamination assessment of remote regions (e.g. the Arctic). And finally, future mercury contamination levels could be assessed by means of the model developed.

Chapter 1

PHYSICAL AND CHEMICAL PROPERTIES OF MERCURY IN THE ATMOSPHERE

Mercury undergoes numerous physical and chemical transformations in the atmosphere. Therefore, understanding and adequate reproduction of properties of mercury and its compounds is a very important condition of realistic simulation. Physical and chemical properties for mercury as well as processes responsible for its transformations in the atmosphere have been already extensively described in the previous MSC-E Reports [*Ryaboshapko et al*., 1998; 1999; *Ilyin et al*., 2000, 2001] However, continuously growing knowledge of mercury behaviour in the atmosphere and modern investigations appearing in the scientific literature constrain us to revise or even substantially modify the model parameterization.

1.1. Mercury forms in the atmosphere

Mercury appears in the atmosphere both in the elemental form and in the form of various chemical compounds. Since properties of the compounds significantly differ from each other and from elemental mercury, it is very important to define the variety of the most important mercury species transported in the atmosphere.

First and the prevailing mercury species is elemental mercury (Hg^0). Due to its physical properties (temperature dependence of saturated vapour pressure) elemental mercury occurs in the atmosphere under the realistic conditions solely in the form of vapour. Even at the absolute temperature minimum over the Earth surface (the Antarctic, Siberia) partial pressure of mercury vapour is several times lower than the pressure of saturated vapour [*Fursov*, 1983; *Lindqvist et al*., 1991].

Besides, atmospheric mercury occurs in the form of different compounds – inorganic and organic. Inorganic compounds include, first of all, mercury chloride ($HgCl_2$) and mercury hydrate ($Hg(OH)_2$). The composition of gaseous inorganic mercury compounds has not been adequately investigated yet [*Ebinghaus et al.*, 1999b].

Organic mercury is represented in the atmosphere mainly by compounds with one and two methyl groups. The first type of compounds include CH_3HgCl, CH_3HgOH, CH_3HgBr etc. and have a generalized name monomethyl mercury (MMM), the second one is $Hg(CH_3)_2$ – dimethyl mercury (DMM).

At last, mercury in the solid phase is incorporated into the composition of aerosol particles. According to [*Schroeder et al.,* 1991], the solid phase mercury in the atmosphere can be presented by the following compounds: HgO, HgS, $HgCl_2$, $HgSO_4$, $Hg(NO_3)_2$.

Atmospheric transport of mercury compounds in the solid phase is mainly determined by properties of particles-carriers. One of the most important aerosol characteristics is the size distribution defining removal processes of mercury from the atmosphere. Under the conditions of continental atmosphere size distribution of particles was studied in [*Milford and Davidson*, 1985]. Mean aerodynamic diameter of aerosols containing mercury was found to be 0.61 μm. G. Keeler and co-workers [*Keeler et al.*, 1995] investigated the composition and size distribution of particulate

mercury in various regions of the USA. It was obtained that maximum of the distribution spectrum is shifted toward larger sizes in contaminated industrial areas, whereas it amounts to 0.68 μm in relatively clean regions.

Another important property of particulate mercury is solubility of its compounds in cloud and precipitation water. This property is essential for mercury chemical transformations in cloud water [*Ryaboshapko et al.*, 2001]. Besides, it defines mercury availability for biota and controls thereby negative impact on the environment.

R. Ebinghaus et al. [1999a] assume that the insoluble part of particulate mercury in precipitation varies from 90% in contaminated regions to 10% in relatively clean ones. Another study of particulate mercury [*Sakata and Marumoto*, 2002] has demonstrated that only 5–50% of aerosol mercury content was leached by dilute hydrochloric acid (0.33 mol/L *HCl*) in a highly contaminated urban area. Presumably, solubility of particulate mercury is even lower in neutral or sub-acid water of the cloud environment. Among mercury compounds occurring in the atmosphere bromide ($HgBr_2$), iodide (HgI_2), sulphide (*HgS*) and oxide (*HgO*) have the lowest solubility. According to [*Brosset and Lord*, 1991] 50% of mercury in rainwater is represented by insoluble compounds. This agrees with conclusions of other researchers [*Fitzgerald et al.*, 1991; *Lamborg et al.*, 1995]. Besides, C. Lamborg and co-workers point out that the portion of particulate mercury in snow is grater than in rainwater.

1.2. Physical and chemical transformations

Mercury transformations in the atmosphere include transitions between the gaseous, aqueous and solid phase, chemical reactions in the gaseous and aqueous environment. Hereafter we shall use term the “aqueous phase” for all species dissolved in cloud water and those in composition of solid particles suspended in a droplet.

Inter-phase equilibrium

All gaseous mercury compounds to this or that extent are soluble in cloud and rain droplets. Droplet sizes are small enough therefore the equilibrium between the solution and gas is established rather rapidly. As a rule, equilibrium states are described by Henry’s law with allowance made for the temperature effect. The same approach can be used for the description of equilibrium between the atmospheric air and sea or lake water surface. In this section for the convenience of comparison the Henry’s law coefficients are given in the dimensionless form (i.e. as the ratio of concentration in the liquid to air concentration).

For the last five years no new publications have been found which could change to any extent the notion of conditions of elemental mercury equilibrium between air and water. Earlier the authors used the following temperature dependence of Henry’s law constant obtained in multiple measurements of its value within the temperature range from 278K to 298K [*Ryaboshapko and Korolev*, 1997]:

$$H_{Hg} = 0.00984 \cdot T \exp\left[2800\left(\frac{1}{T} - \frac{1}{298}\right)\right] \qquad (1.1)$$

This expression gives a value practically coinciding at 278K with that used by W. Schroeder et al. [1991] and by G. Petersen et al. [1998].

For seawater I. Wängberg and co-wokrkers [*Wängberg et al.*, 1999] suggested the following dependence:

$$H_{Hg} = \exp(4633.3 / T_w - 14.52), \qquad (1.2)$$

where T_w is the seawater temperature in K.

Both expressions provide the same result at 25°C but they differ almost 2 times at 0°C. It is difficult to say whether this difference is due to the influence of seawater chemical composition.

It is assumed that the main gaseous mercury compound in the atmosphere is chloride. The most often cited values of its Henry's law constant are $3 \cdot 10^7$ (at 298K) and $8.3 \cdot 10^7$ (at 283K) [*Lidqvist et al.*, 1984]. J. Sommar et al. [1999a] give higher values of the constant for $HgCl_2$ – $4.9 \cdot 10^7$ (at 298K) and $3.6 \cdot 10^7$ (at 323K). A. Ryaboshapko et al. [2001] roughly approximated the temperature dependence of Henry's law constant for mercury chloride in the "air-water" system by the expression:

$$H_{HgCl_2} = 1.054 \cdot 10^5 T \exp\left[5590\left(\frac{1}{T} - \frac{1}{298}\right)\right] \quad (1.3)$$

Henry's law constants of other gaseous mercury compounds and individual reactants for different values of temperature are given in Table 1.1.

As it follows from the table the major part of DMM in the "air-water" system should be in the gaseous state. The reverse relationship should be for CH_3HgOH, $Hg(OH)_2$ and, particularly, for HgO.

Equilibrium conditions of ozone in the "air-water" system were studied in [*Sander*, 1997]. In this work R. Sander has suggested the following expression for temperature dependence of ozone Henry's law constant:

$$H_{O_3} = 9.51 \cdot 10^{-4} T \exp\left[2325\left(\frac{1}{T} - \frac{1}{298}\right)\right] \quad (1.4)$$

Table 1.1. Henry's law constants for mercury compounds and different reactants

Compound	Henry's law constant	Temperature	Reference
$(CH_3)_2Hg$	6.7	273 K	*Lindqvist and Rodhe*, 1985
	3.2	298 K	
	3.2	298 K	*Seigneur et al.*, 1994.
CH_3HgCl	$6.25 \cdot 10^4$	288 K	*Lindqvist and Rodhe*, 1985
	$5.3 \cdot 10^4$	298 K	
	$5.39 \cdot 10^4$	298 K	*Seigneur et al.*, 1994
CH3HgOH	$5.9 \cdot 10^6$	288 K	*Petersen*, 1992
	$3.7 \cdot 10^6$	293 K	
$Hg(OH)_2$	$6.25 \cdot 10^5$	283 K	*Lindqvist and Rodhe*, 1985
	$3.1 \cdot 10^5$	298 K	
	$2.9 \cdot 10^5$	298 K	*Seigneur et al.*, 1994
HgO	$3.2 \cdot 10^6$	?	*Petersen et al.*, 1998
Cl_2	$2.7 \cdot 10^5$ *	?	*Lin and Pehkonen*, 1998
$^{\bullet}OH$	600	298 K	In: [*Lin and Pehkonen*, 1998]
$HO2^{\bullet}$	$4.9 \cdot 10^4$	298 K	In: [*Lin and Pehkonen*, 1998]
SO_2	30	298 K	In: [*Lin and Pehkonen*, 1998]
H_2O_2	$1.8 \cdot 10^7$	298 K	In: [*Lin and Pehkonen*, 1998]

* This constant was obtained on the following assumptions. Chlorine solubility in cloud drops strongly depends on pH and chloride concentration. C.-J. Lin and S. Pehkonen [1998] suggested the formula for calculations of effective Henry's law constant (mole/L/atm):

$$H_{eff} = 7.61 \cdot 10^{-2}\left(1 + \frac{10^{-3.3}}{[Cl^-][H^+]} + \frac{10^{-10.8}}{[Cl^-][H^+]^2}\right)$$

According to data from [*Baltensperger et al.*, 1998; *Couture et al.*, 1998; *Kmiec et al.*, 1998; *Vong et al.*, 1997] $[H^+]$ and $[Cl^-]$ concentrations in the marine atmosphere can be estimated by an order of magnitude as $3.2 \cdot 10^{-5}$ and $\cdot 10^{-4}$ mole/L respectively. Hence it follows that effective Henry's law constant for chlorine will be equal to $1.2 \cdot 10^4$ mole/L/atm or $2.7 \cdot 10^5$ in the dimensionless representation.

Although (as it was demonstrated above) metallic mercury cannot exist in the atmosphere in the liquid or solid state its sorption by aerosol particles is possible. Quantitative characteristics of the process depend first of all on the "gas – solid matter" interface area as well as on the composition of particles.

B. Lyon et al. [1999] considered two types of particles – small (diameter 0.3 μm) and coarse (5.7 μm) and accepted that the distribution in the system is proportional to the contact surface area. The relationship of areas appeared to be equal to 93:7 respectively.

Most likely soot particles possess the highest sorption capability. C. Seigneur et al. [1998] analysed literature data published in [*Krishnan et al*., 1994; *Livengood et al*., 1995; Accurex Environmental, 1995] (cited from [*Seigneur et al*., 1998]) on Hg^0 and *Hg(II)* absorption from the gaseous phase by activated charcoal and estimated redistribution coefficients $K_{a/s}$ in the dimension "liter of air per gram of soot". The coefficient $K_{a/s}$ was estimated to be equal to 10 L/g for Hg^0 and $3 \cdot 10^5$ L/g for *Hg(II)*. C. Seigneur et al. [1998] indicate that it is not clear so far whether activated charcoal and atmospheric particles have the same chemical properties. Besides the redistribution value should depend on the temperature but nothing is known about it as yet.

In the comparison of various mercury liquid-phase chemistry schemes [*Ryaboshapko et al.,* 2001] it was demonstrated that mercury partition in the "liquid – solid matter" system considerably affects mercury accumulation in cloud and rain droplets. Above all it is defined by mercury accessibility to chemical transformations in the liquid phase and non-accessibility in the sorbed state. Soot particles contained in drops may serve as the most probable sorbent.

C. Seigneur and co-workers [*Seigneur et al.*, 1998] also analysed data of [*Thiem et al*., 1976; *Ma et al*., 1996] (cited from [*Seigneur et al*., 1998]) on the absorption of *Hg(II)* from water by activated charcoal and estimated the redistribution coefficient $K_{w/s}$ in the dimension "liter of water per gram of soot". For atmospheric conditions in the first approximation the coefficient is equal to 3700 L/g of *Hg(II)*.

Special experiments with rain water for the determination of partitioning coefficient K_p with shaking of aerosol matter in pure water and for the determination of desorption coefficient K_d showed that these coefficients are of the same order of magnitude [*Seigneur et al*., 1998]. However, K_p varies from 100 to 600 L/g and K_d – from 200 to 1400 L/g. The experiment with adsorption of dissolved forms on sampled aerosol matter made for the determination of the adsorption coefficient K_a evidenced that K_a is lower by an order of magnitude than K_d. Most likely it is connected with the occurrence of insoluble mercury forms (oxide and sulphide) in aerosol matter. The nature of aerosol matter can drastically affect the coefficient values. Values of *pH* actually did not influence the investigated coefficients.

Gas-phase reactions

In the atmosphere there is a number of chemical substances capable of oxidizing elemental mercury and its organic compounds in the gaseous phase. Photochemical processes leading to decay of molecules are also possible. The integral indicator of the significance of this or that reaction for mercury atmospheric cycle is mercury lifetime in the atmosphere relative to a given reaction. Based on this indicator it is reasonable to consider only those reactions, which make a tangible contribution to mercury atmospheric cycle. It is also important to know reaction products since their rate of scavenging from the atmosphere essentially depends on their phase state.

It is recognized that ozone is the most important oxidant in the gas phase. In the majority of modern models describing mercury bahaviour in the atmosphere the reaction rate of oxidation by ozone suggested by

B. Hall [1995] and equal to $(3 \pm 2)\cdot10^{-20}$ cm^3/molec/s at 20°C is used. First of all it should be mentioned that this estimate has an essential uncertainty. B. Hall [1995] also investigated the temperature effect of this reaction at 22°C, 55°C and 75°C. With temperature decrease the reaction rate should decline (activation energy about 10 kJ/mole, pre-exponential multiplier $2.1\cdot10^{-18}$ cm^3/molec/s). With the use of these data we obtained the following temperature dependence of this reaction rate (cm^3/molec/s):

$$k = 2.1\cdot10^{-18}\exp(-1246/T) \qquad (1.5)$$

In a rough assessment mean temperature of the troposphere is 0°C, it gives the oxidation reaction rate equal to $2.2\cdot10^{-20}$ cm^3/molec/s. At the average concentration of ozone in the troposphere $7.5\cdot10^{11}$ molec/cm^3 mean lifetime of elemental mercury in the troposhere relative to this reaction is about 2 years. Therefore this reaction is one of most important in the atmospheric mercury chemistry.

It is difficult to say what compound may be a product of Hg^0 oxidation by ozone. Most probably the oxide is formed. *G. Petersen* and co-workers [*Petersen et al.*, 1998] consider the reaction product to be gaseous. On the contrary experts from *US EPA* [1997] suppose that actually the reaction product is immediately adsorbed by aerosol particles and then behaves itself in the atmosphere in accordance with properties of particles-carriers. We believe if mercury oxide is the product of oxidation by ozone, it cannot exist in the atmosphere as a gas due to its poor volatility [*Sommar et al*., 2001; *Schroeder and Munthe*, 1998]. It should be immediately and irreversibly trapped either by particles or cloud drops.

J. Sommar et al. [1999b; 2001] studied the reaction of elemental mercury oxidation by hydroxyl radical. The reaction can go on in two stages:

$$\begin{aligned} Hg^0_{gas} + {}^{\bullet}OH &\rightarrow {}^{\bullet}HgOH \\ {}^{\bullet}HgOH + O_2 &\rightarrow HgO + HO_2 \end{aligned} \qquad (1.6)$$

Thus, the resulting reaction can be written as follows

$$Hg^0_{gas} + {}^{\bullet}OH \rightarrow HgO + HO_2 \qquad (1.7)$$

with the reaction rate $k = (8.7\pm2.8)\cdot10^{-14}$ cm^3/molec/s.

At the mean concentration of atmospheric hydroxyl 10^6 molec/cm^3 the Hg^0 lifetime relative to this reaction will be less than a year. Thus this reaction may be even more important than the reaction of oxidation by ozone. The high value of the $^{\bullet}OH$ radical oxidation rate has not been confirmed by any independent laboratory yet. Hence one should be careful operating with this high value. The temperature dependence of the reaction rate is also unknown.

The reaction of Hg^0 oxidation by chlorine [*Seigneur et al*., 1994; *Tokos et al*., 1998] may be important for the atmosphere over the ocean:

$$Hg^0_{gas} + Cl_2(\mathrm{g}) \rightarrow HgCl_2(\mathrm{g}), \qquad (1.8)$$

where reaction rate $k \le 4\cdot10^{-16}$ cm^3/molec/s at 25°C. B. Hall (cited from [*Tokos et al.*, 1998]) showed that the reaction rate does not depend on temperature. In the atmosphere near the oceanic water surface chlorine concentration is about $3\cdot10^9$ molec/cm^3. Under these conditions mean lifetime of Hg^0 relative to this reaction will be estimated by days. However, it should be mentioned that in the atmosphere chlorine could exist only at night, only over the ocean and only in the lowest atmospheric layer.

Gaseous hydrogen peroxide may be another oxidant of elemental mercury:

$$Hg^0_{gas} + H_2O_2(\mathrm{g}) \rightarrow Hg(OH)_2(\mathrm{g}). \qquad (1.9)$$

Available in the literature information about this reaction rate is contradictory. For instance, E. Constanttinou et al. [1995] use the rate constant up to $4.1\cdot10^{-16}$ cm^3/molec/s at 25°C. J.J.S.Tokos et al. [1998] give a

considerably lower value – $6 \cdot 10^{-19}$ cm^3/molec/s. It is essential to note the reaction rate should strongly depend on temperature. On the base of data on activation energy (75 kJ/mole) we can suggest the following temperature dependence of the reaction rate constant (cm^3/molec/s):

$$k = 8.4 \cdot 10^{-6} \exp(-9021/T) \qquad (1.10)$$

If, as before, we take that mean temperature of the trposphere is 0°C, then the oxidation rate will be $3.7 \cdot 10^{-20}$ cm^3/molec/s. At the mean atmospheric concentration of gaseous H_2O_2 equal to $2.5 \cdot 10^{10}$ molec/cm^3 elemental mercury lifetime in the atmosphere will be about 30 years. Most likely it is the minimum value since hydrogen peroxide is a daytime oxidant [*Lin and Pehkonen*, 1999]. For this reason gas phase oxidation reaction of Hg^0 by hydrogen peroxide can be neglected.

Mercury organic compounds, for example, DMM are sufficiently rapidly destructed in the atmosphere at the reaction with OH radical [*Niki et al.*, 1983]. The reaction product is either elemental mercury [*Niki et al*., 1983] or MMM [*Schroeder and Munthe*, 1998]. The reaction rate constant is $2 \cdot 10^{-11}$ cm^3/molec/s. At mean radical concentration 10^6 molec/cm^3 atmospheric lifetime of DMM should not exceed several hours [*Lin and Pehkonen*, 1999]. Besides, M. Horvat [1996] points to a possibility of photochemical destruction of DMM leading to even shorter lifetime.

Theoretically mercury reduction in the gas phase to the elemental state is not excluded. For example, photochemical destruction of molecules containing mercury can lead to the formation of Hg^0 but quantitative information on such reactions is not available yet [*Seigneur et al*., 1994].

Aqueous-phase reactions

Schemes of aqueous-phase transformations used in modern models of mercury transport assume a simultaneous action of two mechanisms – oxidation and reduction of elemental mercury. These schemes are described in detail in the work [*Ryaboshapko et al*., 2001]. The main oxidants may be dissolved ozone and chlorine as well as hydroxyl radical formed directly in a droplet. Sulphite complexes and hydroperoxide radical may be reducing agents. Photoreduction of some compounds is also possible. Modern ideas about aqueous-phase mercury chemistry are described in detail in the work [*Lin and Pehkonen*, 1999].

Many investigators studied the reaction of Hg^0 oxidation by ozone in the water environment. C.-J. Lin and S. Pehkonen [1999] take the reaction rate constant equal to $(4.7 \pm 2.2) \cdot 10^7$ $(mole/L)^{-1}s^{-1}$. In order to estimate the uncertainty of this value, Table 1.2 summarizes the rate constants used by different modellers in the chronological order. As it follows from the table the reaction rate published by *J. Munthe* in 1992 is used in models. The dependence of the rate on solution temperature and pH may be neglected. It may be supposed that the reaction with ozone is the basic one for elemental mercury oxidation.

Hg^0 oxidation by hydroxyl radical takes place only in the daytime since the radical itself is a product of photochemical reactions. C.-J. Lin and S. Pehkonen [1997] estimated that the reaction rate is equal to $2 \cdot 10^9$ $(mole/L)^{-1}s^{-1}$. K. Gårdfeldt et al. [2001b] suggest a very close value – $(2.4 \pm 0.3) \cdot 10^9$ $(mole/L)^{-1}s^{-1}$.

H. Herrmann and co-wokers [*Herrmann et al*., 2000] investigated variations of hydroxyl radical concentrations in cloud water. First of all, the concentration depends on the atmosphere pollution by substances capable either to generate radicals or react with them. Besides, there is a strong dependence on a droplet size. In the daytime *OH* concentration variation may be roughly described by the function of square of sine.

Table 1.2. Rate constants of Hg^0 oxidation by ozone in the aqueous phase

Rate constant $(mole/L)^{-1}s^{-1}$	Dependencies		Reference
	on temperature	on pH	
$(4.7 \pm 2.2)\cdot10^7$	Independent	Independent	*Munthe*, 1992
$4.7\cdot10^7$	at 25°C	–	*Seigneur et al.*, 1994
$4.5\cdot10^7$	–	–	*Pleijel and Munte*, 1995
$4.7\cdot10^7$	at 25°C	–	*Constantinou et al.*, 1995
$4.5\cdot10^7$	–	–	*Lin and Pehkonen*, 1997
$4.7\cdot10^7$	at 5°C	–	*Petersen et al.*, 1998
$4.7\cdot10^7$	–	Dependent	*Lin and Pehkonen*, 1998
$(4.7 \pm 2.2)\cdot10^7$	Independent * (5 - 35°C)	Independent * (5.2 - 6.2)	*Lin and Pehkonen*, 1999

* Independent within the interval

The calculated *OH* concentration in water at noon is $3.7\cdot10^{-15}$ mole/L. In this case the constant of pseudo-first order reaction will be $7.4\cdot10^{-6}$ s^{-1} [*Lin and Pehkonen*, 1997]. Aqueous-phase reactions of oxidation by ozone and *OH* radical compete: at the ozone air concentration below 4 ppb radical oxidation prevails. At concentrations more than 10 ppb the contribution of radical reaction is about 20%, and at 20 ppb – only 10%.

Under certain conditions the reaction of Hg^0 oxidation by dissolved chlorine may be important. In solution chlorine may occure in two forms – hypochlorine acid (*HOCl*) and hypochlorite ion (OCl^-), which relationship depends on solution *pH*. Oxidation by chlorine can take place mainly in the ocean atmosphere and only at night since Cl_2 and *HOCl* are decomposed at light. Both hypochlorine acid and pyrochlorite ion can oxidize mercury [*Lin and Pehkonen*, 1999]:

$$HOCl + Hg^0 \rightarrow Hg^{2+} + Cl^- + OH^-, \quad k = (2.09 \pm 0.06)\cdot10^6 \ \ (\text{mole/L})^{-1}\text{s}^{-1} \qquad (1.11)$$

$$OCl^- + Hg^0 \rightarrow\rightarrow Hg^{2+} + Cl^- + OH^-, \quad k = (1.99 \pm 0.05)\cdot10^6 \ \ (\text{mole/L})^{-1}\text{s}^{-1} \qquad (1.12)$$

It was considered earlier that the main agent responsible for the mercury reduction to the elemental state was sulphite ion (SO_3^{2-}) forming unstable complexes with mercury ion [*Munthe et al.*, 1991]. As a result of the complex decays an atom of elemental mercury comes to the aqueous phase. Photoreduction of $Hg(OH)_2$ was indicated also as a possible reduction mechanism [*Pleijel and Munthe*, 1995]. During recent years radical mechanism of reduction at the reaction of mercury ion or dissolved compounds with HO_2 radical was investigated [*Lin and Pehkonen*, 1997; 1998].

Chemistry of mercury sulphite complexes is not sufficiently studied up till now. In a general form the scheme of the sulphite mechanism at present is represented in the following way.

At the first step sulfur dioxide is dissolved in a water drop with the formation of three forms of 4-valent sulfur: non-dissociated H_2SO_3, bisulphite-ion (HSO_3^-), and sulphite-ion (SO_3^{2-}). At real *pH* values of cloud water within the range of 3 - 5 the bulk of S^{IV} is represented by the first two forms, although in any case concentrations of sulphite-ion trace quantities will be higher than concentrations of dissolved mercury.

Sulphite-ion can react with divalent mercury ion forming mercury sulphite. Further it combines with another sulphite-ion producing sulphite-mercury complex [*Constantinou et al.*, 1995]:

$$Hg^{2+} + SO_3^{2-} \leftrightarrow HgSO_3(\text{aq}) \qquad (1.13)$$

$$HgSO_3(aq) + SO_3^{2-} \leftrightarrow Hg(SO_3)_2^{2-} \qquad (1.14)$$

Note that G. Petersen et al. [1998] considers this pathway to be impossible on the assumption that primary the complex is formed. Then it dissociates with the formation of mercury sulphite. In any case mercury sulphite complex dominates among all other mercury compounds with four-valence sulphur [*Lin and Pehkonen,* 1997].

Mercury sulphite and probably sulphite-mercury complex decay and mercury is reduced to the elemental state [*Constantinou et al.*, 1995]:

$$Hg(SO_3)_2^{2-} \rightarrow Hg^0(aq) \qquad (1.15)$$

$$HgSO_3(aq) \rightarrow Hg^0(aq) + SO_3^{2-}. \qquad (1.16)$$

In a general form the intramolecular redox process may be represented by the following reaction chain [*van Loon et al.*, 2000]:

$$Hg^{2+}(aq) + SO_3^{2-}(aq) = Hg^{II}S^{IV}O_3 \rightarrow \rightarrow Hg^0S^{VI}O_3 \rightarrow Hg^0(aq) + S^{VI} \qquad (1.17)$$

Thus the availability of S^{IV} in a drop provides the action of negative feedback increasing elemental mercury concentration in a drop and preventing its additional solution from the ambient air. G. Petersen and co-workers [*Petersen et al.*, 1998] believe that mercury reduction process is limited by reaction of $Hg(SO_3)_2^{-2}$ dissociation. Data on the rate of the indicated reactions are very contradictory. It is demonstrated in Table 1.3.

While considering the importance of sulphite reduction mechanism one should take into account several things. First, if water solution has chloride, mercury ions mainly form mercury chloride [*Prokofiev*, 1981; *Lindqvist et al.*, 1984; *Lin and Pehkonen*, 1998]. At the same time the probability of sulphite compounds formation drastically decreases. Under real atmospheric conditions the content of chloride in cloud water varies from $2\cdot10^{-5}$ to $4\cdot10^{-4}$ mole/L [*Baltensperger et al.*, 1998; *Couture et al.*, 1998; *Kmiec et al.*, 1998]. The content of chloride is particularly high in the atmosphere over the ocean – up to $4\cdot10^{4}$ mole/L [*Vong et al.*, 1997]. Observations in Europe under EMEP [*Ilyin et al.*, 2001] show that chloride content in precipitation is always higher than $2\cdot10^{-6}$ mole/L used in the work [*Petersen et al.*, 1998]. The model analysis of the chemical scheme sensitivity to chloride content demonstrated that actually sulphite mechanism of reduction starts acting only when chloride concentration is lower than $5\cdot10^{-6}$ mole/L [*Ryaboshapko et al.*, 2001].

Second, sulphite in cloud water are rapidly oxidized to sulfate. According to data from [*Lin and Pehkonen*, 1998] in 5 hours sulphite-ion content becomes negligible and the sulphite reduction mechanism ceases to act (it is assumed that at cloud formation the bulk of sulphur dioxide is dissolved in cloud water). It is also important that at high concentrations of sulphite-ion the sufficiently stable complex $Hg(SO_3)_2^{2-}$ (see Table 1.3) is mainly formed [*Lin and Pehkonen*, 1998].

Table 1.3. Reaction rates of sulphite reduction of mercury in the aqueous phase

Reaction	Equilibrium or rate parameter	Temperature	Reference
$Hg^{2+} + SO_3^{2-} \rightarrow HgSO_3$	$5\cdot10^{12}$ M^{-1}	25°C	*Constantinou et al.*, 1995
$HgSO_3 + SO_3^{2-} \leftrightarrow Hg(SO_3)_2^{2-}$	$2.5\cdot10^{11}$ M^{-1}	25°C	*Constantinou et al.*, 1995
$Hg(SO_3)_2^{2-} \rightarrow Hg^0$	$1\cdot10^{-4}$ s^{-1}	25°C	*Constantinou et al.*, 1995
$HgSO_3 \rightarrow Hg^0 + SO_3^{2-}$	0.6 s^{-1}	25°C	*Constantinou et al.*, 1995
$Hg^{2+} + 2SO_3^{2-} \rightarrow Hg(SO_3)_2^{2-}$	$1.1\cdot10^{-21}([SO_2(g)]/10^{-2pH})^2$ s^{-1} *	5°C	*Petersen et al.*, 1998
$Hg(SO_3)_2^{2-} \rightarrow HgSO_3 + SO_3^{2-}$	$4.4\cdot10^{-4}$ s^{-1}	5°C	*Petersen et al.*, 1998
$HgSO_3 \rightarrow Hg^0$	0.6 s^{-1}		*Munthe et al.*, 1991
$HgSO_3 \rightarrow Hg^0$ + products	0.6 s^{-1}		*Lin and Pehkonen*, 1999
$Hg(SO_3)_2^{2-} \rightarrow Hg^0$	0		*Munthe*, 1994
$Hg(HSO_3)^- \rightarrow Hg^0 + S^{VI}$	$4\cdot10^{-6}$ s^{-1}		*Munthe et al.*, 1991

* Concentration of SO_2 is in ppb.

Third, as it was mentioned above the probability of sulphite-ion formation is strongly dependent on solution *pH*. According to [*Petersen et al.*, 1998] the rate of mercury-sulphite complex formation is defined by the solution acidity (see Table 1.3). Model assessments showed [*Ryaboshapko et al.*, 2001] that sulphite reduction mechanism begins to act at *pH* more than 5.

Finally, sulphite reduction rate drastically decreases with temperature decrease. According to [*van Loon et al.*, 2000] at temperature decrease from 25°C to 0°C the rate declines more than 20 times.

C.-J. Lin and S. Pehkonen [1999] consider that in general SO_2 is not important in mercury reduction since sulfur oxidation to 6-valence state goes on quickly. Ozone is the principal oxidant in the continental atmosphere both in the daytime and at night, and in the marine atmosphere – in the daytime. At night chlorine is the main oxidant in the oceanic atmosphere.

A part of oxidized mercury can be represented by hydrate. Under real conditions it can take place only at high *pH* and when chlorides are practically absent. Under the impact of solar light hydrate can decay forming elemental mercury. Z. Xiao and co-workers [*Xiao et al.*, 1994] estimated that even at summer noon in the latitude of Stockholm this reaction is very slow ($k = 3 \cdot 10^{-7}$ s^{-1}).

It is known that the major part of cloud water does not fall out as precipitation but it is evaporated. For modelling of mercury behaviour in the atmosphere the interpretation of mercury fate after a droplet evaporation is important. The literature provides very contradictory information on this issue. Earlier it was supposed [*Lindqvist et al.*, 1991] that reactive oxidized mercury after water evaporation is reduced to the elemental form due to photo-dissociation. Only chemically persistent compounds (like *HgS*) are remained in the solid state. G. Petersen et al. [1998] in their model assume that at drop evaporation all mercury compounds are transferred to the gaseous phase. Experts of US EPA [1997] consider that after drop evaporation an aerosol particle is formed containing in its composition all earlier dissolved and insoluble mercury compounds.

1.3. Arctic mercury depletion

Rising of mercury content in vulnerable Arctic ecosystems and increase of mercury input to human organism in the Arctic is of a particular concern [*AMAP*, 1998]. Only few years ago it was difficult to find any geophysical explanation of increased mercury content in the Arctic. Mercury behaviour in the atmosphere suggests that elevated *Hg* depositions in high latitudes are impossible. Indeed, it is commonly accepted that even if Hg^0 is scavenged form the atmosphere due to dry deposition, the process can be realized only in low and middle latitudes through "soil-plant-atmosphere" interaction [*US EPA*, 1997]. Hg^0 uptake by snow cover is usually disclaimed. Oxidized gaseous and particulate *Hg* has restricted atmospheric lifetime, and their anthropogenic emissions in middle latitudes cannot account for noticeable contribution to total *Hg* deposition in the Arctic [*Petersen et al.,* 2001; *Ilyin et al.*, 2001].

However, recently discovered mercury depletion phenomenon (MDP) during springtime [*Schroeder et al.*, 1998] allows hypothesizing other ways of high *Hg* deposition in the Arctic (and Antarctic). The main point of the MDP consists in abrupt dropping of TGM concentration in high latitudes during springtime. The drop can be very quick (during few hours) and very deep – practically to total disappearance of elemental mercury. In a short time the TGM concentration can sharply rise to its usual values. Sometimes the period of super low Hg^0 concentration can last several hours and even days [*Lu et al.*, 2002; *Lindberg et al.*, 2002; *Berg et al.*, 2001; *Ebinghaus et al.*, 2002]. Sharp droppings can repeat several times, and the total duration of the phenomenon is about 4-6 weeks. Both in the

Northern and Southern Hemisphere the phenomenon can be observed only in springtime [*Lu et al*., 2002; *Ebinghaus et al*., 2002]. In the Northern Hemisphere it lasts from mid-March to mid-June.

Elemental mercury has relatively long atmospheric lifetime and theoretically cannot have such sharp variations [*Junge*, 1972]. Evidently, elemental mercury must be extremely quickly transformed into any other mercury-containing products during MDP. Most likely, they are oxidized mercury compounds presented by either gaseous oxidized forms or particulate oxidized forms. The products were experimentally determined both as reactive gaseous mercury (RGM) and Hg_{part} [*Lu et al*., 2002; *Lindberg et al*., 2002]. The concentration of oxidized mercury can be of the same level as usual TGM concentration (up to 1 ng/m^3). Such concentrations are much higher than those ones, which are typically observed in the vicinity of strong anthropogenic sources.

Very probably, the phenomenon embraces only the first kilometre height of the atmospheric layer [*Ebinghaus et al*., 2002]. This is supported by aircraft measurements of oxidation products [*Schroeder et al*., 2001; *Lindberg et al*., 2002]. For example, at the surface level RGM concentration was 70 pg/m^3, while at 1 km height – only 2 pg/m^3 [*Lindberg et al*., 2002]. The total gaseous mercury (TGM) concentration rises with height and achieves its ordinary values at 1 km [*Schroeder et al*., 2001]. This height is practically coincides with the top of the boundary layer. Hence, since the oxidation process is very fast the vertical profile of oxidation products is opposite to the TGM profile.

It is commonly believed that the sunrise in the Arctic provokes quick photochemical (catalytic) oxidation of elemental mercury in reactions with *Br*-related radicals [*Ebinghaus et al*., 2002]. Recently S. Lindberg et al. [2002] presented a possible mechanism of the *Hg* depletion. The mechanism suggested can be described by several consecutive steps:

1. Occurrence in the atmosphere sea-salt aerosol particles in the frozen form (negative air temperature is an obligatory condition)

2. Influence of UV solar radiation on concentrated on the particle surface *Br*/*Cl* compounds. The compounds can be concentrated on the surface in the process of freezing

3. Formation of halogen radicals and halogen oxide radicals as a result of autocatalytical hetherogenic reactions

4. Destruction of ozone and oxidation of elemental mercury in the following reactions:

$$Br/Cl + O_3 \rightarrow BrO/ClO$$

$$BrO/ClO + Hg^0 \rightarrow HgO + Br/Cl$$

and/or

$$Hg^0 + 2Br/Cl \rightarrow HgBr_2/HgCl_2$$

(preferable reactions)

5. Abrupt stopping step 2 when air temperature is rising above zero. Formation of a water drop instead of the frozen particle and dissolution of the salts homogeneously within the drop.

The mechanism seems to be very reasonable. However, it cannot explain an “explosion” character of the process beginning. In our opinion such a “trigger” is formation of areas of open water near seashore (or polynyas) in ice cover. In springtime ice cover becomes movable due to ice drift provoked by sea currents or wind pressure. Such alternations can be very fast – in few hours a wide area of open water can appear even at low air temperature. In this case the formation of frozen sea-salt aerosol is quite natural. S. Lindberg et al. [2002] showed that elevated levels of RGM accompanied very often with periods of sea-surface roughness and formation of marine aerosol.

S. Lindberg et al. [2002] expect that primary product of elemental mercury oxidation is RGM. Then some RGM can be converted into Hg_{part}. On the contrary, Lu et al. [2002] believe that RGM and Hg_{part} are formed simultaneously, and the formation of Hg_{part} is preferable. T. Berg et al. [2002] also observed simultaneous formation both of Hg_{part} and RGM. Lifetime of Hg_{part} and RGM even in the stable polar atmosphere is much shorter than that of Hg^0, and their deposition should lead to additional *Hg* pollution of the Arctic environment. Measurements of mercury concentration in snow-pack conducted in series with atmospheric observation at Barrow station (Alaska, USA) showed clearly that the depletion phenomenon is accompanied by the rise of mercury content in snow [*Lindberg et al.*, 2002]. Canadian experts provided a broad survey of mercury content in northeastern Canada and Greenland. They found that the depletion phenomenon is widespread and lead to considerable rising of mercury content in snow-pack during springtime [*Lu et al.*, 2002]. However, S. Lindberg et al. [2002] noted that mercury concentration in snow-pack reaches its maximum leeward from polynyas and open water areas. Besides, the concentrations drop with distance from the seashore. These facts confirm that the MDP is closely connected with seashore line.

It was noted in recent works that the depletion is connected with elevated concentrations of *BrO*. Satellite observations showed that both in the Arctic and the Antarctic the zones of elevated *BrO* concentrations have ring shape – they connected with the seashores, and they appear in spring [*Steffen et al.*, 2001; *Drummond*, 2001; *Lu et al.*, 2002; *Ebinghaus et al.*, 2002]. If hypothesis of *BrO* involvement into *Hg* depletion is correct, it means that not the whole Arctic is influenced by the phenomenon but only seashore zones. Most likely, that the central parts of the Arctic and Antarctic are not affected by the MDP. Nowadays it is difficult to say how far southward the phenomenon can be extended. It observed at least within the Polar Circle in the Arctic.

Chapter 2

MODEL DESCRIPTION

2.1. Overview of the model and the computation domain

Hemispheric model of mercury long-range transport (*MSCE-Hem-Hg*) is elaborated as a complex multi-compartment model describing mercury behaviour, transformation, and accumulation in various environmental compartments i.e. the atmosphere, soil, vegetation, seawater etc. As it was mentioned above the main destination of the model is the evaluation of mercury transport to remote areas, investigation of its cycling in the environment for long-term periods, and prediction of future contamination levels. From this point of view the atmosphere is the most dynamic compartment responsible for mercury dispersion over the globe. To date, the atmospheric part of the model has been developed and tested. It considers mercury fate in the atmosphere from its emission till deposition to the Earth surface including numerous physical and chemical transformations. The scheme of model treatment of main mercury processes in the atmosphere is presented in Figure 2.1.

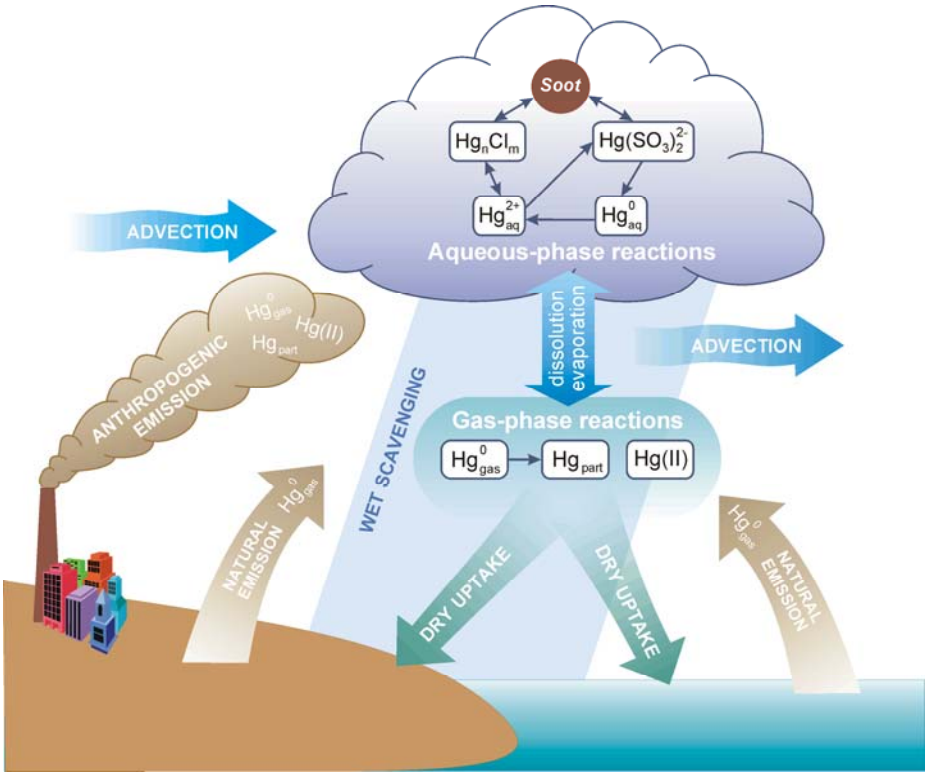

Figure 2.1. *The model scheme of mercury behaviour in the atmosphere*

Mercury enters the atmosphere from anthropogenic and natural sources. They include point (coal-fired power plants, waste incinerators, volcanoes etc.) and diffuse area sources (mill tailings, municipal wastes, geologically enriched soils) [*Jackson*, 1997; *Gustin et al*., 1999]. Whereas anthropogenic emissions contain a number of mercury species (elemental mercury vapour, oxidized gaseous and particulate mercury), natural emissions mostly consist of elemental vapour. Moreover, mercury vapour is emitted to the atmosphere from the sea surface due to marine biota activity [*Kim and Fitzgerald*, 1986]. Detailed description of mercury emission sources is presented in Chapter 3.

Once emitted to the atmosphere mercury is transported through it with the air masses (advective transport) and dispersed by eddy diffusion. During the pathway in the atmosphere mercury species undergo physical and chemical transformations resulting in their mutual redistribution. Thus, elemental mercury is oxidized by such oxidants as ozone and *OH* radical. Besides, it is dissolved in cloud water and takes part in aqueous-phase oxidation and reduction reactions, formation of sulphite and chloride complexes, which are in turn adsorbed by soot particles. The model chemical scheme is described in detail in Section 2.3. Mercury species are removed from the atmosphere by means of surface uptake and precipitation scavenging. The model parameterization of dry and wet deposition processes is considered in Section 2.4.

The model computation domain covers the whole Northern Hemisphere with spatial resolution 2.5° both in zonal and meridional directions. The surface grid structure of the model domain is shown in Figure 2.2. To avoid a singularity at the pole point, peculiar to the spherical coordinates, the grid has a special circular mesh of radius 1.25° including the North Pole. In the vertical direction the model domain consists of eight irregular levels of terrain-following sigma-pressure (σ-p) coordinate defined as a ratio of local atmospheric pressure to the ground surface pressure [*Jacobson*, 1999]. The vertical grid structure of the model is presented in Figure 2.3.

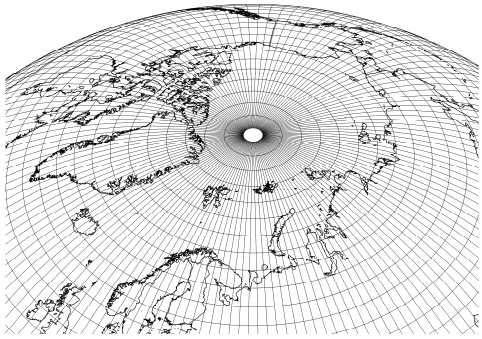

Figure 2.2. *Horizontal grid structure of the model domain. Geographical coordinates with 2.5° × 2.5° resolution and the pole grid cell*

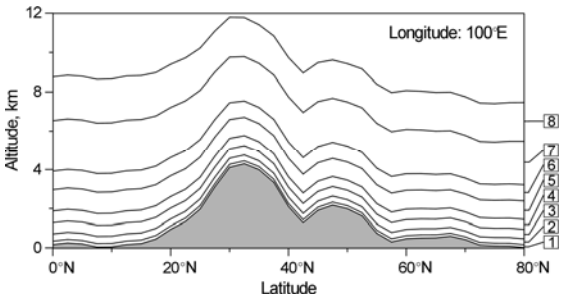

Figure 2.3. *Vertical grid structure of the model domain. Eight terrain-following σ-levels: 1 – σ = 0.99; 2 – 0.96; 3 – 0.91; 4 – 0.85; 5 – 0.77; 6 – 0.68; 7 – 0.55; 8 – 0.4*

2.2. Atmospheric transport

The model description of mercury atmospheric transport is based on the three-dimensional advection-diffusion equation adapted to the (σ–p) coordinate [*Jacobson*, 1999]:

$$\frac{\partial}{\partial t}(q_i p_s) = -\nabla_H \cdot (q_i p_s \mathbf{V}_H) - \frac{\partial}{\partial \sigma}(q_i p_s \dot{\sigma}) + \frac{\partial}{\partial \sigma}\left[K_z \frac{g^2 \rho^2}{p_s^2} \frac{\partial}{\partial \sigma}(q_i p_s)\right] + C_i + S_i - R_i \qquad (2.1)$$

Here $q_i = c_i / \rho$ is mixing ratio of ith mercury species; c_i and ρ are the mercury species volume concentration and the local air density; $\dot{\sigma} = d\sigma / dt$ is the vertical scalar velocity in the σ–p coordinate; ∇_H and $\mathbf{V}_H$ denote horizontal divergence operator and horizontal wind

velocity respectively; K_z is the vertical eddy diffusion coefficient; and g is the gravitational acceleration. In Equation (2.1) we omitted horizontal components of eddy diffusion because of the coarse horizontal grid resolution. The local air density ρ is coupled with air temperature T_a and surface pressure p_s through the equation of state:

$$\rho = \frac{\sigma p_s}{R_a T_a}, \tag{2.2}$$

where R_a is the humid air gas constant.

The first two terms on the right hand side of Equation (2.1) describe horizontal and vertical advection of a pollutant in the atmosphere. The third term represents vertical eddy diffusion, the fourth considers species mutual chemical transformations (C_i), and the last two terms describe bulk pollutant sources (S_i) and removal processes (R_i). Equation (2.1) is solved by means of the time-splitting technique [*Yanenko*, 1971; *Marchuk*, 1975; *McRae et al.*, 1982]. Following this method, Equation (2.1) is decomposed into several separate sub-equations describing different physical and chemical processes, which are solved successively during each time step.

Advection

In spherical coordinates the sub-equation of Equation (2.1) describing horizontal advection has the following form:

$$\frac{\partial}{\partial t}(q_i p_s) = -\frac{1}{R_E \cos\varphi} \times \left[\frac{\partial}{\partial \lambda}(q_i p_s V_\lambda) + \frac{\partial}{\partial \varphi}(q_i p_s V_\varphi \cos\varphi) \right] \tag{2.3}$$

where λ and φ are the geographical longitude and latitude; R_E is the Earth radius; V_λ and V_φ are zonal and meridional components of the wind velocity respectively. Moreover, the former term in the square brackets describes the zonal advective transport, while the latter term represents the meridional one.

Equation (2.3) is numerically solved using Bott flux-form advection scheme [*Bott*, 1989a; 1989b, 1992]. This scheme is mass conservative, positive-definite, monotone, and is characterized by comparatively low artificial diffusion [see e.g. *Dabdub and Seinfeld*, 1994]. In order to reduce the time-splitting error in strong deformational flows the scheme has been modified according to [*Easter*, 1993]. The original Bott scheme has been derived in the Cartesian coordinates. To apply the scheme to the transport in spherical coordinates it has been modified taking into account peculiarities of the spherical geometry. Detailed description of the Bott advection scheme in the spherical coordinates is presented in [*Travnikov*, 2001].

The vertical advection part of Equation (2.1) is written as follows:

$$\frac{\partial}{\partial t}(q_i p_s) = -\frac{\partial}{\partial \sigma}(q_i p_s \sigma). \tag{2.4}$$

This one-dimensional advection equation is solved using the original Bott scheme generalized for a grid with variable step $\Delta\sigma$.

Vertical velocity

The very important issue for any air quality model is the mass consistency. It means that supplied wind and air density fields (surface pressure p_s is a full analog of air density in σ-p coordinate system) should satisfy the continuity equation:

$$\frac{\partial p_s}{\partial t} + \nabla_H \cdot (p_s \mathbf{V}_H) + \frac{\partial}{\partial \sigma}(p_s \sigma) = 0. \tag{2.5}$$

In the terms of an air quality model it implies that the model maintain a uniform mass mixing ratio field of an inert tracer [*Odman and Russel*, 2000]. It is exactly realized only if the air quality model and a meteorological model supplying input data have the same *discretization*, i.e. grid structure, time step, and finite-difference formulation. However, many transport models (including considered one) have discretization different from that

used in the data supplying meteorological model. Besides, time resolution of the meteorological data (6 hours for the model involved) is often considerably lower than the model time resolution defined by the stability condition (15-45 minutes). It requires temporal interpolation of the meteorological data. All mentioned above can lead to a considerable mass inconsistency and the uniform tracer field cannot be maintained. To adjust input meteorological fields to the model discritization vertical wind velocity $\dot{\sigma}$ is calculated from the continuity equation (2.5) at each step using the procedure similar to that suggested in [*Odman and Russel*, 2000].

Since the non-linear advection scheme is used for vertical advection, it is difficult to derive the vertical velocity directly from Equation (2.5). Instead one can solve Equation (2.5) using exactly the same procedure as for Equations (2.3) and (2.4) for one time step and equate the obtained value of surface pressure to that interpolated from the input data. As a result for each vertical column of the computation domain we obtain system of non-linear equations:

$$p_s = F_k(\dot{\boldsymbol{\sigma}}) \qquad k = 1, \ldots, N. \qquad (2.6)$$

Here $\dot{\boldsymbol{\sigma}} = (\dot{\sigma}_1, \ldots, \dot{\sigma}_N)$ is the vector of vertical wind velocities at the upper boundaries of σ-layers, and N is the number of the layers. Solving the equations system (2.6) for $\dot{\boldsymbol{\sigma}}$ at each vertical column and taking into account boundary condition at the surface $\dot{\sigma}_0 = 0$ we obtain field of vertical wind velocities. We apply standard FORTRAN library MINPACK (http://www.netlib.org/minpack/) for the solution of the non-linear equations system (2.6).

Eddy diffusion

Vertical eddy diffusion is described by the following equation:

$$\frac{\partial}{\partial t}(q_i p_s) = \frac{\partial}{\partial \sigma}\left[K_z \frac{g^2 \rho^2}{p_s^2} \frac{\partial}{\partial \sigma}(q_i p_s) \right]. \qquad (2.7)$$

Vertical eddy diffusion coefficient $K_z = K_z(\lambda,\varphi,\sigma)$ is supplied by the atmospheric boundary layer module of the meteorological data preparation system (see Section 3.3). Non-linear diffusion equation (2.7) has been approximated by the second-order implicit numerical scheme in order to avoid restrictions of the time step caused by possible sharp gradients of species mixing ratio $q_i(\sigma)$. The obtained finite-difference equation is solved by means of the sweep method.

Initial and boundary conditions

The model computation domain has two boundaries: upper and equatorial. Long residence time of mercury in the atmosphere requires setting appropriate initial and boundary conditions to take into account mercury contained in the computation domain before the computations and the input fluxes of mercury through the boundaries.

According to the numerous measurements carried out for last decades [e.g. see *Ebinghaus et al.*, 1999a] elemental mercury Hg^0 is more or less uniformly distributed over the Northern Hemisphere (background concentrations are around 1.7 ng/m^3). Vertical distribution of Hg^0 is also rather uniform [*Banic et al.*, 1999]. Therefore we prescribed uniform distribution of elemental mercury concentration at the upper boundary – 0.185 pptv (corresponding to about 1.5 ng/m^3 at 1 atm and 20°C). On the other hand, some gradient of total gaseous mercury (TGM) was observed over the ocean between the Northern and Southern Hemispheres [e.g. see *Lamborg et al.*, 2002]. According to R.Ebinghaus et al. [2001] mean concentrations of TGM over the Northern and Southern Hemispheres are 1.7 and 1.3 ng/m^3 respectively. Elemental mercury makes up the main part of TGM. Summarizing the measurement data from [*Slemr*, 1996] we set the gradient of Hg^0 to 0.05 ng/m^3/degree at the equatorial boundary. Since the residence time of other mercury species in the

atmosphere is considerably shorter we neglected their input through the boundaries.

To fill up the model domain with mercury from anthropogenic sources of different regions and continents (it is necessary for the inter-continental transport assessment) we performed a computation run for the period of one year without any boundary and initial conditions. Then we used the obtained concentrations of mercury species as initial conditions for the regular computation run. Besides, the contribution of different sources to mercury incoming through the upper boundary is assumed to be the same as at the highest atmospheric layer.

2.3. Atmospheric chemistry

The overview of main physical and chemical processes of mercury transformation in the atmosphere is given in Section 1.2. The current model parameterization is mostly based on the chemical scheme developed by G.Petersen et al. [1998]. In order to adjust the original scheme for global long-term calculations it was simplified taking into account only the most important reactions [*Ryaboshapko et al.*, 1999]. Fast irreversible reactions were assumed to be instantaneous, while reversible ones were replaced by appropriate equilibrium conditions. Besides, up-to-date ideas of mercury atmospheric chemistry mentioned in Section 1.2 were also represented.

As it was mentioned in Chapter 1 mercury occurs in the atmosphere in various forms in gaseous, aqueous, and solid phase, which are undergo numerous physical and chemical transformations. The model considers the following mercury forms: gaseous elemental Hg^0_{gas}, gaseous oxidized *Hg(II)*; particulate oxidized Hg_{part}; and four liquid phase forms - elemental dissolved Hg^0_{aq}, mercury ion Hg^{2+}_{aq}, sulphite complex $Hg(SO_3)^{2-}_2$, and aggregate of chloride complexes Hg_nCl_m. The main mercury transformations in the atmosphere are schematically described in the Figure 2.4

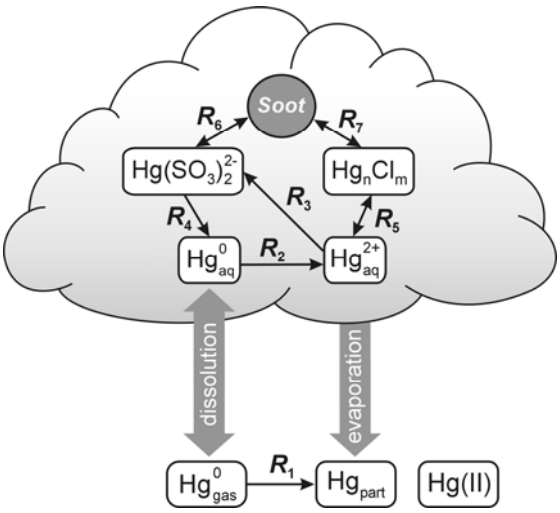

Figure 2.4. *Scheme of physical and chemical transformations of mercury in the atmosphere*

Gaseous phase

Currently, the only gas phase reaction treated in the model is oxidation of elemental mercury by ozone (R_1):

$$Hg^0_{gas} + O_3 \rightarrow Hg(II)_{part} + products \qquad (2.8)$$

Since, ozone is always in plenty under ordinary atmospheric conditions this second-order reaction is described by a first-order rate expression with the reaction rate constant depending on the reactant concentration:

$$R_1 = -\frac{d[Hg^0_{gas}]}{dt} = k_1'[Hg^0_{gas}], \qquad (2.9)$$

$$k_1' = k_1[O_3]_{gas}, \quad k_1 = A\exp(-E_a/(R_{univ}T))$$

where A = 2.1 $\cdot 10^{-18}$ cm^3/(molec·s); E_a = 10.36 kJ/mole; R_{univ} = 8.31 J/(mole·K); and ozone concentration $[O_3]_{gas}$ is in molec/cm^3 [*Hall,* 1995]. It is believed that the product of the reaction is particulate mercury (see Section 1.2). Monthly mean fields of ozone concentration over the whole Northern Hemisphere were taken from [*Wang et al.*, 1998] and then adapted to the model grid (see Section 3.4).

Aqueous phase

In the cloud environment elemental gaseous mercury Hg^0_{gas} is dissolved in cloud water (see Fig. 2.4). This process is described by equilibrium conditions with Henry's low constant (non-dimensional) depending on the air temperature (Eq. 1.1).

Dissolved elemental mercury Hg^0_{aq} is oxidized by ozone producing mercury oxide HgO, which is very short-lived in the liquid phase and is rapidly transformed to the mercury ion Hg^{2+}_{aq} (R_2). Thus, the resulting reaction can be written as follows:

$$Hg^0_{aq} + O_3 \rightarrow Hg^{2+}_{aq} + products\,, \qquad (2.10)$$

with the reaction rate expression:

$$R_2 = -\frac{d[Hg^0_{aq}]}{dt} = k'_2[Hg^0_{aq}]\,; \qquad (2.11)$$

$$k'_2 = k_2 H_{O3}[O_3]_{gas}\,,$$

where k_2 = 7.8·10^{-14} (molec/cm^3)$^{-1}$s^{-1}, ozone concentration $[O_3]_{gas}$ is in molec/cm^3. This reaction rate constant is derived from values presented in Table 1.2 taking into account equilibrium conditions of ozone dissolution in cloud water. Temperature dependence of non-dimensional Henry's low constant H_{O3} for ozone is described by Equation 1.4.

Mercury ion Hg^{2+}_{aq} reacts in the solution with sulphite ions SO^{2-}_3 resulting in the formation of mercury sulphite complex $Hg(SO_3)^{2-}_2$ [*Petersen et al.,* 1998]:

$$Hg^{2+}_{aq} + 2SO^{2-}_3 \rightarrow Hg(SO_3)^{2-}_2\,. \qquad (2.12)$$

The reaction rate is determined by the air concentration of SO_2 and the cloud water pH (see Table 1.3):

$$R_3 = -\frac{d[Hg^{2+}_{aq}]}{dt} = k'_3[Hg^{2+}_{aq}]\,; \qquad (2.13)$$

$$k'_3 = k_3[SO_2]^2_{gas}\cdot 10^{4pH}\,,$$

where k_3 = 1.8·10^{-42} (molec/cm^3)$^{-2}$s^{-1}, and $[SO_2]_{gas}$ is in molec/cm^3. The sulphite complex $Hg(SO_3)^{2-}_2$ is dissociated to mercury sulphite $HgSO_3$, which is unstable, and is readily reduced to Hg^0_{aq}. Thus, the reduction process (R_4) can be described as:

$$Hg(SO_3)^{2-}_2 \rightarrow Hg^0_{aq} + products \qquad (2.14)$$

with the reaction rate expression:

$$R_4 = -\frac{d[Hg(SO_3)^{2-}_2]}{dt} = k_4[Hg(SO_3)^{2-}_2]\,, \qquad (2.15)$$

where k_4 = 4.4·10^{-4} s^{-1}. This process increases the amount of dissolved elemental mercury in a droplet hampering further dissolution of gaseous mercury. Hence, the scheme implies negative feedback controlling elemental mercury uptake from the air.

Mercury ion Hg^{2+}_{aq} also takes part in a number of reactions leading to the formation of various chloride complexes Hg_nCl_m (R_5). These reversible reactions in the first approximation can be replaced by equilibrium concentrations of free mercury ions and mercury in the aggregate of chloride complexes ([$HgCl^+$], [$HgCl_2$], [$HgCl_3^-$], [$HgCl_4^{2-}$]). The equilibrium ratio of the appropriate mercury concentrations depends upon water content of chloride ion $[Cl^-]$ and is defined as follows [*Lurie*, 1971]:

$$r_1 = \frac{[Hg_nCl_m]_{aq}}{[Hg^{2+}_{aq}]} = \frac{[Cl^-]_{aq}}{1.82\cdot 10^{-7}} + \frac{[Cl^-]^2_{aq}}{6.03\cdot 10^{-14}}$$

$$+ \frac{[Cl^-]^3_{aq}}{8.51\cdot 10^{-15}} + \frac{[Cl^-]^4_{aq}}{8.51\cdot 10^{-16}}\,. \qquad (2.16)$$

Sulphite and chloride complexes can be adsorbed and desorbed by soot particles in the aqueous phase (R_6, R_7). Comparatively fast equilibrium of these two reverse processes can also be described by means of "dissolved-to-adsorbed ratio". Based on the appropriate reaction rates it could be taken equal to 0.2 in both cases [*Petersen et al.,* 1998]:

$$r_2 = \frac{[Hg(SO_3)_2^{2-}]_{aq}}{[Hg(SO_3)_2^{2-}]_{soot}} = \frac{[Hg_nCl_m]_{aq}}{[Hg_nCl_m]_{soot}} = 0.2\,.$$

As it was mentioned above one can distinguish three groups of mercury compounds being in equilibrium. The first group (A) contains elemental mercury in the gaseous and dissolved phase; the second one (B) consists of the mercury sulphite complex both dissolved and on soot particles; and the third group (C) includes free mercury ions, dissolved mercury chloride complexes and those on soot particles:

$$A = Hg^0_{gas} + Hg^0_{aq};$$

$$B = \left\{Hg(SO_3)_2^{2-}\right\}_{dis} + \left\{Hg(SO_3)_2^{2-}\right\}_{soot};$$

$$C = Hg^{2+}_{aq} + \left\{Hg_nCl_m\right\}_{dis} + \left\{Hg_nCl_m\right\}_{soot}.$$

According to this simplified scheme and introduced notations mercury transformations in the liquid phase are described by the following system of the first-order differential equations:

$$\begin{cases} \dfrac{d[A]}{dt} = -\alpha k_2'[A] + \beta k_4[B], \\ \dfrac{d[B]}{dt} = -\beta k_4[B] + \gamma k_3'[C], \\ \dfrac{d[C]}{dt} = -\gamma k_3'[C] + \alpha k_2'[A]. \end{cases} \qquad (2.17)$$

Here $\alpha = H_{Hg}L_w / (1 + H_{Hg}L_w)$ is the fraction of mercury in the *A* group corresponding to the dissolved form, and L_w is the non-dimensional liquid water content defined as volume of cloud water per unit volume. Parameter $\beta = r_2 / (1 + r_2)$ denotes mercury fraction of the *B* group in the dissolved phase. Value $\gamma = r_2 / (r_1 + r_2 + r_1 r_2)$ is the fraction of mercury in the *C* group corresponding to the mercury ion Hg^{2+}_{aq}. The analytical solution of the equations system with appropriate initial conditions defines mercury evolution in the aqueous phase during one time step.

The non-dimensional liquid water content L_w is evaluated according to parameterization suggested in [*Hongisto*, 1998]. It is equal to 10^{-7} for clouds without precipitation; $3 \cdot 10^{-7}$ for the large-scale cloudiness with precipitation; and 10^{-6} for the convective cloudiness with precipitation. Cloud cover data for the two types of cloudiness (large-scale and convective) is provided by the meteorological data preparation system (Section 3.3).

Mercury depletion phenomenon

Taking into account general ideas and review of the literature on mercury depletion phenomenon (MDP) presented in Section 1.3 we adopt the following assumptions for the model parameterization.

1. We assume that MDP can occur only over open seawater areas, which were previously covered with ice during winter period. We exclude a possibility of penetration of *BrO* precursors through ice cover. Hence, we think that MDP can take place over coastal zones of the Arctic Ocean. Only those grid cells are taken into account, which cover both land and see.

2. We suppose that the water surface was previously covered with ice if air temperature in a given point was permanently lower than -3°C during wintertime (assumed seawater freezing point). Then in springtime the temperature became higher than 0°C, and ice melting started. Besides, during springtime ice-drift becomes more intensive and areas of open water appear. Conditionally we "switch on" the MDP module if air temperature during previous 24 hours was higher that 0°C. We understand the conventional character of such a "trigger" because open water can appear at low negative temperatures.

3. We assume that total duration of MDP during springtime in any point does not exceed 4 weeks and MDP takes place every day (instantly at noon) during this period. The MDP module can be "switched on" only within the period from April to June.

4. We believe that during the MDP concentration of elemental mercury near the surface layer drops down from its usual level to 0.1 ng/m^3. Oxidation of Hg^0 leads to the formation of RGM (50%) and Hg_{part} (50%). The oxidized products are partly scavenged from the atmosphere within a given modelling grid cell, partly transported outside it and scavenged later.

5. We accept that the MDP covers the lowest 1 kilometre height layer of the atmosphere. Within this layer the intensity of the phenomenon linearly decreases with height to zero at the top of the layer. Hence, during the MDP elemental mercury has rising profile from 0.1 ng/m^3 at the surface to its usual values at 1 km height. Contrary, oxidized forms have dropping profile from their maximum at the surface to their usual values at 1 km height.

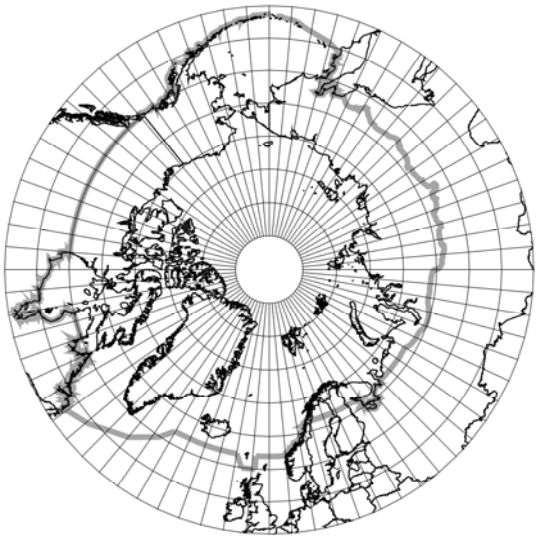

Figure 2.5. *AMAP Arctic area [AMAP, 1998*]

We took the Arctic definition accepted within the AMAP programme (Fig. 2.5). It covers the terrestrial and marine areas north of the Arctic Circle, north of 62°N in Asia and 60°N in North America, modified to include the marine areas north of the Aleutian chain, Hudson Bay, and parts of the North Atlantic Ocean including the Labrador Sea.

2.4. Removal processes

Mercury is removed from the atmosphere due to dry uptake of particulate and gaseous species by the underlying surface and through the scavenging of both the gas-phase and aqueous forms with precipitation. Appropriate sub-equation of Equation (2.1) describing removal processes of ith species is as follows:

$$\frac{\partial q_i}{\partial t} = -(\Lambda_i^d + \Lambda_i^w + \Lambda_i^{aq}) q_i \,, \qquad (2.18)$$

where Λ_i^d, Λ_i^w, and Λ_i^{aq} are the rates of dry, wet deposition and removal of the aqueous phase respectively. Since surface pressure is not changed in this processes, we have divided both parts of the original equation by p_s. All the removal processes are considered in the model successively.

Dry uptake

Particular mercury as well as some gaseous species are removed from the atmosphere through the contact with the underlying surface. They approach the ground surface (soil, rocks, vegetation, water etc.) due to advection, diffusion or sedimentation processes and stick to or react with it. This process is described by a part of Equation (2.18) referred to the surface level:

$$\left.\frac{\partial q_i}{\partial t}\right|_{surf} = -\left.\Lambda_i^d q_i\right|_{surf} \,, \qquad (2.19)$$

where the rate of dry uptake Λ_i^d is proportional to dry deposition velocity V_d^i

$$\Lambda_i^d = V_d^i \left(\frac{g\sigma}{R_a T_a}\right)_{surf} \,. \qquad (2.20)$$

Here subscript *surf* denotes values related to the ground surface. It should be noted that the expression in the parenthesis characterizes

transformation from Cartesian to (σ-p) coordinate system and equals to inverse absolute value of the Jacobian ($J = -R_a T_a/g\sigma$).

In the current version of the model we apply a simplified parameterization of the dry deposition velocity for aerosol particles developed in [*Pekar*, 1996]. This approach is based on measured deposition velocities [*Sehmel*, 1980] as functions of aerosol size (d), roughness of the underlying surface (z_0) and friction velocity parameter (u_*). Reasoning from the analysis of scientific literature (see Section 1.1) it is adopted that mercury particle-carriers have characteristic mass median diameter $d = 0.7$ μm and dry deposition velocities of particulate mercury are described by the following formulas:

$$V_d^{part} = \begin{cases} (0.02u_*^2 + 0.01)(z_0 10^3)^{0.33}, & \text{land} \\ 0.15u_*^2 + 0.013, & \text{sea} \end{cases}$$

Here V_d^{part} is in cm/s, z_0 in m, and u_* in m/s. Currently, only two types of underlying surface are distinguished in the parameterization of dry deposition of particulate mercury (land and seawater surface). It is proposed to introduce specification of dry deposition on different types of land cover (forests, grassland, deserts etc.)

Dry deposition velocity of gaseous oxidized mercury *Hg(II)* is taken the same as for nitric acid $V_d^{oxid} = 0.5$ cm/s due to similarity of their properties [*Petersen et al.*, 1995]. This parameter does not vary seasonally and with different type of the underlying surface.

Dry uptake of elemental gaseous mercury Hg^0_{gas} by various types of underlying surface is not adequately defined yet. Some experts [*US EPA*, 1997] suppose that this type of mercury removal is not an essential sink on a regional and global scale. It is assumed that absorption of Hg^0_{gas} by vegetation takes place only if its concentration exceeds so-called "compensation point" (about 20 ng/m^3). It implies that the absorption is realized only in the immediate vicinity of emission sources [*Lyon et al.*, 1999]. According to another viewpoint [*Lin and Pehkonen*, 1999] dry uptake of elemental mercury is considered to be the dominating mechanism of mercury removal from the atmosphere. T. Bergan and H. Rodhe [2001] also note that elemental mercury uptake is an important mechanism of the global mercury cycle, but it is poorly considered in the literature.

Table 2.1 contains both measured and adopted in various models dry uptake velocities of elemental gaseous mercury under different conditions. The data are presented in the chronological order to reflect the tendencies of the process treatment. As seen from the table the value of deposition velocity varies from zero to first centimeters per second [*Lindberg et al.*, 1998]. The most important parameters affecting dry uptake of elemental mercury are insolation, temperature and type of underlying surface.

Summarizing available data we adopt the following parameterization of the process. There is no dry uptake of elemental gaseous mercury by water surface and land surface not covered by vegetation. It is also absent during nighttime. Over the vegetated surface during daytime dry uptake velocity has the following form:

$$V_d^{gas} = \begin{cases} 0, & T_s \le T_0 \\ A_d \dfrac{T_s - T_0}{T_1 - T_0} \cos\theta_s, & T_0 < T_s \le T_1 \\ A_d \cos\theta_s, & T_s > T_1 \end{cases}$$

Here T_s is the surface temperature, $T_0 = 273$K and $T_1 = 293$K; A_d is equal to 0.03 cm/s for forests and 0.01 cm/s for other vegetation types; θ_s is the solar zenith angle calculated according to [*Jacobson*, 1999].

Table 2.1. Measured and estimated values of dry uptake velocities of elemental gaseous mercury by the underlying surface

Surface type (location)	Conditions	V_d	Method	Reference
Deciduous forest	Warm season	0.01 - 0.1	Measurements	*Lindberg et al.,* 1991
Forest	Winter Summer	0.006 0.12	Modelling	*Lindberg et al.,* 1992
Land (North America)	Always	0	Expert estimates	*Bullock et al.*, 1994
Continents	—	0.05 - 0.1	Expert estimates	*Bloom et al.*, 1994
Land	Daytime	0.005	Expert estimates	*Constantinou et al.*, 1995
Grate Lakes	Always	0	Modelling	*Schroeder,* 1996
Forest	Warm season	>0 (25% of period)	Measurements	*Meyers et al.*, 1996
Land (North America)	Always	0	Expert estimates	*Pai et al.*, 1997
Vegetation	Under CP * Wet leaves	0 >0	Measurements	*US EPA,* 1997
Vegetation	Dry leaves, TGM Wet leaves, TGM	1.3 ± 1.8 0.4 ± 0.3	Measurements	*Lindberg et al.*, 1998
Land (Europe) Water, ice, snow	Warm season Winter, T>0˚C Winter, T<0˚C Always	0.03 0.01 0 0	Expert estimates	*Ryaboshapko et al.,* 1999
Lakes (Sweden)	Warm season	0	Measurements	*Ebinghaus et al.,* 1999
Vegetation	Under CP Over CP	0 0.06	Expert estimates	*Lyon et al.*, 1999
Soil (North America) Forest (North America)	Variable humidity T<0˚C July, Daytime July, Nighttime	0.002 - 0.015 0 up to 0.15 0	Measurements / Modelling	*Xu et al.*, 1999
Continents	Always	0.005	Expert estimates	*Shia et al.*, 1999
Continents Ocean	T<0˚C 0˚C <T<20˚C T>20˚C Always	0.03 0 - 0.03 0 0	Expert estimates	*Bergan and Rodhe,* 2001
Forest Other surfaces	Always	0.001 - 0.03 0	Expert estimates	*Petersen et al.,* 2001
Any surface	Always	0	Expert estimates	*Christensen*, 2001
Soil	Humid, shadow	0.005	Measurements	*Zhang et al.*, 2001
Continents	Always	0.01	Expert estimates	*Seigneur et al.*, 2001

* CP is the compensation point

Wet scavenging

Scavenging of aerosol particles and soluble gases by precipitation is one of the most effective mechanisms of mercury removal from the atmosphere. First of all it concerns particulate Hg_{part} and gaseous oxidized *Hg(II)* mercury forms. Wet scavenging rate Λ_i^w in Equation (2.18) is proportional to precipitation intensity $I_p(\sigma)$ and can be roughly approximated by the following expression:

$$\Lambda_i^w = W_i I_p(\sigma)\left(\frac{g\sigma}{R_a T_a}\right)_{surf} \frac{(q_i I_p)_{surf}}{\int q_i I_p(\sigma) d\sigma}, \qquad (2.21)$$

where W_i is the washout ratio of the ith species defined as a ratio of the species concentration in precipitation to the concentration in the surface air. The last ratio in (2.21) takes into account variation of precipitation intensity with altitude. This approach is aimed at fitting simulated concentration in precipitation of scavenged species to measured ones using empirical values of the washout ratios W_i.

It is accepted that particles containing mercury Hg_{part} behave like sulphate particles with the average washout ratio $W_{part} = 7 \cdot 10^5$ [*Petersen et al.*, 1995; *Iversen et al.*, 1989]. Washout ratio of gaseous oxidized mercury is taken to be equal to that of nitric acid $W_{oxid} = 1.4 \cdot 10^6$ [*Petersen et al.*, 1995; *Jonsen and Berge*, 1995].

Aqueous phase removal

All aqueous-phase mercury species are scavenged from the atmosphere by precipitation with the removal rate:

$$\Lambda_i^{aq} = \frac{g\sigma}{R_a T_a} \frac{\Delta I_p}{L_w \Delta\sigma}, \qquad (2.22)$$

where ΔI_p is the increment of precipitation within a gridcell. It is taken to be zero for negative values. All aqueous-phase species scavenged by precipitation during its falling down return back to the atmosphere in the particulate form if precipitation is entirely evaporated before the ground.

Chapter 3

INPUT INFORMATION

3.1. Natural emission of mercury to the atmosphere: a review

It is clear that the natural atmospheric cycle of mercury took place and varied on the geological scale of time over the course of the Earth existence. Mercury input to the atmosphere from anthropogenic sources in tangible quantities started at the beginning of XIX century [*Melnikov*, 1971; *Pirrone et al.*, 1998].

The atmosphere is an intermediate link in the global mercury cycle. According to various estimates [*Lindqvist and Rodhe*, 1985; *Lamborg et al.*, 2002] the lifetime of elemental mercury, the most long-lived form of mercury in the atmosphere, is about one year. The main mechanism of metallic mercury removal from the atmosphere is its oxidation. The oxidized forms are scavenged faster on the underlying surface – for the periods of days. Aerosol mercury in the lower stratosphere is a special case [*Murphy et al.*, 1998]. Its lifetime can be long and it is defined by the stratospheric-tropospheric exchange.

Mercury in these or those quantities can be found virtually in all the surface media. Elemental and some forms of oxidized mercury due to their volatility are permanently coming to the atmosphere. The Earth surface covered by ice may be considered the only exclusion. Low mercury content in glacier materials and attendant low temperature make glaciers free from mercury emissions to the atmosphere.

High temperature of the Earth mantle zone results in high mercury mobility. It continuously diffuses to the lithosphere surface. In the zones of deep geological fractures these processes go on more intensively. Here are located so-called mercury geochemical belts where mercury concentrations in the upper layer appreciably exceed their average values. In some parts of mercury belts the intensive accumulation of mercury resulted in the formation of deposits and areas of dispersion [*Jonasson and Boyle*, 1971; *Bailey et al.*, 1973]. It is clear that regions with high concentrations in surface rocks are characterized by high mercury emissions to the atmosphere.

Metallic mercury is poorly dissolvable in water. However, various mercury compounds are found everywhere both in fresh and seawater. Concentrations in seawater vary from region to region within an order of magnitude [*Baeyens et al.*, 1991]. Physical-chemical processes in surface layers of water lead to the formation of volatile forms – elemental and methylated mercury. In its turn it causes supersaturating of surface water layers relative to air concentrations. Sometimes, levels of supersaturating can reach four orders of magnitude [*Baeyens et al.*, 1991]. When the equilibrium is disturbed mercury flux to the atmosphere from the ocean should take place.

According to the character of natural mercury emissions to the atmosphere the Earth surface may be divided into five main types: (1) glaciers (with zero emission), (2) sea water, (3) background soils, (4) soils of the mercury belts and (5) soil (or rocks) of mercury deposits areas. Within the scales of oceans and continents the fresh water reservoirs should be referred to appropriate types of land due to their insignificant sizes.

Seawater emission

Numerous measurements of mercury concentrations simultaneously in air and water showed that everywhere water is

supersaturated by elemental mercury and by DMM. According to Henry's law "excessive mercury" enters the atmosphere. Both fresh and marine waters are supersaturated by the volatile mercury forms, and at present it is difficult to say whether mechanisms of mercury excess formation in sea and fresh water differ. According to measurements of K. Gårdfeldt et al. [2001a] the emission from fresh water is by an order of magnitude higher than from seawater. However, since fresh water reservoirs have incommensurably smaller surface on the global scale we can omit their contribution to the global emission.

There are two hypotheses relative to the role of biota in mercury emissions from the water surface. For example, J. Kim and W. Fitzgerald [1986] indicate a direct connection between mercury emission intensity and biological productivity in water. On the other hand, A. Amiot [1995] found that the removal of particles, bacteria and colloids from lake water samples does not influence the concentration of dissolved elemental mercury. The more so, sample sterilization slightly increases the concentration of dissolved Hg^0.

One of the first measurements of mercury emissions from seawater was made by V. Fursov [1983]. His data evidence that the mean mercury flux to air from the surface of the Aral Sea is 1.6 ± 0.3 ng/m^2/h. Unfortunately, this paper does not answer the question whether observations were made round the clock and what was the season. For the first time J. Kim and W. Fitzgerald [1986] assessed the role of the ocean on the global scale. They measured mercury flux to the atmosphere in the east of the equatorial Pacific in the zone of elevated biological productivity. It was found that the highest mercury concentrations in water are characteristic of cold, enriched by nutrients zones in equatorial upwelling. In the North Atlantic R. Mason et al. [1998] estimated mean emission value equal to 11 μg/m^2/y. On the average over the World Ocean the emission intensity is 6.5 μg/m^2/y [*Lindqvist et al.*, 1991]. T. Bergan and H. Rodhe [2001] accept in their model that emissions from the sea surface smoothly change from the equator to the poles from about 9 to 0 μg/m^2/y.

If the emission intensity of the sea surface is proportional to area of "air-water" contact then the availability of dependence on wind speed (on sea roughness) becomes natural. W. Baeyens et al. [1991] found that the emission intensity varies from 0.05 to 0.74 ng/m^2/h depending on the wind speed. When on wave crests appear "white horses" the intensity can increase up to 20 ng/m^2/h. The authors suggest an empirical formula for the dependence of mercury flux from the ocean on the wind speed within the range from 0 to 30 m/s:

$$F_{Hg} = 0.43 + V^{1.13} + (V/10)^{4.25},$$

where mercury flux F_{Hg} is in μg/m^2/y; wind velocity V is in m/s.

K. Gårdfeldt et al. [2001a] found that seawater emission in the region of the western coast of Sweden is on the average 0.61 ng/m^2/h at the range from –2.72 to +8.84 ng/m^2/h. Thus in their experiments the water surface was mercury sink time to time though on the whole the flux was directed from water to air. The flux increased with temperature increase. It was explained by solubility decline with temperature growth and correspondingly the supersaturating increase.

For the central part of the Baltic Sea mean diurnal flux in summer (average temperature 17.3°C) was about 1 ng/m^2/h and in winter (average temperature 3.3°C) decreases as much as 2 times [*Wängberg et al.*, 1999]. The authors did not find a pronounced diurnal cycle and came to the conclusion that the flux was a function of water temperature and wind speed. Mean annual emission intensity for the Baltic Sea as a whole was estimated equal to 7 μg/m^2/y.

In addition to elemental mercury seawater is obviously supersaturated by dimethylated mercury. There is small number of DMM flux measurements. This complicates the

determination of integral values. R. Pongatz and K. G. Heumann [1999] measured DMM in different regions of the World Ocean at different depths. They found that the depth profile of DMM concentrations actually coincides with the profile of chlorophyll-a. According to their assessment DMM flux to the atmosphere from the basin of the Antarctic Ocean (between 51 and 71 latitudes) amounts to 210 t/y and from the Arctic Ocean – 240 t/y. Even neglecting the contribution of the other oceans this value indicates the significance of DMM emission input to the global atmospheric mercury cycle.

Background soils

Mercury content in soils outside the geochemical mercury belts varies several times all over the world. For cultivated soils A. Vinogradov [1957] gives the range from 0.03 to 0.07 ppm. V. Fursov [1983] investigated Eurasian soils in detail and found a wider range (0.03-0.09 ppm). Mercury content in the US soils is even more variable – from 0.008 to 0.4 ppm [*US EPA*, 1997]. Most likely the upper limit belong to soils of a geochemical mercury belt. For the US clean soils S. Wilson [1968] estimates the variation range from 0.02 to 0.04 ppm.

The capacity of the soil reservoir relative to mercury is at least by three orders of magnitude higher than that of the atmosphere (see Chapter 5). In soil mercury is chemically toughly bound [*Biester and Nehrke*, 1997]. For the most part it is in the oxidized form, often as humic complexes. To destruct these complexes and to remove mercury it is necessary to heat soil samples to 220-320°C. Mercury lifetime in soil relative to its volatilization is from hundreds to thousands years [*Trakhtenberg and Korshun*, 1990; *Ebighaus et al.*, 1999a] therefore in comparison with the reservoir capacity the annual emission amount is very low.

The interpretation of data on mercury emission from soil is impeded by the fact that for the most part of a year soils are covered by vegetation. It is supposed that soils emit mercury and vegetation above soil can partly uptake it via the gas exchange process [*Lindberg et al.*, 1992]. To assess the global natural emissions to air the net flux from given vegetation ecosystem is important. Unfortunately these data are very scares in the literature because it is difficult technically to make an experiment above the canopy of a forest with height 20 - 30 m.

At present two main methods of soil emission assessment are in use: the chamber method on the soil surface and method of measurement of the vertical concentration gradient in the atmosphere. Both methods are quite rough. The comparison of the methods [*Poissant et al.*, 1999] demonstrated that the correlation is comparatively low. Therefore it is impossible to obtain sufficiently accurate estimates of mercury fluxes from soil to air. The situation is aggravated by the fact that the flux direction can alternate depending on ambient conditions.

Table 3.1 gives emission intensity values measured by different methods. As it follows from the table the emission fluxes from soils vary within a wide range – up to two orders of magnitude. It is important that all the measurements were carried out in middle latitudes. There are no data on tropical forests, savannas and deserts. In addition the table shows that the emission intensity has clear diurnal and seasonal variations, i.e. depends on ambient conditions. The authors of the works presented in the table point out that as the ambient condition changes the flux not only can drop to zero but also changes its direction.

Investigations carried out round the clock and over a year show that soil temperature and insolation intensity are the most important external factors. Only a minor fraction of mercury in soil is represented by the elemental form, the bulk – by the oxidized form. It means that while emitting oxidized mercury should be reduced. This process takes place with energy consumption.

Table 3.1. Intensity of mercury emissions to the atmosphere from background soils (ng/m^2/h)

Region	Measurement methods and conditions	Flux	Reference
USSR Republics of Central Asia	(C) *	5.9	*Fursov*, 1983
USSR Republics of Central Asia	(G) *	2.6	*Fursov*, 1983
Canada, Ontario	Average for the Province for a year	0.18	*Innanen*, 1998
Canada, Nova Scotia	(C)	0.3 – 2.3	*Boudala et al.*, 2000
Canada, South Quebec	Grass, vegetation, noon	8.3	*Poissant and Casimir*, 1998
USA, Tennessee	Mean value	5	*Kim et al.*, 1995
USA, Tennessee	(C), shadowed soil under the forest canopy, daytime, summer	2-7	*Carpi and Lindberg*, 1998
USA, Tennessee	(C), open field, daytime, summer	12 – 45	*Carpi and Lindberg*, 1998
USA, forests of middle latitudes. Similar forests make up 25% of all the forests on the Earth	(G), grown up deciduous forest, mean value	37	*Lindberg et al.*, 1998
USA, forests of middle latitudes	(G), planting of spruce	7.8	*Lindberg et al.*, 1998
USA forest soils	Mean value	<0.2	*Munthe*, 1993
USA, Tennessee	Summer-autumn	7.5 ± 7	*Schroeder and Munthe*, 1998
USA deciduous forests	Mean value	100 ± 80	In: [*Schroeder and Munthe*, 1998]
USA deciduous forests	(G), mean annual value	10 – 50	In: [*Schroeder*, 1995]
USA deciduous forests	(G), mean for warm season	-2.2 – 7.5	In: [*Schroeder*, 1995]
The southern part of UK	Mean value	7	*Lee et al*., 1998
Sweden, boreal forests	Mean annual value	0.11	*Lindqvist et al*., 1991
Sweden, deciduous forests	(C), summer, daytime	1.4	In: [*Schroeder*, 1995]
Sweden, coniferous forests	(C), summer, daytime	0.3 – 0.6	In: [*Schroeder*, 1995]
Sweden, coniferous forests	(C), mean annual value	-1.1 – 1.0	In: [*Schroeder*, 1995]
Sweden, field	(C), summer, daytime	0.1 – 0.9	In: [*Schroeder*, 1995]
Sweden, soils	Mean flux, summer	1.1 ± 0.4	*Schroeder et al.*, 1989
South-western Sweden	Soil, T > 10°C	0.3	*Xiao et al*., 1991
USA, agricultural field	July, mean value	37	*Xu et al*., 1999
USA, deciduous forests	July, mean value	24	*Xu et al*., 1999
USA, mixed forests	July, mean value	18	*Xu et al*., 1999
Boreal forests	Mean value	1 – 10	*Schroeder and Munthe*, 1998
Natural land	Global value	2 – 7	*Bergan and Rodhe*, 2001

* (C) – chamber method; (G) – gradient method

Reduction mechanisms can be both biotic and abiotic. In the first case the intensity of biotic reduction should depend on temperature and it should drop to zero at soil freezing. In the second case the reduction process can take place on the surface as result of photolysis of mercury-containing complexes. Most likely both mechanisms are in operation simultaneously.

A number of works confirm obvious dependence of the emission intensity on soil temperature [*Bouldala et al*., 2000; *Carpi and Lindberg*, 1998; *Zhang et al.*, 2001; *Engle et al.*, 2001]. Thus, on evidence of *F. Bouldala et al.* [2000] soil temperature is the most important parameter defining the intensity of mercury emission. The flux from soil may be parameterized by an equation of Arrhenius type:

$$\ln(F_{Hg}) = -E_a/(R_{univ}T_s) + C\,, \qquad (3.1)$$

where F_{Hg} is the mercury emission flux; E_a is the activation energy; R_{univ} is the universal gas constant; and T_s is the surface temperature; and C is a constant. In all following dependencies the emission flux is in ng/m^2/h and T_s is in K.

For Canadian forest soils it was obtained that E_a = 14.6 kcal/mole, C = 25.7 (when soil temperature was measured at 0.5 cm depth) [*Bouldala et al*., 2000].

In the same geographical region A. Carpi and S. Lindberg [1998] studied the dependence of mercury emissions intensity from background soils to the air on external factors. Soil temperature and insolation were taken as the main factors. Like previous authors they found that the dependence of the flux on temperature might be described by the Arrhenius type equation (3.1). In measurements the activation energy varied from place to place from 18 to 24.9 kcal/mole. For practical use the authors expressed temperature dependence as simple regression equations for two forest sites and two cites in an open field (T_0 is equal to 273 K):

Undisturbed forest soil (under canopies):

$$\log F_{Hg} = 0.059(T_s - T_0) - 0.6$$
$$\log F_{Hg} = 0.028(T_s - T_0) + 0.2$$

Open field, cultivated soil:

$$\log F_{Hg} = 0.043(T_s - T_0) + 0.2$$
$$\log F_{Hg} = 0.057(T_s - T_0) - 1.7$$

Coefficients of these equations point to a high space variability of the emission, which depends not only on temperature. It should be noted that measurement sites were located at rather small distance from each other.

L. Poissant and A. Casimir [1998] also found that dependence of the emission on temperature obviously follows the Arrenius type equation (3.1). When temperature was measured at 5 cm depth the activation energy value was found as 20.5 kcal/mole. In this case the flux can be estimated using the simplified equation:

$$F_{Hg} = -1.0548 \cdot 10^4 / T_s + 36.161 .$$

For background soils of Michigan State of the USA the emission intensity is on the level of 2 ng/m^2/h at variations from 1.4 to 2.4 ng/m^2/h [*Zhang et al*., 2001]. Only in one very shadowed place at high moisture content it was found that the intensity of mercury absorption by soil is -0.3 ng/m^2/h corresponding to dry uptake rate about 0.005 cm/s. On the open field the flux was appreciably higher – 7.6±1.7 ng/m^2/h. According to these authors the emission intensity first of all depends on insolation and to less extent on temperature, although the correlation with temperature is high and clear linear dependence is observed:

$$F_{Hg} = 0.6382(T_s - T_0) - 9.3892 .$$

This regression equation was derived for the totality of forest and open-field sites.

The authors of the work [*Zhang et al*., 2001] consider mercury exchange in the system "air-soil" as the surface physical-chemical process based on adsorption. The linear relationship between $\ln F_{Hg}$ and 1/T is interpreted as evidence that the exchange process is a process of zero order. For background soils of Michigan the calculated activation energy value is 29.4 kcal/mole. It is noticeably higher than for other background soils.

For comparison values of the activation energy of mercury emission obtained by different researchers are summarized in Table 3.2.

Table 3.2. Activation energy of mercury natural emission from background soils (kcal/mole)

Location	E_a	Reference
Tennessee, USA	17.3 - 25.8	*Kim et al*., 1995
Tennessee, USA	18.0 - 24.9	*Carpi and Linberg*, 1998
Quebec, Canada	20.5	*Poissant and Casimit*, 1998
Michigan, USA	29.4	*Zhang et al*., 2001

H. Zhang et al. [2001] also found that soil temperature is directly connected with insolation. The regression equation for the totality of all forest and open sites looks as follows:

$$T_s = T_0 + 0.022 S_R + 14.9 .$$

Here and further the solar radiation flux S_R is in W/m^2.

Summer measurements of emissions from soils covered by grass in Canadian Province South Quebec made by L. Poissant and A. Casimir [1998] showed that diurnal variations of soil emissions coincide with variations of insolation. At night the flux was observed on the level of 1 ng/m^2/h. In the daytime the flux value lagged behind of solar radiation peak.

According to [*Carpi and Lindberg*, 1998] the sunlight makes greater impact than temperature. On exposure to soil the sunlight reduces oxidized mercury to elemental one. In one of experiments a linear dependence of mercury flux logarithm upon the solar radiation flux S_R (W/m^2) was obtained:

$$\log F_{Hg} = 0.0013 S_R + 0.3$$

S. Lindgerg et al. [1998] found that the intensity of mercury emissions by mature forests of middle latitudes is about 70 μg/m^2/y, by young planting – 30 μg/m^2/y and by forest soils – 2 μg/m^2/y. Their global assessment of mercury natural emission from land is presented in Table 3.3.

Table 3.3. Global natural emissions of mercury from land [*Lindberg et al*., 1998] (t/y)

Surface type	Area, km^2	Range of emission values
Forests		
Boreal forests	$1.37 \cdot 10^7$	10 - 100
Temperate forests	$1.04 \cdot 10^7$	300 - 700
Tropical forests	$1.76 \cdot 10^7$	540 - 1200
Soils		
Non-forested soils		500 - 1000
Forested soils (winter)		80 - 160
Total		**1400 - 3200**

Besides, the mercury flux from soil is highly correlated with the water vapor flux [*Poissant and Casimir*, 1998]:

$$F_{Hg} = 42.64 F_{H_2O} + 1.4965 .$$

In its turn it means that the higher air humidity R_H (%) the lower emission:

$$F_{Hg} = -0.0633 R_H + 7.4026$$

Wetting of soil by rain is another factor affecting the soil emission intensity [*Lindberg et al.,* 1999; *Benesch et al.*, 2001; *Carpi and Lindberg*, 1998; *Engle et al*., 2001]. The mechanism of the phenomenon is not clear so far. S. Lindberg et al. [1999] believe that three reasons are possible: (1) the substitution of elemental mercury atom by water molecule on the sorption surface; (2) rapid reduction of oxidized mercury in the aqueous phase; (3) displacement of soil air by water. Most likely the wetting effect is of a short-time character and it cannot affect long-term values of the emissions. For instance, in experiments of H. Zhang et al., [2001] watering of soil by water amount 11 mm caused a rapid growth of the flux from 3.0 to 5.6 ng/m^2/h (the increase by 87% during 15 minutes). Water molecules possess higher capability to absorption by the surface of soil particles than elemental mercury atoms.

Mercury enriched soils

Soils of the mercury belts contain essentially more mercury than background soils. Besides in these cases the variability of values is also considerably higher. For mercury anomaly in the zone of a mercury belt *I. Trakhtenberg and* M. Korshun [1990] give the range of *Hg* content in soils from 0.3 to 12 ppm. Mercury content is even higher in desert soils of Nevada – up to 25 ppm [*Engle et al*., 2001]. O. Lindqvist et al. [1991] believe that mean annual emission value within the mercury geochemical belts is 10 μg/m^2/y.

It is natural that the mercury flux to air should be higher the higher is its content in soil. M. Gustin et al. [1999b] investigated this dependence both in laboratory and under field conditions. The experiment results can be approximated by the linear regression equation:

$$\log F_{Hg} = 1.10 \cdot \log C_{Hg} + 0.52 \text{ (in laboratory);}$$

$$\log F_{Hg} = 1.26 \cdot \log C_{Hg} + 0.25 \text{ (in field),}$$

where mercury concentration in soil C_{Hg} is in ppm. Within the range of 1 - 1000 ppm both

equations give close results (at least by the order of magnitude).

American and European specialists carried out a series of investigations of soil mercury emissions within the geochemical mercury belt in Nevada, the USA [*Gustin et al.*, 1999a]. The maximum mercury flux reached 600 ng/m^2/h. In work [*Engle et al.*, 2001] it was found that mean diurnal emission is about 17 ng/m^2/h. At night when temperature dropped down to -4°C the emission actually ceased and it reached its maximum at noon (temperature +20°C). The authors approximated the diurnal emission variation by Gauss curve with maximum at noon. Under laboratory conditions it was also observed that at constant temperature the enhancement of illumination leads to the sharp increase of mercury release.

S. Lindberg et al. [1995] investigated mercury emission (being more precise re-emission) from earlier polluted soils. This kind of soils rather relates to anthropogenically enriched ones. They obtained the following linear dependence of the emission flux from contaminated soils upon the soil temperature within the range 7 - 29°C:

$$\log F_{Hg} = 0.065 T_s - 17.1$$

One can approximately assess the activation energy for this flux within the given temperature interval as 25.2 kcal/mole. This value agrees with the activation energies of background soils (see Table 3.1)

Other lithospheric sources

Appreciable mercury emissions on relatively local scales result from volcanic activity. On fumarole fields of Kilauea volcano F. Davies and G. Notcutt [1996] found extremely high concentrations of TGM – from 2.7 to 40.6 μg/m^3. According to the estimate of *S. Siegel* and B. Siegel [1984] mercury flux only from this volcano is 260 t/y. From the evidence of J. Nriagu and C. Decker [2001] during 1980 – 2000 European volcanoes released 40 tonnes of mercury, volcanoes of both Americas – 2160 tonnes and in the whole World – 7182 tonnes. Thus mean annual value for all the volcanoes is 360 t/y though it is clear that this flux is highly sporadic. W. Fitzgerald [1996] obtained appreciably lower values (from 20 to 90 t/y). He believes that the volcanic contribution to the global mercury cycle does not exceed 3%.

Forest fires and biomass burning can also make a certain contribution to natural emissions. In reality these sources can hardly be purely natural sources. J. Nriagu [1989] estimated the flux only from wild forest fires as 20 t/y. P. Artaxo et al. [2000] found very high mercury concentrations in air during the season of biomass burning in Brazil (up to 1 μg/m^3). From their viewpoint mercury can enter the atmosphere both from the burning biomass itself and from soil being heated.

Global natural emission estimates

It is interesting to compare estimates of global natural emission intensities obtained by different authors and used in global models. For the convenience the data are collected in Table 3.4 separately for land and sea surface.

Sufficiently simple estimates evidence that very high values of emissions contradict measurement data. For instance, the upper limit of mercury atmospheric content is a reliable value – about 6000 tonnes. If the flux is equal, for example, to $1.9 \cdot 10^5$ t/y, then mercury lifetime in the atmosphere should be about 10 days. In its turn it means that an essential vertical gradient of concentration should be observed. Since in reality any pronounced gradient is not detected, natural emission of about 10^4 t/y and higher seems unreasonably overestimated.

Table 3.4. Natural mercury emissions to the atmosphere

Emission value, t/y			Reference	Note
Land	Ocean	Total		
		$1.9 \cdot 10^5$	*Jaworowski et al*., 1981 (quoted in *Geological Survey of Canada*, 1995)	
	2900		*Kim and Fitzgerald*, 1986	±1800 t/y
730	1770	2500	*Nriagu*, 1989	
		3000	*Lindqvist et al*., 1991	From 2000 to 9000 t/y
		$2.9 \cdot 10^4$	*Geological Survey of Canada*, 1995	3500 t/y for Canada only
1000	2000	3000	*Fitzgerald and Mason*, 1996	1400 t/y of re-emission from the ocean
1400-3200			*Lindberg et al*., 1998	
1000			*Carpi and Lindberg*, 1998	
700			*Ebinghaus et al*., 1999a	500 t/y in mercury belts
2000	2000	4000	*Seigneur et al*., 2001	1500 t/y of re-emission from land
1320	1100	2420	*Bergan and Rodhe*, 2001	Without re-emission
1000	800	1800	*Lamborg et al.,* 2002	400 t/y of re-emission from the ocean

3.2. Emission data

Anthropogenic sources

Anthropogenic constituent of mercury emission to the atmosphere dominates over industrial and urbanized regions of the world. To evaluate the anthropogenic input of mercury in the Northern Hemisphere we utilize the latest available global emission inventory for 1995 [*Pacyna and Pacyna*, 2002]. The digital emission data were provided by the Arctic Monitoring and Assessment Programme (AMAP) in the framework of UNEP/GEF project. The original dataset has global coverage with resolution 1°×1° and mercury chemical speciation into three forms: elemental Hg^0, gaseous oxidized Hg^{2+}, and particulate Hg_{part}. To adapt the emission to the model input it has been redistributed to the model grid (2.5°×2.5°) assuming uniform distribution over a grid cell.

Spatial distribution of anthropogenic mercury emission density in the Northern Hemisphere is presented in Figure 3.1 (for each species individually). As seen from the figures the most significant emission sources are in Eastern Asia, Europe and the Eastern part of North America. Some emissions are also in Hindustan and Arabian Peninsula. The total anthropogenic mercury emission from the Northern Hemisphere is estimated as 1885 tonnes per year.

In order to assess the inter-continental mercury transport the whole hemispheric emission field was divided into several continents and regions (see Fig. 3.2): Europe, Africa, North America, South America, and Asia. Moreover, the last one was subdivided into three regions: Western, Central, and Southern Asia; Eastern and South-eastern Asia; and Asian Russia.

Relative contributions of each continent or region to the total mercury emission in the Northern Hemisphere are presented in Figure 3.3. According to the diagram more than half (50%) of the total mercury is emitted from Eastern and Southeastern Asia. Considerable emissions are also in Europe (18%), Western, Central, and Southern Asia (15%), and North America (10%). The contribution of other regions does not exceed 8%.

Annual emissions of each mercury species from different continents in the Northern hemisphere are summarized in Table 3.5. It should be noted that average speciation (over continents of the Northern Hemisphere) is approximately 58% of Hg^0, 33% of Hg^{2+}, and 9% of Hg_{part}.

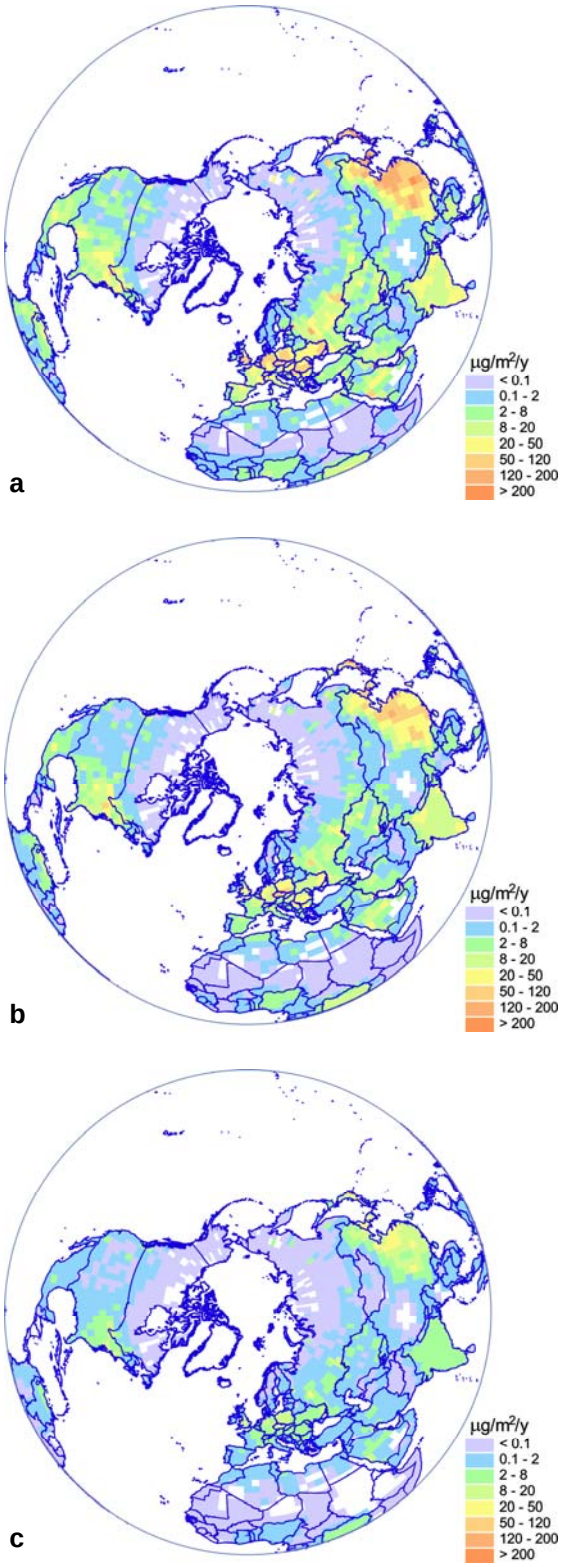

Figure 3.1. *Spatial distribution of mercury anthropogenic emissions density in the Northern Hemisphere in 1995: (a) – Hg^0; (b) – Hg^{2+}; (c) - Hg_{part}*

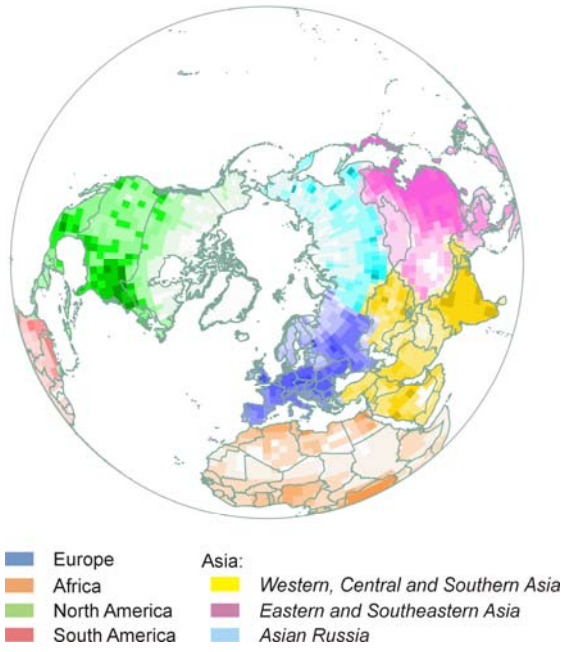

Figure 3.2. *Division of the total emission field into the continents and regions (scale ranges are the same as in Figure 3.1)*

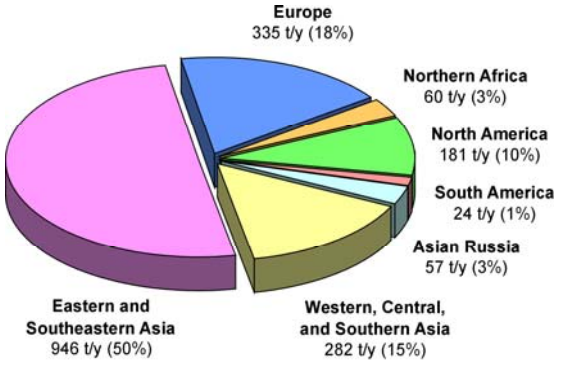

Figure 3.3. *Relative contribution of different continents and regions to the total anthropogenic emission of mercury in the Northern Hemisphere*

Table 3.5. Annual anthropogenic emission of mercury species in the Northern Hemisphere, t/y

Region	Hg^0	Hg^{2+}	Hg_{part}
Europe	207.0	100.3	27.3
Africa	33.0	21.7	5.4
North America	98.8	63.8	18.3
South America	14.3	8.0	2.0
Western, Central, and Southern Asia	152.9	103.0	25.8
Eastern and Southeastern Asia	549.1	315.1	81.6
Asian Russia	38.6	14.8	4.1

Natural sources

Mercury emission from natural sources makes up a significant part of total mercury input to the atmosphere (up to 70%). It is clear that the correct assessment of mercury exchange between the atmosphere and other environmental compartments (soil, seawater etc.) could be obtained only from a comprehensive multi-compartment model. However, the developed atmospheric transport module requires detailed enough natural emission data to provide adequate air concentration levels and deposition fields. In particular, it relates to the spatial distribution of mercury emission intensity over the Earth surface. Reasonable estimates of natural emission based on literature data (Section 3.1) could be an acceptable compromise in this situation.

Unfortunately, available estimates of the global natural emission of mercury are very uncertain. The most reasonable of them vary from 700 to 3200 t/y for the continents and from 600 to 2900 t/y for the World Ocean (Table 3.4). In the current assessment we decided to base on the estimates suggested by C. Seigneur et al. [2001] – 2000 t/y from land and 2000 t/y from the ocean. As it was mentioned in Section 3.1 we distinguish five types of the Earth surface: (1) glaciers, (2) seawater, (3) background soils, (4) soil of the geochemical mercury belts, and (5) soil of mercury deposit areas. Mercury emission fluxes differ for different surface types.

Glaciers of the Northern Hemisphere include Greenland, permanent ice of the Arctic and high-mountain glaciers. It is presumed that there is no mercury emission from this type of the surface.

To distribute mercury emission over the ocean we accepte the idea suggested by J. Kim and W. Fitzgerald [1986] that mercury emission intensity is proportional to biological productivity in seawater. For this purpose we utilize monthly mean data on the ocean primary production of carbon described in [*Behrenfeld and Falkowski*, 1997] and available through the Internet (http://marine.rutgers.edu/opp/). According to the data global primary productivity is equal to $4.6 \cdot 10^{13}$ kg C/y.

Spatial distribution of annual primary production in the ocean of the Northern Hemisphere (including internal seas) adapted to the model grid is presented in Figure 3.4. As seen from the figure the highest values of primary productivity relate to coastal parts of the ocean in the middle and low latitudes and to internal seas (Baltic, Black, Caspian). Another feature of the distribution is elevated values of the production in the Atlantic corresponding to Gulf Stream and absence of production near the pole.

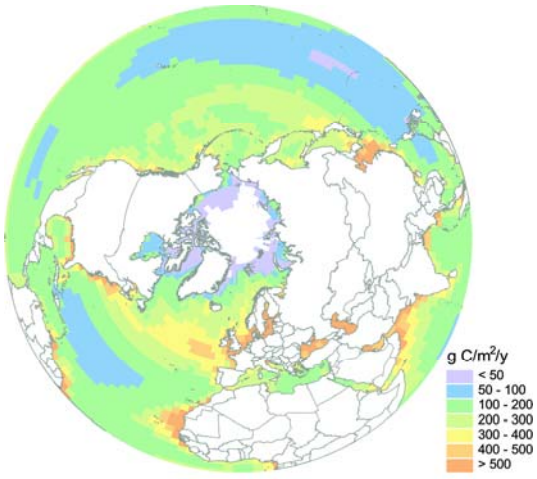

Figure 3.4. *Spatial distribution of annual primary production of carbon in the ocean of the Northern Hemisphere [Behrenfeld and Falkowski, 1997]*

Figure 3.5. *Generalized map of geochemical mercuriferous belts (magenta color) and productive deposit areas (red color) in the Northern Hemisphere [Jonasson and Boyle, 1971; Gustin et al., 1999a]*

Dividing global mercury emission from the ocean adopted above ($2 \cdot 10^6$ kg/y) by the global primary production one can estimate the proportionality coefficient as $4.3 \cdot 10^{-8}$ (approximately 4 times lower than the value $1.6 \cdot 10^{-7}$ from [*Kim and Fitzgerald*, 1986]). Since about 60% of the global ocean primary production falls on the Northern Hemisphere we assess the total ocean mercury emission in the Northern Hemisphere as 1200 t/y.

The entire continental area in the Northern Hemisphere constitutes approximately 75% of the global land area (excluding Greenland and the Antarctic). Thus, the total natural emission of mercury from land in the Northern Hemisphere can be roughly assessed as 1500 t/y. Mercury flux from the land significantly depends on soil mercury content. From this point of view we divide land surface into three categories according to the adopted soil classification: background soils, soils of mercury belts, and soils of mercury deposits. Location of geochemical mercuriferous belts and productive mercury deposits areas are schematically shown in Figure 3.5. These data were generalized from [*Jonasson and Boyle*, 1971; *Gustin et al.*, 1999a] and adapted to the model grid. In the current assessment we do not take into account any influence of vegetation on the emission process.

As it was mentioned in Section 3.1 temperature dependence on mercury emission flux can be described by an Arrhenius type equation. Besides, empirically derived activation energies of the process have close values both for background (17.3-29.4 kcal/mole) and for enriched soils (25.2 kcal/mole). To parameterize the temperature dependence we choose value 20 kcal/mole for all soil types. On the contrary, we consider pre-exponential factor depending on the soil type: the factor for background soil is five times lower than for soils of the mercury belts, and ten times lower than for the deposits areas. Besides, the emission flux is assumed to be zero for negative values of the soil temperature in the centigrade scale. Fitting total land emission in the Northern Hemisphere to the adopted value we obtain the following temperature dependence of the mercury flux from soil:

$$F_{Hg} = \begin{cases} A_s \exp(-10^4 / T_s), & T_s > T_0 \\ 0, & T_s \le T_0 \end{cases} \qquad (3.2)$$

Here mercury flux F_{Hg} is in ng/m^2/h; A_s is equal to $6.4 \cdot 10^{14}$ for background soils, $3.2 \cdot 10^{15}$ for the mercury belts, and $6.4 \cdot 10^{15}$ for deposit areas; surface temperature T_s is in K and T_0 = 273 K. Currently we do not consider dependence of the mercury emission flux on insolation. It is assumed that mercury is emitted to the atmosphere in the elemental form both from land and from the ocean.

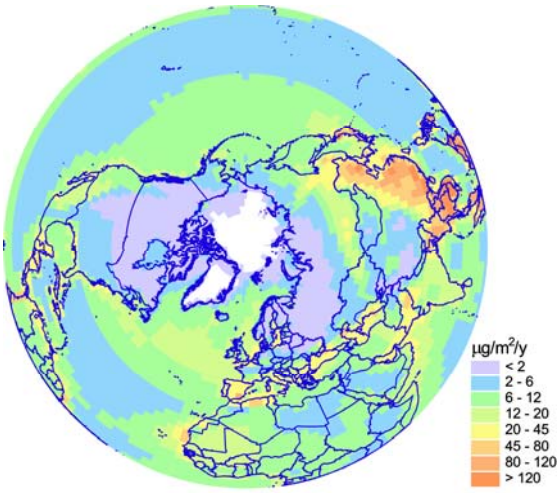

Figure 3.6. *Spatial distribution of mean annual natural emission density of mercury in the Northern Hemisphere*

Resulting spatial distribution of mean annual mercury emission from natural sources is shown in Figure 3.6. As one can see from the figure the highest mercury emissions from land corresponding to mercuriferous belts and deposit areas (compare with Fig. 3.5) varies from 15 µg/m^2/y at the middle latitudes to more than 120 µg/m^2/y at the low latitudes. One should note that these values could be higher in warm seasons. Mercury fluxes at the high latitudes are considerably lower even for the mercury belts due to low soil temperature.

Mean annual emission flux of mercury from background soils amounts to several μg/m^2/y.

Emission flux from seawater varies from 2 μg/m^2/y in the Middle Pacific to more than 20 μg/m^2/y in internal seas and coastal waters at low latitudes. In the Arctic ocean emission flux drops below 1 μg/m^2/y. There is no mercury emission from Greenland and from seawater near the pole because of permanent glaciers.

Figures 3.7.a and 3.7.b illustrate seasonal variation of natural mercury emission. As one can see variation of land emission flux is considerably higher (up to an order of magnitude) than that of seawater due to greater amplitude of land surface temperature alteration. Moreover, a significant part of the surface has no mercury emission in wintertime due to negative surface temperatures.

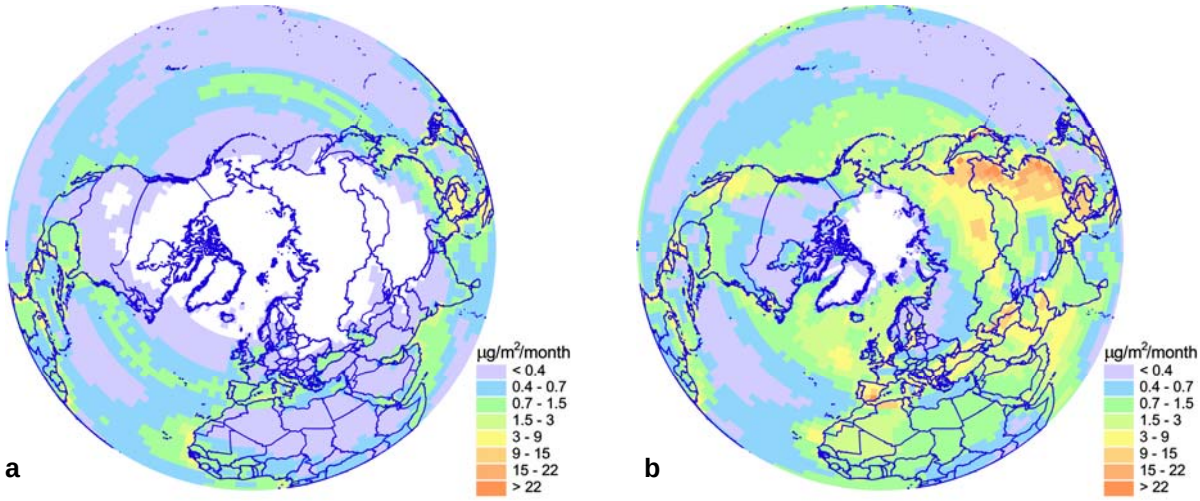

Figure 3.7. *Spatial distribution of monthly mean natural emission density of mercury in the Northern Hemisphere in January (a) and in July (b)*

3.3. Meteorological and geophysical input

Meteorological data necessary for the model operation is supplied by the low atmosphere diagnostics system (SDA) developed in co-operation with Hydro-meteorological Centre of Russia. The system provides 6-hour weather prediction data along with estimates of the atmospheric boundary layer (ABL) parameters and covers the Northern Hemisphere with the model spatial resolution. SDA system consists of a hydrodynamic prognostic model, ABL post-processor, and data storage system. As the input information it utilizes objective analysis data performed by Hydro-meteorological Centre of Russia. Besides, it employs weekly mean data on ocean surface temperature and sea ice distribution for the evaluation of the boundary conditions. Meteorological parameters supplied by the SDA system are listed in Table 3.6.

Some of the model processes (e.g. dry uptake of elemental mercury) require information on land cover of the Earth surface. For this purpose we use 25-category land cover dataset from NCAR Mesoscale Modeling System (MM5) [*Guo and Chen*, 1994]. The data are available through the Internet (http://www.mmm.ucar.edu/mm5/). Since the model formulation does not require highly detailed specification, the original 25-category data were reduced to five general categories (urban, forests, grassland, bare land, and glaciers) and redistributed over the model grid.

Table 3.6. Meteorological parameters supplied by the low atmosphere diagnostics system (SDA)

Parameter	Notation	Type
Wind velocity	V_λ, V_φ	bulk
Air temperature	T_a	bulk
Surface pressure	p_s	surface
Precipitation rate	I_p	bulk
Water vapour mixing ratio	q_w	bulk
Large-scale cloudiness	C_L	bulk
Convective cloudiness	C_C	bulk
Surface temperature	T_s	surface
Vertical eddy diffusion coefficient	K_z	bulk
Roughness of the underlying surface	z_0	surface
Friction velocity	u_*	surface
Monin-Obukhov length	L_{MO}	surface
Soil humidity	M_s	surface
Snow cover height	h_s	surface

Figure 3.8 demonstrates spatial distribution of forests in the Northern Hemisphere according to resulting data. In this interpretation forests include deciduous and coniferous forests of the high and middle latitudes, evergreen tropical forests, wooden wetland, and mixed forests.

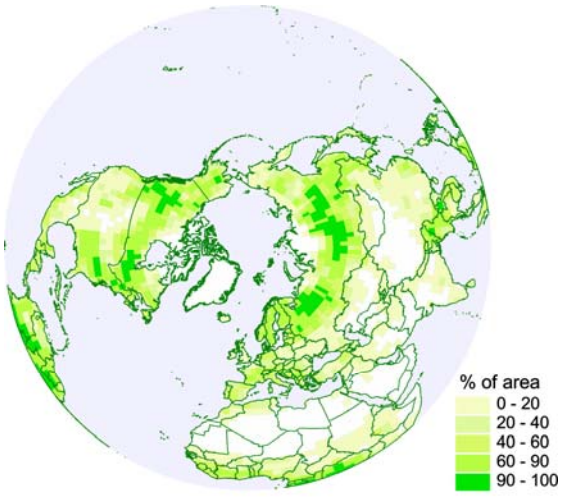

Figure 3.8. *Fraction of the area covered by forests in the Northern Hemisphere*

3.4. Reactants

As it was mentioned in Chapter 1 mercury species take part in chemical reactions of oxidation and reduction both in the gaseous and aqueous phase. To describe chemical transformations one has to know spatial and temporal distribution of the reactants concentration (such as ozone and sulfur dioxide) in the atmosphere.

Global monthly mean data on ozone and SO_2 concentration in the atmosphere were kindly presented by Dr. Malcolm Ko [*Wang et al.*, 1998; *Chin M. et al.*, 1996]. The original data were interpolated to the model grid for the Northern Hemisphere. The resulting data are briefly described below.

Spatial distribution of ozone concentration in the lowest model layer is demonstrated in Figure 3.9. As seen from the figure elevated values of ozone concentration occur in the middle latitudes around the Northern Hemisphere. The highest ozone concentrations correspond to elevated regions of the Earth surface (within the model grid resolution): the Himalayas, the Rocky Mountains, Greenland etc. Figure 3.10 shows vertical profiles of ozone concentration in the atmosphere. Each line of the plot demonstrates mean annual ozone concentration averaged along a latitude as a function of altitude above the sea level. Blue, green, and red lines correspond to the North Pole, 45 °N, and the Equator respectively. According to the figure, ozone concentration increases with altitude in all cases. Besides, the increment is greater for high latitudes than for low ones. Thus, one can expect more intensive mercury oxidation by ozone at the upper troposphere.

Figure 3.11 shows spatial distribution of sulfur dioxide concentration in the surface air of the Northern Hemisphere. The highest concentrations of SO_2 correspond to the most industrially loaded regions such as Europe, the eastern part of North America, Far East and etc. As it is shown in Figure 3.12 SO_2

concentration decreases with altitude practically at all latitudes (except slight growth at high altitudes over the equator). The elevated value of SO_2 concentration in the ground air of the middle latitudes (green line) reflects location of main sulfur sources.

Besides, for the aqueous-phase chemistry cloud water was characterized by *pH* equal to 4.5 and water content of chloride ion $[Cl^-]$ as much as $7 \cdot 10^{-5}$ mole/L [*Acker et al.*, 1998].

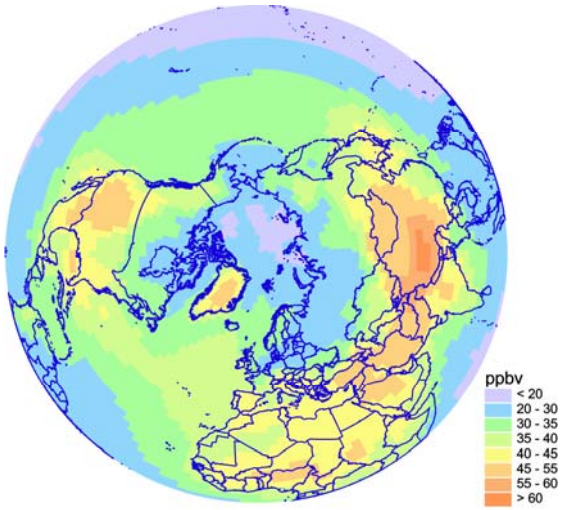

Figure 3.9. *Spatial distribution of ozone concentration in the ground air of the Northern Hemisphere*

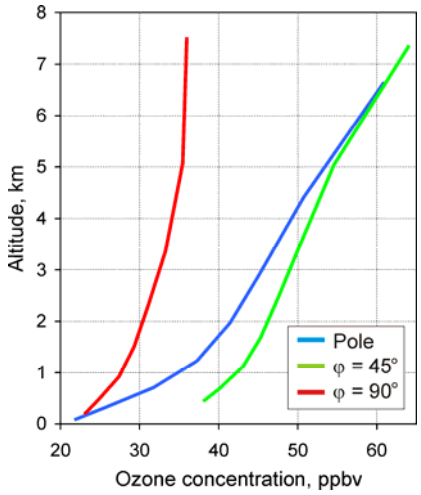

Figure 3.10. *Vertical profiles of ozone concentration averaged along different latitudes of the Northern Hemisphere*

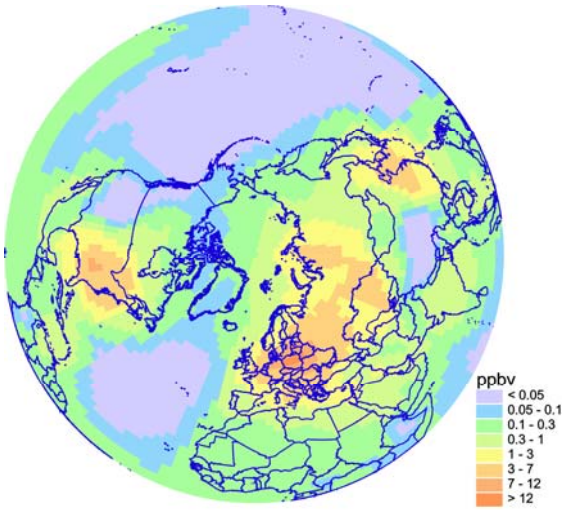

Figure 3.11. *Spatial distribution of SO_2 concentration in the ground air of the Northern Hemisphere*

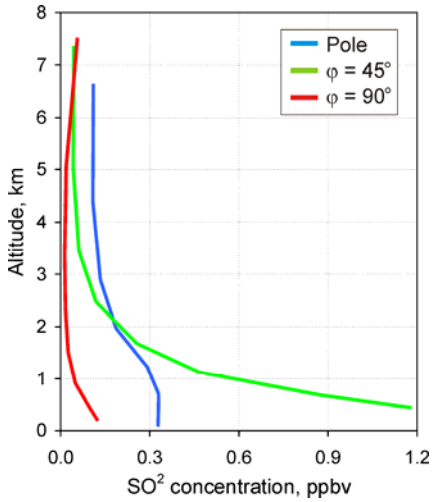

Figure 3.12. *Vertical profiles of SO_2 concentration averaged along different latitudes of the Northern Hemisphere*

Chapter 4

ATMOSPHERIC TRANSPORT OF MERCURY IN THE NORTHERN HEMISPERE (preliminary results for 1996)

Pilot calculations of atmospheric mercury transport in the Northern Hemisphere have been performed for 1996 by means of the developed model. The calculation run for the period of one year have been carried out using emission data described in Section 3.2 and the appropriate initial and boundary conditions (Section 2.2). Preliminary results of the computations are presented and discussed below.

4.1. Concentrations in the ambient air and deposition fluxes

Mercury concentration in the ambient air and its deposition fluxes to the ground is the primary information characterizing negative impact of the pollutant on the human health and the environment. On the other hand, the deposition flux is an important component of the mercury exchange between the atmosphere and other environmental compartments.

Figure 4.1 shows calculated fields of mean annual concentration of mercury forms in the surface air of the Northern Hemisphere. Spatial distribution of elemental gaseous mercury (Hg^0) is presented in Figure 4.1.a. According to the modeling results elemental mercury is more or less uniformly distributed over the Northern Hemisphere. This fact agrees with numerous measurements carried out for last several decades [e.g. see *Ebinghaus et al.*, 1999a]. As seen in the figure Hg^0 concentration in the Northern Hemisphere varies from about 1 ng/m^3 (under local conditions) in elevated remote regions (Greenland, the Himalayas) to several ng/m^3 in industrialized areas. One can clearly distinguish two the most contaminated regions: Far East with concentrations up to 5 ng/m^3 and Europe (more than 2 ng/m^3). High values of gaseous mercury concentration in these regions can be explained by significant mercury emissions both anthropogenic and natural (see Figures 3.1.a and 3.6). There are pronounced gradients of Hg^0 concentration in the Atlantic and Pacific Oceans. In both cases concentration decreases from high latitudes (2 ng/m^3 and 1.8 ng/m^3 in the Atlantic and Pacific respectively) to the equator (about 1.5 ng/m^3). It agrees with gradients of total gaseous mercury (TGM) measured over the oceans [*Slemr*, 1996; *Lamborg et al*., 2002]. Elevated concentrations in the Northern Pacific can be explained mostly by airborne transport from East-Asian sources. In the Northeastern Atlantic the main contribution to elemental mercury content in the ambient air is made by European sources, however some influence of American sources and local evasion of mercury from the sea surface are also possible. Low values of the concentration in the equatorial parts of the Atlantic and Indian Oceans can be possibly explained by the adopted boundary conditions (Section 2.2).

Figure 4.1.b demonstrates spatial distribution of particulate mercury in the ambient air. Besides in Southeast Asia and Europe, comparatively high concentrations of particulate mercury occur in Hindustan and the Arabian Peninsula being consistent with the emission data (Fig. 3.1.b).

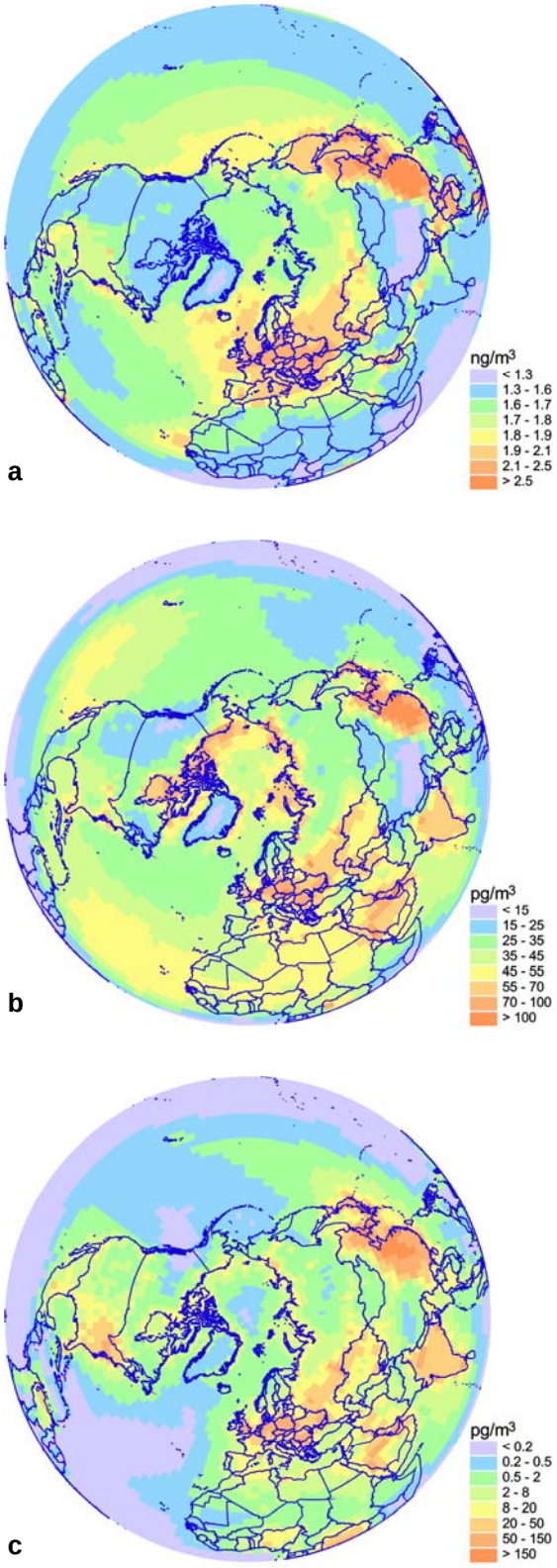

Figure 4.1. *Spatial distribution of mean annual concentration of mercury forms in the surface air of the Northern Hemisphere: (a) – elemental (Hg^0); (b) – particulate (Hg_{part}); (c) – gaseous oxidized (Hg^{2+})*

Another feature of the concentration pattern is elevated particulate mercury content in the coastal areas of the Arctic Ocean. This is a direct consequence of the mercury depletion phenomenon (MDP). According to the model parameterization of MDP (Section 2.3) during springtime elemental mercury in the lower troposphere is partially transformed to particulate and gaseous oxidized forms in the vicinity of the Arctic coast. Results of the phenomenon are clearly seen in the figure.

Spatial distribution of gaseous oxidized mercury concentration is shown in Figure 4.1.c. Since in the current version of the chemical scheme this mercury form does not take part in chemical transformations its distribution pattern has a shape similar to that of a tracer with high removal characteristics: high concentrations in the emission regions and significantly lower in remote ones. Influence of MDP in this case seems considerably weaker because of higher deposition rates in comparison with the particulate form.

Figure 4.2 presents distribution field of annual deposition flux of total mercury in the Northern Hemisphere.

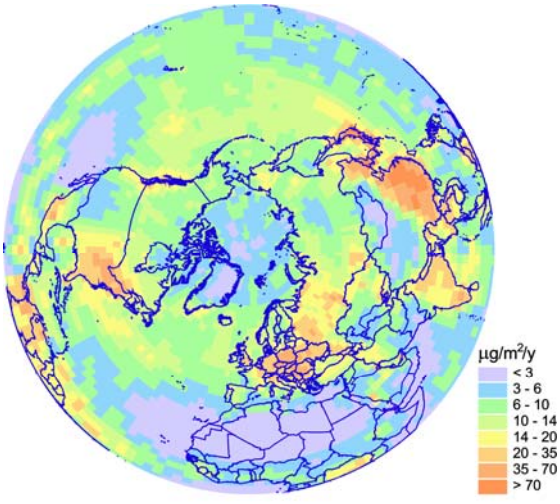

Figure 4.2. *Annual deposition density of total mercury in the Northern Hemisphere*

As seen from the figure the most considerable fluxes take place in the middle latitudes. The highest depositions are in the main emission regions: Southeast Asia, Europe, and the eastern part of North America. As for the rest, the deposition pattern, to some extent, corresponds to the annual precipitation amount field, since wet deposition plays a dominating role in the mercury removal process. Influence of MDP on the deposition fluxes within the Arctic region is not clearly seen in the figure because of the coarse color range scale. More detailed consideration of the MDP effect is presented in Section 4.4.

4.2. Verification of the modelling results

To verify the modelling results the calculated mercury concentrations in the air and deposition fluxes were compared with available monitoring data and results obtained by the regional MSCE-HM model.

Comparison with measurements

Currently, only limited number of measurement data on the annual basis is available for 1996 from the EMEP monitoring network [*Berg and Hjellbrekke*, 1998]. The monitoring stations involved in the comparison are listed in Table 4.1.

Table 4.1. Monitoring stations of the EMEP network involved in the model verification

Station	Code	Latitude	Longitude
Westerland	DE1	54°55'N	8°18'E
Zingst	DE9	54°26'N	12°44'E
Pallas	FI96	67°58'N	24°7'E
Mace Head	IE31	53°19'N	9°54'W
Spitsbergen	NO42	78°54'N	11°53'E
Lista	NO99	58°06'N	6°34'E
Rörvik	SE2	57°25'N	11°56'E
Bredkälen	SE5	63°51'N	15°20'E
Vavihill	SE11	56°01'N	13°09'E
Aspvreten	SE12	58°48'N	17°23'E

Comparison of the observed and modeled annual wet deposition fluxes is presented in Figure 4.3. As seen from the figure the modelled values satisfactorily conform to the measured ones. For some stations (SE2, SE5, SE11, SE12) agreement is perfect, for some other is worse. However, for the majority of the stations the discrepancy does not exceed a factor of two.

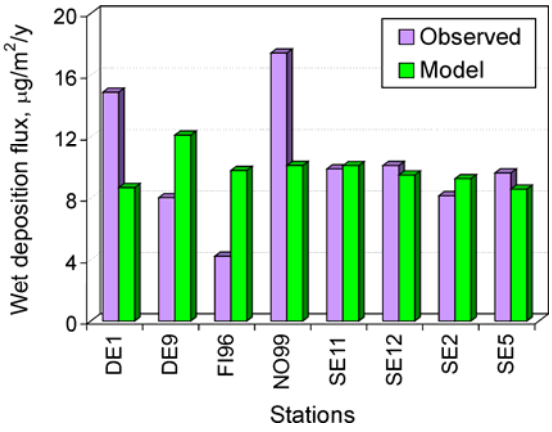

Figure 4.3. *Observed and modeled annual wet deposition fluxes of mercury*

Figure 4.4 shows observed and modeled mean annual mercury concentrations in the ambient air. Only four annual measurements are available for 1996. In all the cases modelling results slightly overestimate measured values, but the discrepancy does not exceed 30%.

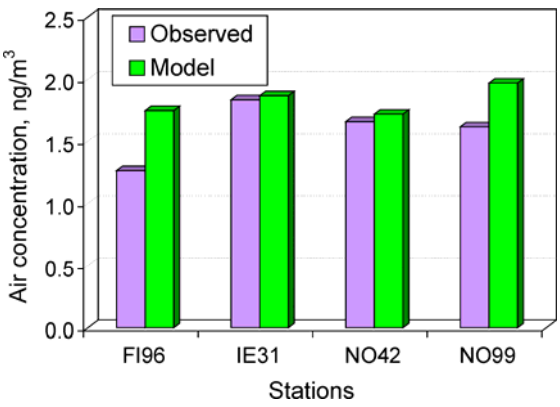

Figure 4.4. *Observed and modeled mean annual mercury concentrations in the ambient air*

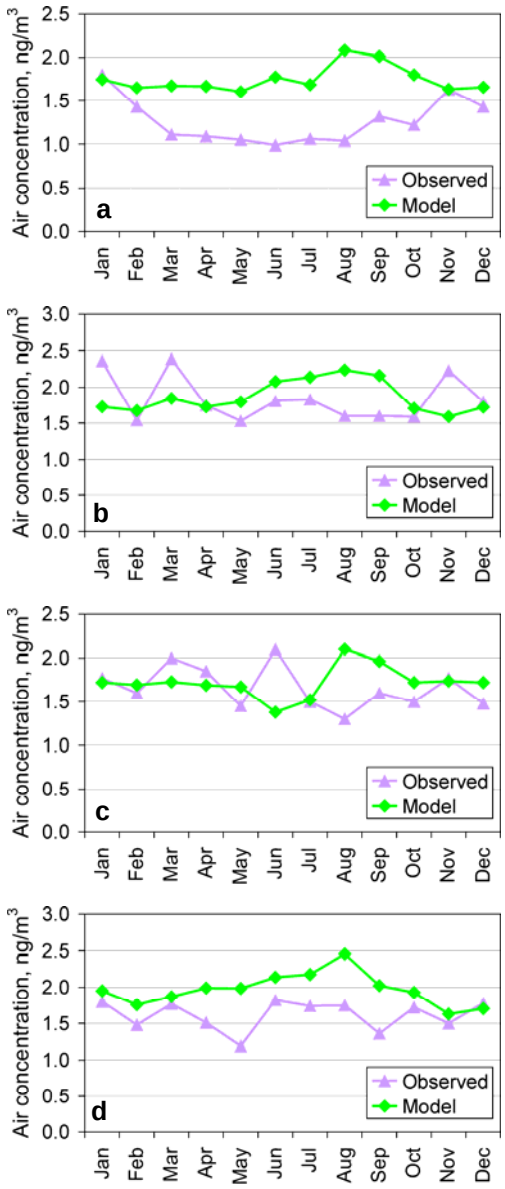

Figure 4.5. *Monthly mean mercury concentrations in the ambient air in 1996: (a) – FI96; (b) – IE31; (c) – NO42; (d) – NO99*

For more detail comparison we also consider seasonal variation of the calculated values. Figure 4.5 shows observed and modelled monthly mean mercury concentrations in the ambient air for 4 monitoring stations presented in Figure 4.4 (Pallas, Mace Head, Spitsbergen, and Lista). As one can see from the figures in spite of promising agreement of the annual mean values, their monthly mean variations considerably differ. In some cases the modelling results reflect general tendencies of the observed values, but cannot reproduce sort-term variations. Coarse resolution of the model grid is a possible explanation.

It is clear that the comparison only with European stations cannot provide a comprehensive verification of the hemispheric model. For more thorough analysis measurements from other regions of the Northern Hemisphere (e.g. North America, Asia, the oceans) should be involved.

Comparison with the regional MSCE-HM model

Besides, the modelling results were compared with those obtained by the regional MSCE-HM model. This is a three-dimensional Eulerian-type model covering the EMEP region with spatial resolution 50 km × 50 km. The MSCE-HM model applies the mercury chemical scheme similar to that of the hemispheric one. Each model used its own meteorological data for 1996. The same mercury anthropogenic emission inventory for 1995 [*Pacyna and Pacyna*, 2002] was utilized for the comparison. Only European emission sources were considered in both cases. Natural mercury emission was neglected as well as initial and boundary conditions.

Results of the comparison are presented in Figures 4.6 and 4.7. Figure 4.6 shows mean annual mercury concentration in the air obtained both by the hemispheric and regional models. Taking into account essentially different spatial resolution of the models one can conclude that both spatial distributions have a similar shape. The areas with the most significant mercury concentrations in general coincide in both cases. The hemispheric model is unable to reproduce the highest peaks of concentration because of lower spatial resolution. The models produce close mercury air concentrations in remote regions. In general the hemispheric model predicts more significant mercury transport outside the domain eastward. Spatial distribution of mercury annual deposition flux is shown in Figure 4.7. The deposition fields obtained by both the models look similar. The main distinction is more considerable depositions in remote regions (the Atlantic and Africa) predicted by the hemispheric model.

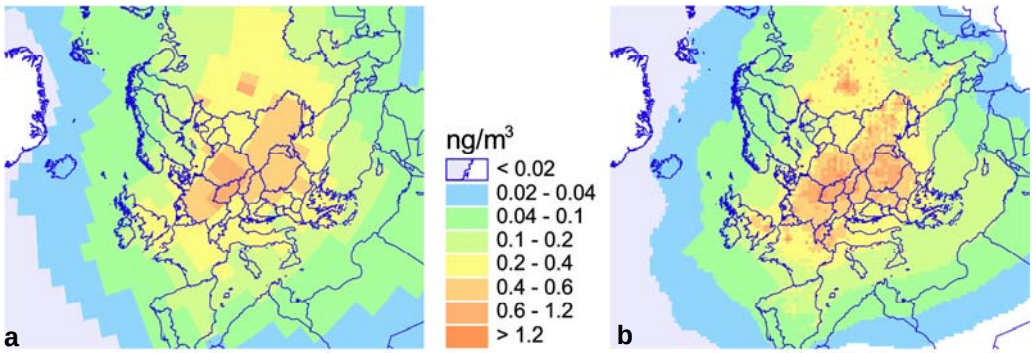

Figure 4.6. *Spatial distribution of mean annual mercury concentration in the surface air obtained by the hemispheric (a) and regional MSCE-HM (b) models*

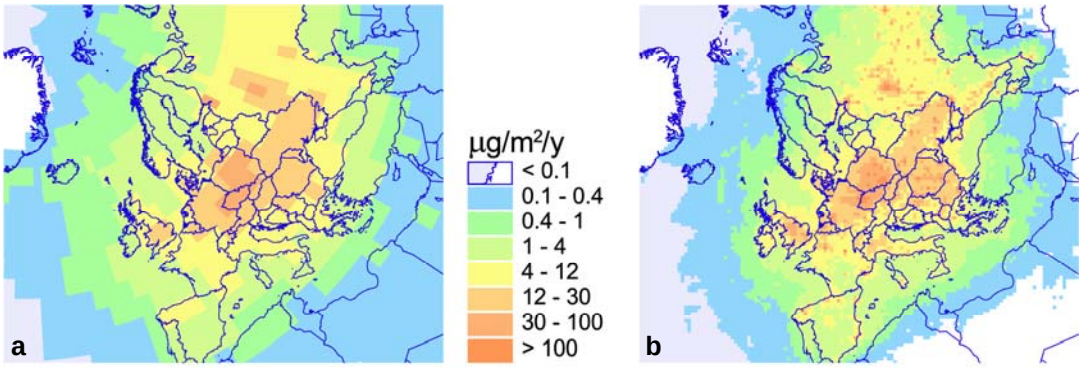

Figure 4.7. *Spatial distribution of total annual mercury deposition obtained by the hemispheric (a) and regional MSCE-HM (b) models*

4.3. Inter-continental mercury transport

Lifetime of elemental mercury, being a principal part of the entire mercury content in the atmosphere, amounts to one year or even more. It makes possible mercury transport over very long distances from emission sources to any remote areas of the World. Particularly, mercury emitted from one continent can reach and deposit to another one. This point is very important for the regional modelling where the pollutant transport across the boundaries can make a significant contribution to the whole pollutant content within the region.

The inter-continental transport is illustrated on the example of Europe. Figure 4.8 shows annual deposition field of mercury from European anthropogenic sources. Red rectangle in the figure depicts the EMEP domain. As seen from the figure mercury from European sources is transported and deposits almost all over the Northern Hemisphere. The most intensive depositions are in the middle latitudes being consistent with the general precipitation pattern. The lowest depositions are in Africa.

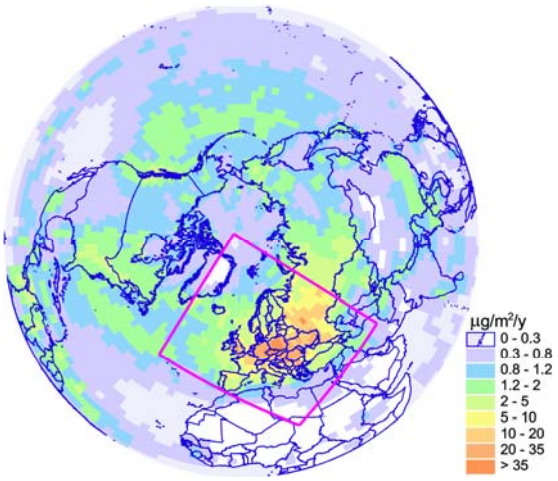

Figure 4.8. *Annual deposition field of mercury from European anthropogenic sources. The red rectangle depicts the EMEP domain*

Deposition of mercury to Europe from different sources of the Northern Hemisphere has also been investigated. The total annual mercury deposition to Europe amounts to about 200 t/y. Figure 4.9 demonstrates relative contribution of different regions of the Northern Hemisphere to the entire European deposition. Unidentified sources describe mercury coming through the equator. The highest depositions are from European anthropogenic sources (54%). A significant contribution is also made by natural sources (29%). It should be noted that the category "natural sources" includes natural emission sources both from Europe and from other regions of the Northern Hemisphere.

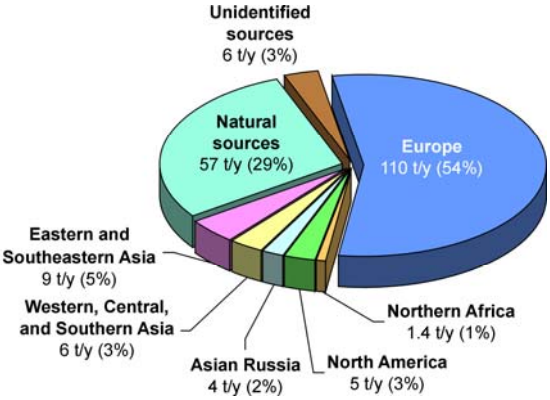

Figure 4.9. *Relative contributions of different regions to the entire mercury deposition to Europe. Natural sources include both European and other natural sources of the Northern Hemisphere*

Deposition from anthropogenic sources of other regions and continents amounts to 14%. Thus, up to 46% of the entire mercury deposition to Europe is from outer anthropogenic sources of other continents and from natural sources.

Figure 4.10 shows spatial pattern of annual mercury deposition to the EMEP domain from European anthropogenic sources (a) and from natural and external anthropogenic sources (b). As one can see from the figure European sources prevails over external ones only in the central part of the EMEP domain. On the other hand, external and natural sources make up more significant contribution in the Atlantic and Arctic Oceans, Northern Europe, Africa and Asian part of the EMEP domain.

Modelling results illustrating the inter-continental transport are summarized in Table 4.2. Rows of the table represent mercury sources located in different continents and regions of the Northern Hemisphere. Columns contain values of mercury annual deposition to different receptors. Three last rows represent mercury depositions from natural sources, unidentified sources (mercury coming trough the equator), and total deposition to the region.

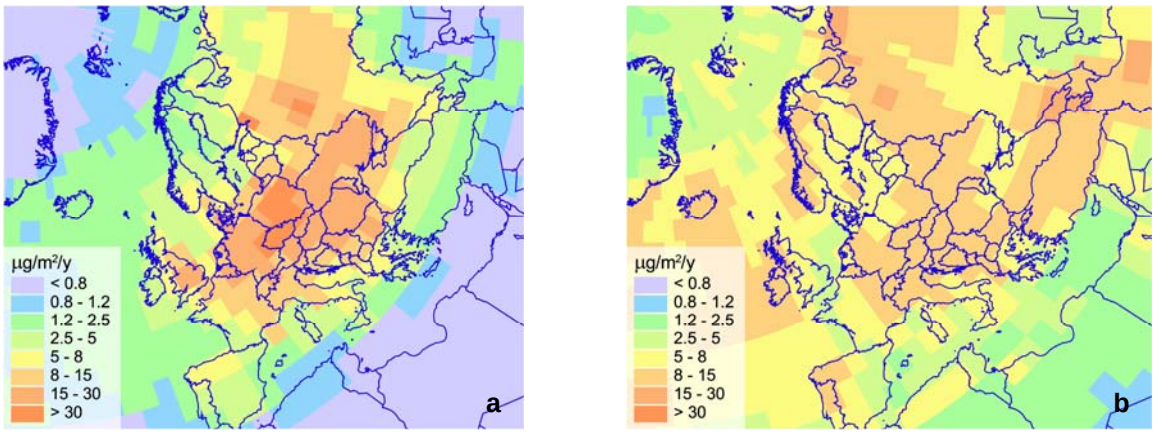

Figure 4.10. *Spatial distribution of annual mercury deposition to the EMEP domain: (a) – from European anthropogenic sources; (b) – from external anthropogenic and global natural sources*

Table 4.2. Annual budget of mercury in the Northern Hemisphere. Rows represent mercury sources; columns contain mercury deposition to different receptors, t/y

Sources	Receptors					
	Europe	Africa (northern part)	North America	Asian Russia	Western, Central, and Southern Asia	Eastern and Southeastern Asia
Europe	**109.7**	5.7	25.7	20.4	15.6	11.7
Africa (northern part)	1.4	**20.8**	1.5	0.7	1.7	1.0
North America	5.4	1.7	**73.2**	5.1	3.8	3.8
Asian Russia	3.8	0.8	6.6	**16.4**	4.2	3.2
Western, Central, and Southern Asia	6.2	4.4	9.1	7.9	**85.6**	14.1
Eastern and Southeastern Asia	9.3	2.9	26.9	15.9	7.6	**224.6**
Natural sources	57.1	25.3	125.1	66.2	46.4	72.3
Unidentified sources	6.2	14.8	21.1	6.5	9.6	25.3
Total	199.2	76.5	289.3	139.0	174.6	356.0

4.4. Atmospheric mercury input to the Arctic

The Arctic contamination represents a special case of the inter-continental transport. Remote location of the Arctic from the main industrial regions and its sensitive ecosystem make it particularly important for the hemispheric pollution assessment. Preliminary results of the atmospheric mercury transport and deposition to the Arctic are presented below.

Figure 4.11 shows spatial distribution of annual mercury deposition to the Arctic. The Arctic is presented by so-called "AMAP domain" described in Section 2.3. To examine the effect of mercury depletion phenomenon on the Arctic contamination, two computation runs have been conducted: taking into account MDP (Figure 4.11.a) and neglecting it (Figure 4.11.b). In the former case total mercury deposition to the Arctic region runs into 244 t/y, whereas in the latter one – 200 t/y.

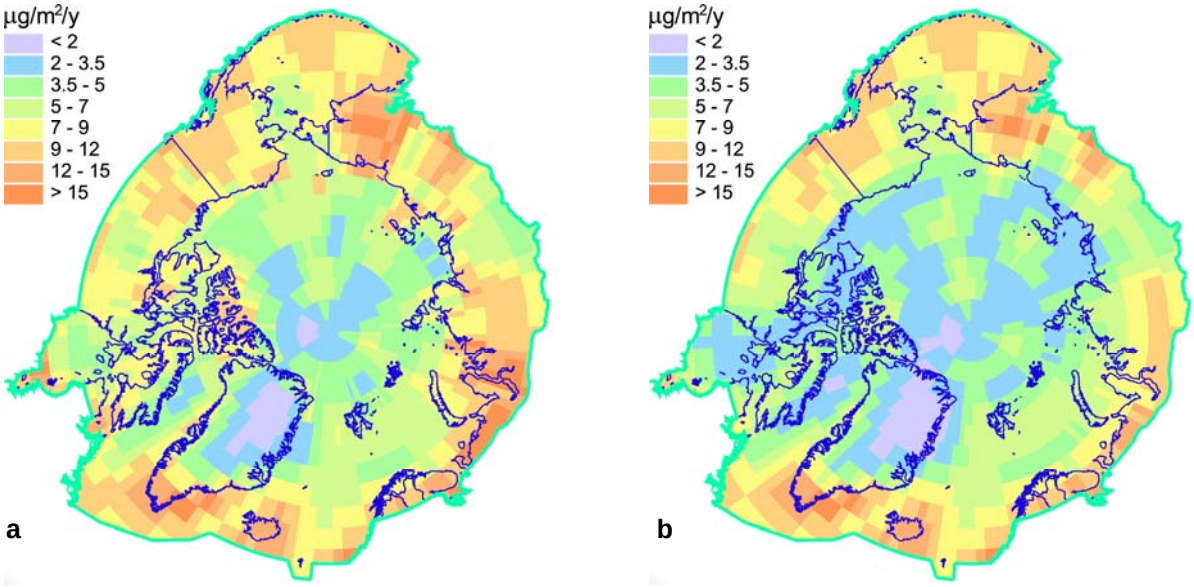

Figure 4.11. *Spatial distribution of annual mercury deposition to the Arctic (within the AMAP domain): (a) – computation with MDP; (b) – without MDP*

As seen from Figure 4.11.a the most significant mercury depositions (more then 15 μg/m^2/y) are in the Northern Atlantic, European part of the Arctic, and Eastern Siberia. The lowest depositions are in Greenland and near the Pole. Comparing Figures 4.11.a and 4.11.b one can conclude that MDP leads to more noticeable mercury deposition in coastal areas of the Arctic Ocean: the Queen Elizabeth Islands, Hudson Bay, Gulf of the Ob River etc. In spite of short-term character of the phenomenon, it can increase several times the annual deposition flux in these areas.

The influence of different regions and continents on the Arctic mercury contamination has also been investigated. Figure 4.12 shows relative contribution of the regions to the total annual mercury deposition to the Arctic region. As one can see the most significant contribution is made by natural emission sources (55%). However, anthropogenic sources also make up a considerable part of the total deposition (about 40%). The highest depositions are from Europe (37 t/y) and from eastern and southeastern Asia (27 t/y). North America, Western, Central and Southern Asia, and Asian part of Russia contribute close values (about 10 t/y each).

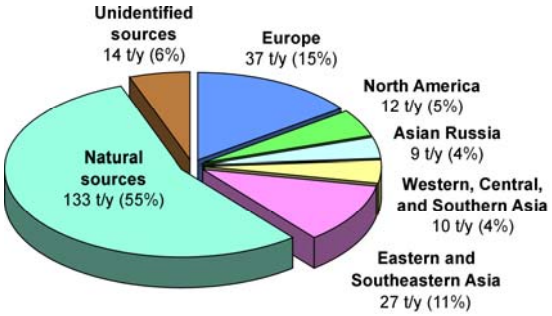

Figure 4.12. *Relative contributions of different regions to the entire mercury deposition to the Arctic*

Chapter 5

MULTI-COMPARTMENT MODEL OF MERCURY CYCLING IN THE ENVIRONMENT: BASIC TENETS

Mercury properties presume rather intensive migration of this element not only in the atmosphere but in other mediums as well. Before noticeable human impact on the environment there was a self-sustained natural cycle of mercury. In a simplified way it may be represented as an input of elemental mercury to the planet surface from deep layers of the lithosphere, its incorporation to redox processes in the surface geospheres, burial in oceanic bottom sediments in the oxidized form, sinking of the bottom sediments into the mantle where at high temperature mercury returns to its original elemental form. Mercury content in these or those mediums could vary with external conditions at different geological epochs.

Mercury has been known since ancient time, noticeable growth of its content in the environment began 500 years ago [*US EPA*, 1997], but a tangible human impact on its cycle may be dated back to the end of XVIII century or the beginning of XIX century. In this period two unique properties of mercury – capability to dissolve gold (to produce amalgam) and rapidly volatilize if heated – started to be used. It makes the basis for the simplest way of gold production, which is used up till now (mainly illegally). The growth of gold mining required essential amounts of metallic mercury. An important point was that mercury irrevocably vanished from the process to the environment.

Later on the anthropogenic incorporation of mercury to the planetary cycle was connected with mercury use as liquid electrodes, in pesticide production, for thermometers etc. At present the most important source of mercury input to the environment is combustion of fossil fuels contained mercury.

Among other metals originality of mercury is in its capability to accumulate in individual geochemical reservoirs and then long enough (according to lifetime in a given reservoir) to re-emit to the atmosphere. In other words when the anthropogenic flux is changed or completely ceased the input of the accumulated anthropogenic mercury to the atmosphere will continue for many years. Accordingly negative effects associated with mercury accumulation in biota will be also dragged on in time.

To describe accumulation and re-emission processes it is necessary to have a dynamical model operating with the entire period of anthropogenic impact. It is clear that it cannot be very detailed with short time steps. In principle the extent of model detailed elaboration should be adequate to modern knowledge on concentrations, fluxes, forms and other characteristics of the mercury cycle in the environment. There is no sense to distinguish and consider these or those geochemical reservoirs if no information about them is available. Thus, *a priory* it is clear that a multi-compartment model should be of a box type. On the other hand, it should have enough spatial resolution to provide input information for operational atmospheric transport models of regional and global levels. The concept of box approach was evolved in the models of I. Jonasson and R. Boyle [1971]; Abramovsky et al. [1978]; F. Ribeyre et al. [1991]; R. Hudson et al. [1995]; T. Jackson [1997] and C. Lamborg et al. [2002].

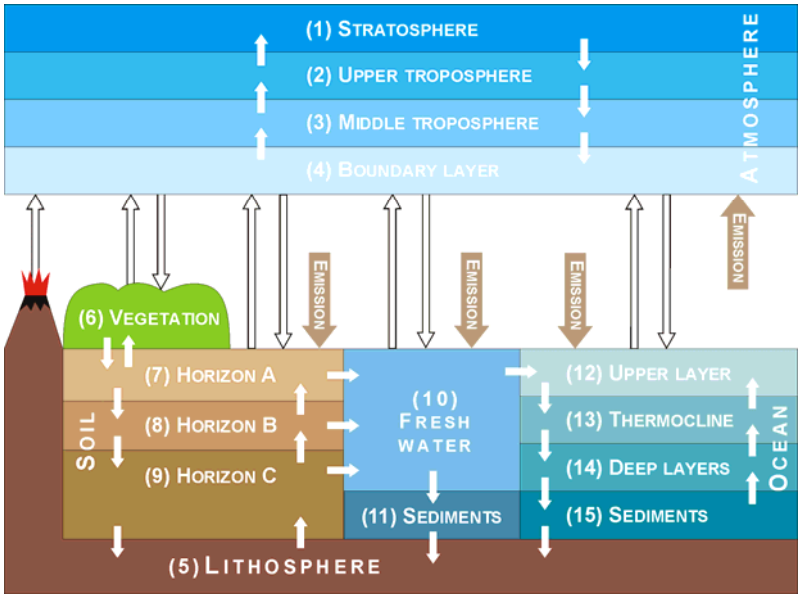

Figure 5.1. *General scheme of mercury cycling in the environment*

The objective of this chapter is to formulate main statements of the multi-compartment model. At first we consider the scheme of all main geochemical compartments. Then the analysis of required information adequacy will be made for each box separately. We hope that with the use of such an approach it is possible to develop a simple and reliably defined model scheme. It is clear that within the framework of the MSC-E activity the main attention will be paid to the atmosphere.

From the viewpoint of geophysical notion about the dynamics of geospheres each of them has a number of units, to which one may apply the notion of “well mixed” reservoir. It is accepted *a priori* that with regard to mercury this approach will lead to an excessive detalization. In future either new information about some units will be available or groups of units will be combined to one.

Figure 5.1 shows an idealized (at present too detailed) scheme of mercury cycling in the environment. The suggested scheme consists of 15 individual units. Since the difference in atmospheric concentrations between the North and South Hemispheres is experimentally determined reliably enough then for model verification it is reasonable to divide each unit in the northern and southern parts as it was done by T. Bergan and H. Rodhe [2001] and C. Lamborg et al. [2002]. Below we consider the level of our knowledge of each unit and decide whether it is reasonable to incorporate this or that unit to the developing model. Among numerous characteristics of each unit first of all we concentrate our attention on such parameters as mercury content, lifetime and values of fluxes to neighboring reservoirs.

In the atmosphere it is possible to distinguish four zones with very different characteristics of mercury mixing and scavenging: planetary boundary layer (approximately 0 - 1.5 km); the middle troposphere (1.5 - 5 km); the upper troposphere (5-12 km) and the stratosphere. The lithosphere is represented as one unit. As a rule the lithosphere is covered by soils, which can be divided into 3 units. The soils permanently or during certain seasons are covered by vegetation. Fresh water bodies as the underlying surface have bottom sediments. The ocean (including seas) is divided into 4 units - the upper layer from the surface to thermocline (0-100 m), the thermocline layer (100-1000 m), deep ocean layers (from 1000 m to the bottom), and bottom sediments.

The stratosphere (Unit 1) is an atmospheric unit important for modelling since it defines conditions at the upper boundary of the entire system. It may be said *a priori* that before anthropogenic impact the stratosphere was in equilibrium with the troposphere. The information about this mercury box is very poor. It may be assumed that mercury concentration coming from the troposphere to the stratosphere is 1 ppt(m). The air flux from the troposphere to the stratosphere (Flux 2-1) is about $9 \cdot 10^{14}$ t/y [*Reiter*, 1968]. Hence the corresponding flux of mercury is 90 t/y. Most likely in the stratosphere elemental mercury is oxidized by ozone that is confirmed by revelation of stratospheric mercury aerosol layer [*Murphy et al*., 1998]. If we conceive that aerosol particles containing mercury by their characteristics are close to radioactive particles, then their lifetime in the stratosphere should be about a year [*Junge*, 1963]. Consequently mercury mass in Unit 1 by an order of magnitude is 100 tonnes. It is important that the stratosphere is a sink of elemental mercury and a source of aerosol mercury for the troposphere. The ratio of gaseous and aerosol mercury in air coming from the stratosphere is not known so far. It may be only supposed that high ozone content and long residence time in the stratosphere make the aerosol form dominating.

The upper troposphere (Unit 2) is characterized by dominating gas-phase processes of mercury oxidation. The probability of the drop aqueous phase of cloud water is negligible at this height therefore liquid phase redox processes may be ignored in this compartment. Exchange processes with the stratosphere (Fluxes 2-1 and 1-2) may be prescribed on the base of calculations of troposphere-stratosphere air mass transport. Exchange fluxes with the middle troposphere (Fluxes 3-2 and 2-3) are prescribed by the meteorological analysis.

The mixing ratio of elemental mercury in this unit may be slightly lower than near the ground surface since descending vertical profile of the mixing ratio should exist. P. Pai et al. [1997] accept in their model that elemental mercury mass concentration at the boundary with the stratosphere is 70% of its near surface value. C. Banic et al. [1999] did not find any difference between concentrations near the ground and at the height of 7 km (within limits of measuring accuracy). In the rough estimation the current mass of mercury in Unit 2 may be 2000 tonnes.

There is rather high probably that the atmosphere in Unit 3 has liquid cloud drops. Consequently here both gas phase and aqueous phase reactions can take place. Exchange fluxes with the upper troposphere (Fluxes 3-2 and 2-3) and with the boundary layer (Fluxes 4-3 and 3-4) can be prescribed by the meteorological analysis. The nowaday mercury mass in Unit 3 may be estimated by the value of 2000 tonnes.

The planetary boundary layer (Unit 4) is of a particular interest since just here the most significant processes defining mercury deposition pattern at least on the regional scale take place. Probability of occurrence of liquid-drop clouds here is high. Here short-lived oxidants such as chlorine are in action. Here the phenomenon of elemental mercury spring depletion is evolving in high latitudes. Finally mercury from natural (except for high volcanoes) and anthropogenic sources arrives here.

At present anthropogenic mercury emission is assessed as 2140 t/y [*Lamborg et al*., 2002] and the bulk of it is realized in the latitudinal band between 40 °N and 60 °N. Approximately half of anthropogenic emission is represented by elemental mercury, 30% - by gaseous compounds of divalent mercury and 20% - by aerosol particles containing mercury.

Mercury transport directly from the lithosphere (Flux 5-4) takes place either in regions of volcanic activity (200 t/y) or in mountain and desert regions free of soil and with elevated content of mercury in mountain rocks (Kyrgyzstan, Nevada desert). Mercury exchange between soil and the atmosphere (Fluxes 7-4 and 4-7) is clearly not in

equilibrium - the soil is more a source than a sink [*Xiao et al.*, 1991; *Zhang and Lindberg*, 1999; *Boudala et al.*, 2000]. Modern estimates of the net flux to the atmosphere from soils vary from 200 t/y [*Ebinghous et al.*, 1999a] to 1160 t/y [*Lindberg et al.*, 1998]. It is considered that natural emissions from Units 5 and 7 are represented only by elemental mercury.

It has been found experimentally that vegetation can both absorb and emit mercury to the atmospheric boundary layer. The flux value and direction has an explicit diurnal cycle that is connected with vegetation respiration. Most likely Fluxes 6-4 and 4-6 are in equilibrium on prolonged time intervals.

Both for fresh and marine water natural emission (10-4 and 12-4) and uptake fluxes (4-10 and 4-12) are obviously not balanced. The water surface is almost always an emitter and very seldom – absorber.

An overall content of mercury in Unit 4 can be assessed as 1100 tonnes. This estimate is based on sufficiently reliable measurements in both hemispheres. On the global level this mass is mainly represented by elemental mercury. In industrial regions, however, the contribution of the oxidized forms may be pronounced. Oxidized mercury (gaseous or aerosol) has a comparatively short half-life – from hours to days. In general Unit 4 may be considered as most thoroughly studied.

The lithosphere (Unit 5) by itself is not of a great interest for us since all the processes in it have characteristic time appreciably exceeding the period of human existence. Only note that the mercury Clarke factor (mass ratio) in the upper part of the Earth's crust is estimated by value $7.7 \cdot 10^{-6}$ % [*Smirnov et al.*, 1972] and the total mercury content in the upper layer of 1 km depth is 10^9 tonnes [*Trahtenberg and Korshun*, 1990].

The major part of continental surface is covered by seasonal or permanent vegetation (Unit 6). Mercury does not take part in the vital activity of vegetation. It is difficult to say whether commonly encountered forms of mercury are toxic for vegetation. In spite of a neutral character relative to vegetation metabolism processes there is an evidence of exchange between leaves/needles and air. There is a popular hypothesis on "compensation point" – the threshold concentration of mercury in air, above which the absorption by vegetation and below which emission takes place. Depending on vegetation kind the "compensation point" can vary from 10 to 20 ng/m^3. Such high concentrations may be only near a source of mercury emission to the atmosphere. At the same time absorption is occasionally observed at considerably lower concentrations. It means that the theory about the "compensation point" is not universal. Root input from soil to the crown is virtually absent [*Schroeder and Munthe*, 1998]. Mercury accumulation in leaves/needles cannot be of a long-term character, hence mercury lifetime in Unit 6 most likely runs into hours-days. Wood also contains some quantity of mercury. When a plant dies mercury come into soil. At present it is difficult to judge about the reservoir (6) capacity. Most likely it is relatively small.

Soil (Units 7-9) is a very important reservoir for mercury cycle. Firstly, soil is a geochemical buffer on the mercury pathway from the lithosphere to the atmosphere. Here it is often accumulated in a natural way to concentrations exceeding characteristic values for underlying mountain rocks. Secondly, it is considered that the bulk of anthropogenic mercury (90-95%) earlier released to the atmosphere at present is in soils [*Fitzgerald and Mason et al.*, 2001; Oliveira et al., 2001]. According to data of W. Schroeder and J. Munthe [1998] $2 \cdot 10^5$ tonnes of mercury have entered soil from the atmosphere since 1890. The «soil-atmosphere» system was conceptually considered in [*Zhang and Lindberg*, 1999].

Although a part of mercury in soil is represented by its elemental form in soil air and in the sorbed form, the major part is in the composition of mercury organic complexes [*Shuster*, 1991]. It means that mercury soil chemistry is closely connected with carbon

chemistry [*Yin et al.*, 1997] and with biotic processes. This is confirmed by the fact that mercury emissions from soil to air stops when temperature drops to 0°C [*Xiao et al*., 1991]. Mercury organic complexes are chemically stable compounds and release mercury when heated to about 220°-320°C (*Biester and Nehrke*, 1997). It confirms the fact of a long life of mercury in soil – hundreds or possibly thousands of years. The major part of mercury in soil is present as non-volatile compounds and only when they are transformed to elemental or methylated forms they can volatilize to the atmosphere [*Schroeder and Munthe*, 1998]. The lifetime relative to emission to the atmosphere (flux 6-4) is in the interval from 150 to 400 years [*Abramovsky et al*., 1978; *Wallschläger et al*., 2000; *Trakhtenberg and Korshun*, 1990] and relative to hydrological leaching (Fluxes 7-10, 8-10 and 9-10) – from 300 to 10000 years [*Abramovsky et al.*, 1978*; Wallschläger et al.*, 2000; *Lee et al.*, 1998]. W. Fitzgerald and R. Mason [1996] consider that runoff from soil to rivers is 200 t/y at present and before human activity was 60 t/y.

From the viewpoint of soil structure three horizons (*A*, *B*, and *C*) with different carbon content are distinguished. According to data of V. Fursov [1983]; E. Schuster [1991] and T. Matilainen et al*.* [2001] the highest mercury content is in the upper horizon abundant in carbon. For example, in Kazakhstan soils horizon *A* contains 0.058 ppb and in horizons *B* and *C* mercury concentration is lower – 0.044 and 0.034 ppb respectively [*Fursov*, 1983]. On the whole mercury content in soil varies within an order of magnitude ~10^{-2} ppb [*Vinogradov*, 1957; *Williston* 1968; *Prokofiev*, 1981; *Fursov*, 1983; *Johansson et al.*, 1991]. It is possible to evaluate the total mercury mass in the soil reservoir on the following assumption. The savanna and sparse growth of trees area is $3 \cdot 10^{13}$ m^2 at soil depth 5 cm (maximum organic carbon content). The area of forests is $4.5 \cdot 10^{13}$ m^2 at soil depth 15 cm. The area of agricultural land is $1.5 \cdot 10^{13}$ m^2 at soil depth 20 cm. We take soil density equal to 1.3 t/m^3. Mean concentration of mercury in soil we estimate as 0.05 ppm. Hence mercury mass in the soil reservoir is $7.5 \cdot 10^6$ tonnes. It is three orders of magnitude higher than mercury mass in the atmosphere.

Due to anthropogenic activity soils may be directly contaminated by mercury (without atmospheric impact). Estimates of the annual anthropogenic input of mercury to the upper soil horizon are within a wide range – from 1570 to 15000 t/y [*Nriagu and Pacyna*, 1988; *Thornton et al*., 1995]. At present the information about mercury fluxes from one horizon to another (Fluxes 7-8, 8-7, 8-9, 9-8) is scarce. It is possible that under the conditions of severe anthropogenic pollution mercury may be transported to the underlying rocks (Flux 9-5) [*Yin et al*., 1997]. Under natural conditions, however, Flux 5-9 is realized, which in combination with atmospheric depositions balances removal fluxes from soil.

On the global scale fresh water reservoirs (Unit 10) contain only a minor fraction of water. Mercury concentrations in rivers and lakes vary within a very wide range – from 0.1 to 100 ng/L [*US EPA*, 1997]. If we take that mean concentration is 5 ng/L and the overall volume of fresh water is $1.9 \cdot 10^{17}$ liters [*Henshaw et al*., 2000] then mercury mass in reservoir (10) should be less than 1000 tonnes. F. Ribeyre et al*.* [1991] has developed on a conceptual level the model of mercury behaviour in a fresh water reservoir.

Mercury input to the fresh water reservoir takes place due to direct anthropogenic discharge, depositions from the atmosphere directly on the water surface (Flux 4-10), drainage on the catchment area (Fluxes 7-10, 8-10 and 9-10). The assessment of direct anthropogenic discharge ranges from 80 to 7000 t/y [*Thornton et al.*, 1995]. From the reservoir mercury enters the atmosphere in the elemental form (Flux 10-4) and to the ocean in the dissolved form and as particulate dregs (Flux 10-12).

On the global scale the fresh water reservoir should not play a noticeable role – this unit is a transit in the mercury transport from soils to the World Ocean. Some fraction of mercury is

buried in sediments (Flux 10-11) and in the long run comes to the lithosphere (Flux 11-5). Mercury concentrations in bottom sediments are relatively low – about 0.02 ppm [*Kannan and Falandysz*, 1998] but they are growing continuously: During the industrial period they increased 3-6 times [*Fitzgerald et al*., 2001]. It can be supposed that the flux from bottom sediments of the fresh water systems to the lithosphere (Flux 11-5) is negligible on the global level.

The ocean is a significant mercury reservoir (Units 12, 13, and 14), though concentrations of the dissolved mercury form are low – from 0.2 to 2.4 ng/L [*Baeyens*, 1991]. If we take 0.5 ng/L as a mean value then the total mercury mass is about $7 \cdot 10^5$ tonnes. It is by an order of magnitude lower than the total content in soil. In view of considerably different velocities of water mass mixing it is reasonable to divide the ocean into three independent layers. The upper layer (Unit 12) is most dynamic and it is capable to exchange mercury with the atmosphere for the period of decades [*Lamborg et al.*, 2002]. From the viewpoint of mercury migration this layer is sufficiently well studied. The next layer (Unit 13) has characteristic time of water mass exchange – about 200 years [*Lamborg et al.*, 2002]. Processes in the deep ocean (Unit 14) go on very slowly (about several thousands of years). Actually there is no data on concentration distribution in Units 13 and 14. Some idea on mercury content levels in deep waters may provide measurements in upwelling zones [*Mason et al.*, 1994].

At first mercury enters the upper oceanic layer as a result of direct anthropogenic discharges, depositions with atmospheric precipitation (Flux 4-12) and riverine runoff (Flux 10-12). The last flux is mainly represented by the solid phase of riverine particulate dregs, which lifetime in the ocean is not long. Mercury contained in the composition of discharged particles falls out on the oceanic bottom near river mouths [*Lamborg et al*., 2002]. Dissolved mercury compounds are readily sorbed by organic matter, ferrous and manganese hydrates, calcium phosphates, silicates and settle on the bottom as particles [*Barabanov*, 1985].

Oceanic bottom sediments (Unit 15) are the final sink of mercury in the global geochemical system. Most likely mercury is buried once and for all as sulphide in anaerobic bottom sediments [*Horvat*, 1996]. The pattern of mercury behaviour in seawater is clear qualitatively but quantitative estimates of fluxes in deep oceanic layers are absent. Mercury lifetime in the ocean as a whole is assessed as $3.2 \cdot 10^3$ years and in bottom sediments – $2.5 \cdot 10^8$ years [*Benjamin and Honeyman*, 2000]. A. Prokofiev [1981] estimates mercury lifetime in the ocean by an order of magnitude higher – from $2.6 \cdot 10^4$ to $4.2 \cdot 10^4$ years. Mercury concentration in sediments of the southern Baltic is about 0.2 ppm [*Kannan and Falandysz*, 1998], in the Black Sea – 0.6 ppm [*Smirnov et al.*, 1972]. Capacities of the described above environmental reservoirs are summarized in Table 5.1.

Table 5.1. Capacity of the environmental reservoirs

Reservoir	Capacity, t
1. Stratosphere	100
2. Upper troposphere	2000
3. Middle troposphere	2000
4. Planetary boundary layer	1100
5. Lithosphere	10^9
6. Vegetation	n/a *
7. Soil (horizon A)	$7.5 \cdot 10^6$
8. Soil (horizon B)	
9. Soil (horizon C)	
10. Fresh water bodies	1000
11. Fresh water sediments	n/a
12. Ocean (upper layer)	$7 \cdot 10^5$
13. Ocean (thermocline)	
14. Ocean (deep layers)	
15. Ocean sediments	n/a

* n/a – not available

As was mentioned a real increase of mercury concentration in different compartments due to human activity began about 500 years ago and continued in all the countries till the middle of the 70s of XX century [*US EPA*, 1997]. During recent 20 years rapid changes of spatial distribution of anthropogenic mercury emissions take place all over the

world. In industrialized countries mercury emission has sharply decreased whereas in developing ones it rapidly increases. At present in regard to anthropogenic mercury emission China takes the first place in the world – 460 t/y [*Pacyna et al.*, 1999]. On the whole, during XX century mean growth rate of air mercury concentration was estimated by W. Fitzgerald [1995] as 0.6% per year.

To review the said above the following proposals of mercury multi-compartment model development can be suggested:

➢ Refining parameters of mercury mass transfer between the troposphere and stratosphere. It is important to have an idea about chemical processes in the stratosphere. Certainly the stratosphere is an important reservoir for modelling.

➢ To simplify the model Units 2, 3 and 4 may be combined to one unit “troposphere”.

➢ The lithosphere is of interest only as a natural source of mercury emission to the atmosphere. This flux may be important and it should be refined.

➢ During short periods of time vegetation can play an important role in the mercury cycle. Most likely this unit should be present in the model but its characteristics need refinement.

➢ Since actually nothing is known about mercury migration between soil horizons it is reasonable to consider soil as one unit. It is important to refine parameters of mercury circulation in soil itself and values of mercury removal from this unit.

➢ It is likely that in global modelling the fresh water reservoir (Units 10 and 11) can be neglected.

➢ Since actually nothing is known about mercury behaviour in deep oceanic layers and time periods of water mass mixing greatly exceed the historical period of mercury cycle variation, Units 14 and 15 may be ignored. In this situation Unit 13 becomes the final unit of the mercury cycle.

➢ It is necessary to have sufficiently reliable information about variations of global anthropogenic emissions at least during recent 200 years. At the same time it is important to assess changes in emission speciation during this period. In addition it is necessary to make more precise estimates of direct mercury input to soil and water systems.

The simplified scheme of mercury cycling in the environment is presented if Figure 5.2. According to the scheme multi-compartment model is to consist of 7 most important units: (1) stratosphere, (2) troposphere, (3) lithosphere, (4) soil, (5) vegetation, (6) upper ocean layer, (7) ocean thermocline. Mercury is emitted to the troposphere, soil and upper ocean layer from anthropogenic sources. Besides, it enters the troposphere directly from the lithosphere. The only output of mercury from the system is burial from the thermocline to deep layers and further to the ocean sediments.

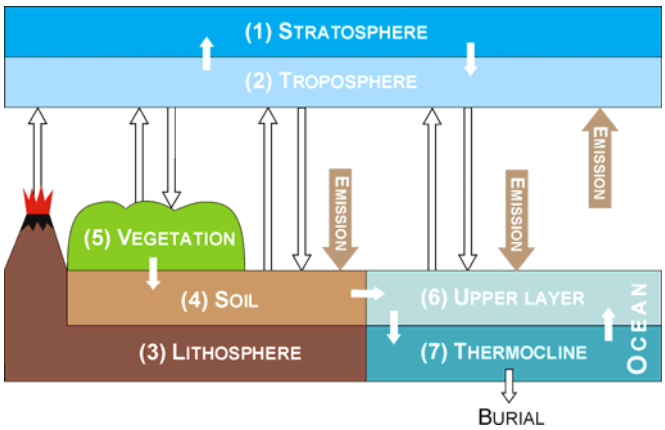

Figure 5.2. *Simplified scheme of mercury cycling in the environment*

CONCLUSIONS

The multi-compartment model of mercury transport and contamination on the hemispheric (in perspective - the global) scale is currently under development in Meteorological Synthesizing Centre East of EMEP. The following conclusions resume the current stage of the model development.

- The atmospheric module describing long-range airborne mercury transport, transformation and deposition to the ground has been elaborated.

- Survey of mercury physical and chemical properties in the atmosphere was accomplished. The model chemical scheme of mercury transformations has been brought into conformity with the contemporary scientific researches.

- Necessary input information for modelling of mercury transport on the hemispheric scale has been collected. The data include anthropogenic emissions, meteorological and geophysical data, and air concentrations of the reactants taking part in chemical reactions. Besides, natural emission of mercury was evaluated basing on the literature survey.

- Pilot calculations of mercury transport and depositions in the Northern Hemisphere were carried out for 1996. Mercury concentration levels in the ambient air as well as deposition fluxes were assessed and discussed.

- The modeling results were compared with available monitoring data and with modelling results obtained by the regional model. The comparison conducted has shown a satisfactory agreement between the modelled and observed values as well as between both the models.

- The inter-continental transport of mercury in the Northern Hemisphere has been assessed. According to the preliminary results more then 40% of mercury deposition to Europe is from external anthropogenic and global natural sources.

- The influence of different regions and continents on the Arctic mercury contamination has also been investigated. It was obtained that anthropogenic mercury input to the Arctic from the atmosphere make up a considerable part of the total deposition (about 40%).

- Basic principles of the multi-compartment model of mercury dispersion and cycling in the environment have been formulated. The most important environmental compartments were selected; the main inter-compartmental exchange fluxes were pointed out. General steps of the model development were outlined.

Acknowledgments

The authors deeply appreciate national experts and outer contributors who supplied the required information and data:

Dr. Malcolm Ko from *Atmospheric Chemistry and Dynamics Group of Atmospheric and Environmental Research (USA)* for the global data on ozone and sulfur dioxide content in the atmosphere;

Prof. Henning Rodhe from *Department of Meteorology of Stockholm University (Sweden)* for the global data on sulfur dioxide content in the atmosphere;

Dr. Dorota Colber from *Institute of Marine and Coastal Sciences at Rutgers the State University of New Jersey (USA)* for the global data on the ocean primary productivity.

Besides, the authors are very grateful to **Dr. Rulf Ebinghaus** from *Institute of Physical and Chemical Analysis of GKSS Research Center (Germany)* and **Dr. Christian Seigneur** from *Atmospheric and Environmental Research (USA)* for general informative support.

Finally, we are sincerely thankful to all **MSC-E team** and especially to **Mrs. Larissa Zayavlina** for editing the manuscript as well as to **Ms. Irina Strizhkina** and **Mrs. Svetlana Yevdokimova** for its preparing and publishing.

REFERENCES

Abramovsky B. P., Anokhin Yu. A., Ionov V. A., Nazarov I. M., and Ostromogilsky A. H. [1977] Estimation of global mercuty balance and critical limits of mercury emission to the atmosphere. In: Nazarov I. M. (Ed.), Atmospheric Pollution as an Ecological Factor. Issue of Institute of Applied Geophysics **39**, Gydrometeoizdat, Moscow, 4-19.

Acker K., Moller D., Wieprecht W., Kalass D., and Auel R. [1998] Investigations of ground-based clouds at the Mt. Brocken. Fresenius. *Anal. Chem.* **361**, 59-64

AMAP [1998] *AMAP Assessment report: Arctic pollution issues*. Arctic Monitoring and Assessment Programme (AMAP), Oslo, Norway. 859 p.

Amiot M., Lean D., Mierle G., and McQueen D. J. [1995] Volatilization of Hg from lakes mediated by solar radiation. Proceedings of 1995 Canadian mercury network workshop, 29-30 September 1995, York University, Toronto, Ontario, Canada

Artaxo P., Campos de R. C., Fernandes E. T., Martins J. V., Xiao Z., Lindqvist O., Fernandes-Jimenez M. T., and Maenhaut W. [2000] Large scale mercury and trace element measurements in the Amazon basin. *Atmos. Environ.* **34**, 4085-4096

Baeyens W., Leermakers M., Dedeurwaerder H., and Larsens P. [1991] Modelization of the mercury fluxes at the air-sea interface, *WASP* **56**, 731-744

Bailey E. H., Clark A. L., and Smith R. M. [1973] Mercury. *U.S. Geol. Surv. Prof. Pap.* **821**, 410-414

Banic C. M., Schroeder W. H., and Steffen A. [1999] Vertical distribution of total gaseous mercury in Canada. Book of abstracts, 5th International Conference on Mercury as a Global Pollutant, 23-28 May 1999, Rio de Janeiro.

Baltensperger U., Schwikowski M., Jost D. T., Nyeki S., Gäggeler H.W., and Poulida O. [1998] Scavenging of atmospheric constituents in mixed phase clouds at the high-Alpine site Jungfraujoch. Part I: Basic concept and aerosol scavenging by clouds. *Atmos. Environ.* **32**, 3975-3983

Barabanov V. F. [1985] *Geochemistry*. Nedra, Leningrad, 423 p. (in Russian)

Behrenfeld M.J. and Falkowski P.G. [1997] Photosynthetic derived from satellite-based chlorophyll concentration. *Limnol. Oceanogr*., **42**(1), 1-20

Benesch J. A., Gustin M. S., Schorran D. E., Coleman J., Jonson D. A., and Lindberg S. E. [2001] Determining the role of plants in the biogeochemical cycling of mercury on an ecosystem level. Book of Abstracts, 6th International Conference on Mercury as a Global Pollutant, 15-19 October 2001, Minamata, Japan

Benjamin M. M. and Honeyman B. D. [2000] Trace Metals. In: Jacobson M., Charlson R., Rodhe H., and Orians G. (Eds.), Earth System Science. From Biogeochemical Cycles to Global Change. Academic Press, San Diego, pp. 377-418

Boudala F. S., Folkins I., Beauchamp S., Tordon R., Neima J., and Johnson B. [2000] Mercury flux measurements over air and water in Kejimkujik national park, Nova Scotia. *WASP* **122**, 183-202

Berg T. and Hjellbrekke A.-G. [1998] Heavy metals and POPs within the ECE region. EMEP/CCC Report 7/98, Norwegian Institute for Air Research, Kjeller, Norway

Berg T., Sekkester S., Steines E., Valdal A., and Wibetoe G. [2001] Arctic springtime deplition of mercury as observed in the European Arctic. Book of Abstracts, 6th International Conference on Mercury as a Global Pollutant, 15-19 October 2001, Minamata, Japan

Berg T., Sekkesæter S., Solberg S., Steines E., Valdal A.-K., and Wibetoe G. [2002] Arctic springtime depletion of mercury in Svalbard. Book of abstracts of Symposium "EUROTRAC-2", 11-15 March 2002, Garmisch-Partenkirchen, Germany

Bergan T. and Rodhe H. [2001] Oxidation of elemental mercury in the atmosphere; constraints imposed by global scale modelling. *J. Atm. Chem.* **40**, 191-212

Biester H. and Nehrke G. [1997] Quantification of mercury in soils and sediments - acid digestion versus pyrolysis. *Fresenius Journal of Analytical Chemistry* **358**(3), 446-452

Bloom N., Bullock O. R., Church T. M., Coffey P., Engstrom D. R., Fitzgerald W. F., France D., Gill G. A., Hopke P. K., Iverfeldt A., Jansen J. J., Keeler J., Lindberg S. E., Lindqvist O., Meagher J. F., Munthe J., Olmez I., Petersen G., Porcella D. B., Schroeder W. H., Seigneur C., and Turner R. [1994] Mercury Atmospheric Processes: A Synthesis Report. Expert panel on mercury atmospheric processes, March 16-18, 1994, Tampa, Florida, USA

Bott A. [1989a] A positive definite advection scheme obtained by nonlinear renormalization of the advective fluxes. *Monthly Weather Review* **117**, 1006-1015

Bott A. [1989b] Reply to comment on "A positive definite advection scheme obtained by nonlinear renormalization of the advective

fluxes." *Monthly Weather Review* **117**, 2633-2636

Bott A. [1992] Monotone flux limitation in the area-preserving flux-form advection algorithm. *Monthly Weather Review* **120**, 2592-2602

Brosset C. and Lord E. [1991] Mercury in precipitation and ambient air – a new scenario. *WASP* **56**, 493-506

Bullock O. R., Benjey W. G. and Keating M. H. [1994] Modeling of regional scale atmospheric mercury transport and deposition using RELMAP. In: Baker J. E. (Ed.) Atmospheric deposition of contaminants to the Great Lakes and coastal waters. SETAC Technical Publications Series, Pensacola, Florida, 323-347

Carpi A. and Lindberg S. E. [1998] Application of a teflon^{TM} dynamic flux chamber for quantifying soil mercury flux: tests and results over background soil. *Atmos. Environ.* **32**(5), 873-882

Chin M. et al. [1996] A global three-dimensional model of tropospheric sulfate, *J. Geophys. Res.* **101**, 18667-18690

Christensen J. [2001] Modelling of Mercury with the Danish Eulerian Hemispheric Model. The International Workshop on Trends and Effects of Heavy Metals in the Arctic, 18-22 June 2001, McLean, Virginia, USA

Constantinou E., Wu X. A., and Seigneur C. [1995] Development and application of a reactive plume model for mercury emissions. *WASP* **80**, 325-335

Couture M. D., Banic C. M., Schemenauer R. S., Leaitch W. R., and Wiebe H. A. [1998] Comparison of the chemistry of fog water from mountain sites and cloud water from airborne platforms. In: R. S. Schemenauer and H. Bridgman (Eds.) Proceedings of the First International Conference on Fog and Fog Collection. International Development Research Center, Ottawa, Canada, 109-112

Dabdub D., Seinfeld J. H. [1994] Numerical advective schemes used in air quality models – sequential and parallel implementation. *Atmos. Environ.* **28**, 3369-3385

Davies F. and Notcutt G. [1996] Biomonitoring of atmospheric mercury in the vicinity of Kilauea, Hawaii. *WASP* **86**, 275-281

Drummond J. R. [2001] The view from above: Passive sounding of the troposphere from space. *IGAC Newsletter* **25**, 2-6

Easter R. C. [1993] Two modified versions of Bott's positive-definite numerical advection scheme. *Monthly Weather Review* **121**, 297-304

Ebinghaus R., Tripathi R. M., Walischlager D., and Lindberg S. E. [1999a] Natural and anthropogenic mercury sources and their impact on the air-surface exchange of mercury on regional and global scales. In: Ebinghaus R., Turner R. R., Lacerda de L. D., Vasiliev O., and Salomons W. (Eds.) Mercury contaminated sites. Springer, Berlin, 3-50

Ebinghaus R., Turner R. R., Lacerda de L. D., Vasiliev O., and Salomons W. (Eds.) [1999b] *Mercury contaminated sites*. Springer, Berlin. 538 p.

Ebinghaus R., Temme C., Kock H. H., Löwe A., and Schroeder W. H. [2001] Deplition of atmospheric mercury concentrations in the Antarctic. Book of Abstracts, 6th International Conference on Mercury as a Global Pollutant, 15-19 October 2001, Minamata, Japan

Ebinghaus R., Kock H. H., Temme C., Einax J. W., Löwe A. G., Richter A., Birrows J. P., Schroeder W. H. [2002] Antarctic Springtime Depletion of Atmospheric Mercury. *Environ. Sci. Technol.* **36**, 1238-1244

Engle M. A., Gustin M. S., and Zhang H. [2001] Quantifying natural source mercury emissions from the Ivanhoe mining district, north-central Nevada, USA. *Atmos. Environ.* **35**, 3987-3997

Fitzgerald W. F., Mason R. P., and Vandal G. M. [1991] Atmospheric cycling and air-water exchange of mercury over mid-continental lacustrine regions. *WASP* **56**, 745-767

Fitzgerald W. F. [1995] Is mercury increasing in the atmosphere? The need for an Atmospheric Mercury Network (AMNET). *WASP* **80**, 245-253

Fitzgerald W. F. [1996] Mercury Emission from Volcanoes. Book of abstracts, Fourth International Conference on Mercury as a Global Pollutant, 4-8 August 1996, Hamburg, Germany

Fitzgerald W. F. and Mason R. P. [1996] The global mercury cycle: oceanic and anthropogenic aspects. In: Baeyens W., Ebinghaus R. Vasiliev O. (Eds.), Global and Regional Mercury Cycles: Sources, Flaxes and Mass Balances. NATO-ASI-Series, Kluwer Academic Publishers, Dordrecht, The Netherlands, 85-108

Fitzgerald W. F., Lamborg C. H., Tseng C.-M., Engstrom D. R., Damman A. W. H., Benoit J. M., and Balcom P. H. [2001] Book of Abstracts, 6th International Conference on Mercury as a Global Pollutant, 15-19 October 2001, Minamata, Japan

Fursov V. [1983] *Gaseous mercury method of prospecting of rock mineral fields*. Nauka, Moscow, 203 p. (in Russian)

Geological Survey of Canada [1995] The significance of natural sources of metals in the environment. Report prepared for the UN-ECE LRTAP (HM) Convention, 28 May 1995

Guo, Y.-R., and S. Chen [1994] Terrain and land use for the fifth-generation Penn State/NCAR mesoscale modeling system

(MM5): Program TERRAIN. NCAR Technical Note NCAR/TN-397+IA, National Center for Atmospheric Research, Boulder, Colorado, USA

Gustin M. S., Lindberg S., Marsik F., Casimir A., Ebinghaus R., Edwards G., Hubble-Fitzgerald C., Kemp R., Kock H., Leonard T., London J., Majewski M., Montecinos C., Owens J., Pilote M., Poissant L., Rasmussen P., Schaedlich F., Schneeberger D., Schroeder W., Sommar J., Turner R., Vette A., Wallschlaeger D., Xiao Z., and Zhang H. [1999a] Nevada STORMS project: Measurement of mercury emissions from naturally enriched surfaces. *J. Geophys. Res*. **104**(D17), 21831-21844

Gustin M. S., Rasmussen P., Edwards G., Schroeder W., and Kemp J. [1999b] Application of a laboratory gas exchange chamber for assessment of in situ mercury emissions. *J. Geophys. Res*. **104**(D17), 21873-21878

Gårdfeldt K., Feng X., Sommar J., Lindqvist O. [2001a] Total gaseous mercury exchange between air and water at river and sea surfaces in Swedish coastal regions. *Atmos. Environ.* **35**, 3027-3038

Gårdfeldt K., Sommar J., Strömberg D., and Feng X. [2001b] Oxidation of atomic mercury by hydroxyl radicals and photoinduced decomposition of methylmercury in the aqueous phase. *Atmos. Environ.* **35**, 3039-3047

Hall B. [1995] The gas phase oxidation of mercury by ozone. *WASP* **80**, 301-315

Henshaw P. C., Charlson R. J., and Burges S. J., [2000] Water and the hydrosphere. In: Jacobson M., Charlson R., Rodhe H., and Orians G. (Eds.), Earth System Science. From Biogeochemical Cycles to Global Change. Academic Press, San Diego, 109-131

Herrmann H., Ervens B., Jacobi H.-W., Wolke R., Nowacki P., and Zellner R. [2000] CAPRAM2.3: A chemical aqueous phase radical mechanism for tropospheric chemistry. *J. Atm. Chem.* **36**, 231-284

Hongisto M. [1998] HILATAR, a regional scale grid model for the transport of sulphur and nitrogen compounds. FMI Contributions No. 21, Finnish Meteorological Institute, Helsinki, Finland

Horvat M. [1996] Mercury analysis and specification in environmental samples. In: Baeyens W., Ebinghaus R. Vasiliev O. (Eds.), Global and Regional Mercury Cycles: Sources, Flaxes and Mass Balances. NATO-ASI-Series, Kluwer Academic Publishers, Dordrecht, The Netherlands, 1-31

Hudson R. J. M., Gherini S. A., Fitzgerald W. F., and Porcella D. B. [1995] Anthropogenic influences on the global mercury cycle: a model-based analysis. *WASP* **80**, 265-272

Ilyin I., Ryaboshapko A., Travnikov O., Berg T., Hjellbrekke A.-G., and Larsen R. [2000] Heavy metal transboundary air pollution in Europe: monitoring and modelling results. EMEP Report 3/2000, Meteorological Synthesizing Centre - East, Moscow, Russia

Ilyin I., Ryaboshapko A., Afinogenova O., Berg T., and Hjellbrekke A.-G. [2001] Evaluation of transboundary transport of heavy metals in 1999. Trend analysis. EMEP Report 3/2001, Meteorological Synthesizing Centre - East, Moscow, Russia

Innanen S. [1998] The ratio of anthropogenic to natural mercury release in Ontario: Three emission scenarios. *The science of the Total Environment* **213**, 25-32

Iversen T., Saltbones J., Sandnes H., Eliassen A., and Hov O. [1989] Airborne tronsboundary transport of sulphur and nitrogen over Europe - model descriptions and calculations. EMEP/MSC-W Report 2/89, Meteorological Synthesizing Centre - West, Oslo, Norway

Jackson T. A. [1997] Long-range atmospheric transport of mercury to ecosystems, and the importance of anthropogenic emissions - a critical review and evaluation of the published evidence. *Environ. Rev.* **5**, 99-120.

Jacobson M. Z. [1999] *Fundamentals of atmospheric modeling*. Cambridge University Press. 656 p.

Jonasson I. R. and Boyle R. W. [1971] Geochemistry of mercury. Spatial Symposium on Mercury in Man's Environment, Environment Canada, 15-16 February 1971, Ottawa, Canada pp. 5-21

Johansson K., Aastrup M., Andersson A., Bringmark L., and Iverfeldt A., [1991] Mercury in Swedish forest soils and waters – assessment of critical load. *WASP* **56**, 267-281

Jonsen J.E. and E. Berge [1995] Some preliminary results on transport and deposition of nitrogen components by use of Multilayer Eulerian Model. EMEP/MSC-W Report 4/95, Meteorological Synthesizing Centre – West, Oslo, Norway

Junge C. E. [1963] *Air chemistry and radioactivity*. Academic Press, New York and London, 382 p.

Junge C. [1972] The cycle of atmospheric gases – natural and man made. *Quarterly Journal of the Royal Meteorological society* **98**(418), 711-729

Kannan K. and Falandysz J. [1998] Speciation and concentrations of mercury in certain coastal marine environment. *WASP* **103**, 129-136

Keeler G., Glinsorn G., and Pirrone N., [1995] Particulate mercury in the atmosphere: its

significance, transport, transformation, and sources. *WASP* **80**, 159-168

Kim J. P. and Fitzgerald W. F. [1986] Sea-air partitioning of mercury in the Equatorial Pacific Ocean. *Science* **231**, 1131-1133

Kim K.-H., Lindberg S. E. and Meyers T. P. [1995] Micrometeorological measurements of mercury vapor fluxes over background forest souls in eastern Tennessee. *Atmos. Environ.* **29**(2), 267-282

Kmiec G., Zwozdziak A., Acker K., and Wieprecht W. [1998] Cloud/fog water chemistry at high elevation in the Sudeten mountains, south-western Poland. In: Proceedings of the First International Conference on Fog and Fog Collection, Vancouver, Canada, July 19-24, 1998, 69-72

Lamborg C. H., Fitzgerald W. F., Vandal G. M., and Rolfhus K. R. [1995] Atmospheric mercury in northern Wisconsin: sources and species. *WASP* **80**, 189-198

Lamborg C. H., Fitzgerald W. F., O'Donnell J., and Torgersen T. [2002] A non-steady-state compartmental model of global-scale mercury biogeochemistry with interhemispheric atmospheric gradients. Geochimica et Cosmochimica Acta **66(**7), 1105-1118

Lee D. S., Dollard G. J., and Pepler S. [1998] Gas-phase mercury in the atmosphere of the United Kingdom. *Atmos. Environ.* **32**(5), 855-864

Lin C.-J., and Pehkonen S. O. [1997] Aqueous free radical chemistry of mercury in the presence of iron oxides and ambient aerosol. *Atmos. Environ.* **31**, 4125-4137

Lin C.-J., and Pehkonen S. O. [1998] Two-phase model of mercury chemistry in the atmosphere. *Atmos. Environ*. **32**, 2543-2558

Lin C.-J., and Pehkonen S. O. [1999] The chemistry of atmospheric mercury: a review. *Atmos. Environ.* **33**, 2067-2079

Lindberg S. E., Turner R. R., Meyers T. P., Taylor G. E., and Schroeder W. H. [1991] Atmospheric concentrations and deposition of Hg to a deciduous forest at Walker Branch Watershed, Tennessee, USA. *WASP* **56**, 577-594

Lindberg S. E., Meyers T. P., Taylor G. E., Turner R. R., and Schroeder W. H. [1992] Atmospheric-surface exchange of mercury in a forest: results of modeling and gradient approaches. *J. Geophys. Res*. **97**, 2519-2528

Lindberg S. E, Kim K.-H., Meyers T. P., and Owens J. G. [1995] Micrometeorological gradient approach for quantifying air/surface exchange of mercury vapor: Test over Contaminated Soils. *Environ. Sci. Technol.* **29**, 126-135

Lindberg S. E., Hanson P. J., Meyers T. P., and Kim K.-H. [1998] Air/surface exchange of mercury vapor over forests – the need for a reassessment of continental biogenic emissions. *Atmos. Environ.* **32**, 895-908

Lindberg S. E., Zhang H., Gustin M., Vette A., Marsik F., Owens J., Casimir A., Ebinghaus R., Edwards G., Fitzgerald C., Kemp J., Kock H., London J., Majewski M., Poisant M., Pilote M., Rasmussen P., Schaedlich F., Schneeberger D., Sommar J., Turner R., Wallschlager D., Xiao Z. [1999] Increases in mercury emissions from desert soils in response to rainfall and irrigation. *J. Geophys. Res*. **104**, 21879-21888

Lindberg S. E., Brooks S., Lin J., Scott K., Meyers T., Landis M., and Stevens R. [2001] The dynamic oxidation of mercury in the Arctic troposphere: mercury scociation in air and accumulation in snow at point Barrow Alaska. Book of Abstracts, 6th International Conference on Mercury as a Global Pollutant, 15-19 October 2001, Minamata, Japan

Lindberg S. E., Brooks S., Lin C.-J., Scott K. J., Landis M. S., Stevens R. R., Goodsite M., and Richter A. [2002] Dynamic oxidation of gaseous mercury in the Arctic troposphere at polar sunrise. *Environ. Sci. Technol.* **36**, 1245-1256

Lindqvist O., Jernelo:v A., Johansson K., and Rodhe H. [1984] Mercury in the Swedish environment: Global and local sources. National Swedish Environment Protection Board, Report PM 1816, 91 p.

Lindqvist O. and Rodhe H. [1985] Atmospheric mercury - a review. *Tellus* **37B**, 136-157

Lindqvist O., Johanson K., Aastrup M., Anderson A., Bringmark L., Hovsenius G., Hakanson L., Iverfeld A., Meili M., and Timm B. [1991] Mercury in the Swedish environment – recent research on causes, consequences and corrective methods. *WASP* **55**, 1-261

Loon L. van, Mader E., and Scott S. L. [2000] Reduction of the aqueous mercuric ion by sulfite: UV spectrum of HgSO3 and its intermolecular redox reaction. *J. Phys. Chem.* **104A**, 1621-1626

Lu J. Y., Schroeder W. H., Barrie L. A., Steffen A., Welch H. E., Martin K., Lockhart W. L., Hunt R. V., Boila G., Richter A. [2001] Magnification of atmospheric mercury deposition to polar regions in springtime: the link to tropospheric ozone depletion chemistry. *Geophys. Res. Letters.* **28**(17), 3219-3222

Lurie Yu. Yu. [1971] *Handbook for Analytical Chemistry*. Khimiya, Moscow, 454 p.

Lyon B., Rice G., Bullock O. R., and Selby P. [1999] Modelling the local scale atmospheric fate of anthropogenic mercury emissions. In: Mercury as a Global Pollutant. 5th International Conference, Rio de Janeiro, May 23-28, 1999. Book of abstracts, p. 110

Marchuk G. I. [1975] *Methods of numerical mathematics*. Springer-Verlag, New York. 316 p.

Mason R. P., O'Donnell J. and Fitzgerald W. F. [1994] Elemental mercury cycling within the mixed layer of the equatorial Pacific Ocean. In: Watras C.J. and Huckabee J.W. (Eds.) Mercury Pollution: Integration and Synthesis. Lewis Publishers, pp. 83-97

Mason R. P., Rolfhus K. R., and Fitzgerald W. F. [1998] Mercury in the North Atlantic. *Marine Chemistry* **61**, 37 – 53

Matilainen T., Verta M., Korhonen H., Uusi-Rauva A., and Niemi M. [2001] Beavior of mercury in soil profiles: impact of increased precipitation, acidity and fertilization on mercury methylation. *WASP* **125**, 105-119

McRae G. J., Goodin W. R., Seifeld J. H. [1982] Numerical solution of the atmospheric diffusion equation for chemically reacting flows. *Journal of Computational Physics* **45**, 1-42

Melnikov S. M. [1971] *Metallurgy of Mercury*, Metallurgy, Moscow, 472 p.

Meyers T. P., Hall M. E., Lindberg S. E., and Kim K. [1996] Use of the modified Bowen-ratio technique to measure fluxes of trace gases. *Atmos. Environ.* **30**, 3321-3329

Milford J. B. and Davidson C. I. [1985] The size of particulate trace elements in the atmosphere – a review. *JAPCA* **35**(12), 1249-1260

Munthe J., Xiao Z. F. and Lindqvist O. [1991] The aqueous reduction of divalent mercury by sulfite. *WASP* **56**, 621-630

Munthe J. [1992] The aqueous oxidation of elemental mercury by ozone. *Atmos. Environ.* **26A**, 1461-1468

Munthe J. [1993] Mercury in the Atmosphere: Emissions, Transformations, Deposition and Effects. IVL Rapport 1110, Swedish Environment Research Institute, Göteborg, Sweden

Munthe J. [1994] The atmospheric chemistry of mercury: kinetic studies of redox reactions. In Watras C. J. and Huckabee J. W. (Eds.) Mercury Pollution: Integration and Synthesis, Lewis Publishers, Ann Arbor, Michigan, 273-279

Murphy D. M., Thomson D. S., and Mahoney T. M. [1998] In situ measurements of organics, meteoritic meterial, mercury and other elements in aerosols at 5 to 19 kilometers. *Science* **282**, 1664-1669

Niki H., Maker P. D., Savage C. M., and Breitenbach L. P. [1983] A long-path Fourier transform study at the kinetics and mechanism for the HO-radical initiated oxidation of dimethyl mercury. *J. Phys. Chem*. **87**, 4978-4981

Nriagu J. O. and Pacyna J. M. [1988] Quantitative assessment of worldwide contamination of air, water and soils by trace metals. *Nature* **333**, 134-139

Nriagu J. O. [1989] A global assessment of natural sources of atmospheric trace metals. *Nature* **338**, 47-49

Nriagu J. O. and Decker C. [2001] Worldwide emissions of mercury from volcanoes. Book of Abstracts, 6th International Conference on Mercury as a Global Pollutant, 15-19 October 2001, Minamata, Japan

Odman M. T. and Russell A. G. [2000] Mass conservative coupling of non-hydrostatic meteorological models with air quality models. In: Gryning S.-E. and Batchvarova E. (Eds.) Air pollution modelling and its application XIII. Kluwer Academic/Plenum Publishers, New York, 651-660

Pacyna J. M., Scholtz T., and Pirrone N. [1999] Global emissions of mercury to the atmosphere. Book of abstracts, 5th International Conference on Mercury as a Global Pollutant, 23-28 May 1999, Rio de Janeiro

Pacyna, E. G. and Pacyna J. M. [2002] Global emission of mercury from anthropogenic sources in 1995. *WASP* **137**(1), 149-165

Pai P., Karamchandani P., and Seigneur C. [1997] Simulation of the regional atmospheric transport and fate of mercury using a comprehensive Eulerian model. *Atmos. Environ*. **31**, 2717-2732

Pekar M. [1996] Regional models LPMOD and ASIMD. Algorithms, parametrization and results of application to Pb and Cd in Europe scale for 1990. EMEP/MSC-E Report 9/96, Meteorological Synthesizing Centre - East, Moscow, Russia

Petersen G., Iverfeldt A. and J. Munthe [1995] Atmospheric mercury species over central and northern Europe. Model calculations and comparison with observations from the nordic air and precipitation network for 1987 and 1988. *Atmos. Environ*. **29**, 47-67

Petersen G., Munthe J., Pleijel K., Bloxam R. and A.V.Kumar [1998] A comprehensive Eulerian modeling framework for airborne mercury species: Development and testing of the tropospheric chemistry module (TCM). *Atmos. Environ.* **32**(5), 829-843

Petersen G., Bloxam R., Wong S., Munthe J., Krüger O., Schmolke S., and Kumar A. V. [2001] A comprehensive Eulerian modelling framework for airborne mercury species: model development and applications in Europe. *Atmos. Environ*. **35**, 3063-3074

Pirrone N., Allegrini I., Keeler G. J., Nriagu J. O., Rossman R., and Robbins J. A. [1998] Historical atmospheric mercury emissions and depositions in North America compared to mercury accumulations in sedimentary records. *Atmos. Environ.* **32**(5), 929-940

Pleijel K., and Munte J. [1995] Modeling the atmospheric mercury cycle - chemistry in fog droplets. *Atmos. Environ.* **29**, 1441-1457

Poissant L. and Casimir A, [1998] Water–air and soil–air exchange rate of total gaseous mercury measured at background sites. *Atmos. Environ.* **32**(5), 883-893

Poissant L., Pilote M., and Casimir A. [1999] Mercury flux measurements in a naturally enriched area: correlation with environmental conditions during the Nevada Study and Tests of the Release of Mercury From Soils (STORMS). *J. Geophys. Res*. **104**(D17), 21845-21857

Pongratz R. and Heumann K.G. [1999] Production of methylated mercury, lead and cadmium by marine bacteria as a significant natural source for atmospheric heavy metals in polar regions. *Chemosphere* **39**(1), 89-102

Prokofiev A. K. [1981] Chemical forms of mercury, cadmium and zink in fresh water systems. Advances in Chemistry **50**, 54-84 (in Russian)

Reiter E. R. [1968] Stratospheric-tropospheric exchange processes. *Rev. Geophysics and Space Physics* **14**(4), 459-474

Ribeyre F., Boudou A., and Maury-Brachet R. [1991] Multicompartment ecotoxicological models to study mercury bioaccumulation and transfer in freshwater system. *WASP* **56**, 641-652

Ryaboshapko A. and Korolev V. [1997] Mercury in the atmosphere: estimates of model parameters. EMEP/MSC-E Report 7/97, Meteorological Synthesizing Centre - East, Moscow, Russia

Ryaboshapko A., Ilyin I., Gusev A. and O. Afinogenova [1998] Mercury in the Atmosphere of Europe: Concentrations, deposition patterns, transboundary fluxes. EMEP/MSC-E Report 7/98, Meteorological Synthesizing Centre - East, Moscow, Russia

Ryaboshapko A., Ilyin I., Gusev A., Afinogenova O., Berg T. and Hjellbrekke A.-G. [1999] Monitoring and modelling of lead, cadmium and mercury transboundary transport in the atmosphere of Europe. Joint report of EMEP centres: MSC-E and CCC, EMEP Report 3/99, Meteorological Synthesizing Centre – East, Moscow, Russia

Ryaboshapko A., Ilyin I., Bullock R., Ebinghaus R., Lohman K., Munthe J., Petersen G., Segneur C., Wangberg I. [2001] Intercomparison study of numerical models for long-range atmospheric transport of mercury. Stage I: Comparison of chemical modules for mercury transformations in a cloud/fog environment. EMEP/MSC-E Technical report 2/2001, Meteorological Synthesizing Centre – East, Moscow, Russia

Sakata M. and Marumoto K. [2002] Formation of atmospheric particulate mercury in the Tokyo metropolitan area. To be published in *Atmos. Environ*.

Sander R. [1997] Henry's law constants available on the Web. EUROTRAC Newsletter, No. 18, 24-25 (www.mpch-mainz.mpg.de/~sander/ res/henry)

Schroeder W.H., Munthe J., and Lindqvist O. [1989] Cycling of mercury between water, air, and soil compartments of the environment. *WASP* **48**, 337-347

Schroeder W. H., Yarwood G., and Niki H. [1991] Transformation processes involving mercury species in the atmosphere. *WASP* **56**, 653-666

Schroeder W. H. [1995] Environmental measurements and results of mercury volatilization rates ("fluxes") from soil and lake surfaces. Proceedings of 1995 Canadian mercury network workshop, 29-30 September 1995, York University, Toronto, Ontario, Canada

Schroeder W. H. [1996] Estimation of atmospheric input and evasion fluxes of mercury to and from The Great Lakes. In: Baeyens W., Ebinghaus R. Vasiliev O. (Eds.), Global and Regional Mercury Cycles: Sources, Flaxes and Mass Balances. NATO-ASI-Series, Kluwer Academic Publishers, Dordrecht, The Netherlands, 109-121

Schroeder W. H. and Munthe J. [1998] Atmospheric mercury - an overview. *Atmos. Environ.* **32**, 809-822

Schroeder W., Anlauf K., Barrie L. A., Lu J., Steffen A., Schneeberger D., and Berg T. [1998] Arctic springtime depletion of mercury. *Nature* **394**, 331-332

Schroeder W. H., Edwards G. C., Rasmussen P. E., Kemp R. J., Dias G., Wallace D., Steffen A., and Lu J. Y. [2001] Mercury: Rising? Or falling? Book of Abstracts, 6th International Conference on Mercury as a Global Pollutant, 15-19 October 2001, Minamata, Japan

Schuster E. [1991] The behavior of mercury in the soil with special emphasis on complexation and adsorption processes - a review of the literature. *WASP* **56**, 667-680

Sehmel G. A. [1980] Particle and gas dry deposition: a review. *Atmos. Environ.* **14**, 983-1011

Siegel S. M. and Siegel B. Z. [1984] First estimate of annual mercury flux at the Kilauea main vent. *Nature* **309**, 146-147

Seigneur C., Wrobel J. and Constantinou E. [1994] A chemical kinetic mechanism for atmospheric inorganic mercury. *Environ. Sci. and Technol*, **28**(9), 1589-1597

Seigneur C., Abeck H., Chia G., Reinhard M., Bloom N. S., Prestbo E., and Saxena P. [1998] Mercury adsorption to elemental carbon (soot) particles and atmospheric

particulate matter. *Atmos. Environ.* **32**, 2649-2657

Seigneur C., Karamchandani P., Lohman K., Vijayaraghavan K., and Shia R.-L. [2001] Multiscale modeling of the atmospheric fate and transport of mercury. *J. Geophys. Res*. **106**(D21), 27795-27809

Shia R.-L., Seigneur C., Pai P., Ko M., Sze N. D. [1999] Global simulation of atmospheric mercury concentrations and deposition fluxes. *J. Geophys. Res.* **104(**D19), 23747-23760

Slemr F. [1996] trends in atmospheric mercury concentrations over the Atlantic ocean and the Wank Summit, and the resulting concentrations on the budget of atmospheric mercury. In: Baeyens W., Ebinghaus R. Vasiliev O. (Eds.), Global and Regional Mercury Cycles: Sources, Flaxes and Mass Balances. NATO-ASI-Series, Kluwer Academic Publishers, Dordrecht, The Netherlands, 33-84

Smirnov V. I., Kuznetsov V. A., Ozerova N. A., and Fedorchuk V. G. [1972] News in mercury geochemistry v. XIV, No 4, 17-30 (in Russian).

Sommar J., Strömberg D., and Lindqvist O. [1999a] Distribution equilibrium of mercury (II) chloride between water and air applied to flue gas scrubbing. In: Mercury as a Global Pollutant. 5th International Conference, Rio de Janeiro, May 23-28, 1999. Book of abstracts, p. 129

Sommar J., Gårdfeldt K., Feng X., and Lindquist O. [1999b] Rate coefficients for gas-phase oxidation of elemental mercury by bromine and hydrocyl radicals. In: Mercury as a Global Pollutant. 5th International Conference, May 23-28, 1999, Rio de Janeiro, Brazil. Book of abstracts, p. 87

Sommar J., Gårdfeldt K., Strömberg D., and Feng X. [2001] A kinetic study of the gas-phase reaction between the hydroxyl radical and atomic mercury. *Atmos. Environ*. **35**, 3049-3054

Steffen A., Schroeder W. H., Hoenniger G., Platt U., Fuentes J., Lawson W., Strachan W. [2001] Springtime experiments during Canadian high Arctic atmospheric mercury depletion events. Book of Abstracts, 6th International Conference on Mercury as a Global Pollutant, 15-19 October 2001, Minamata, Japan

Thornton I., Ramsey M., and Atkinson N. [1995] Metal in the Global Environment: Facts and Misconceptions. International Council on Metals and the Environment, 103 p.

Tokos J. J. S., Hall B., Calhoun J. A., and Prestbo E. M. [1998] Homogeneous gas-phase reaction of Hg^0 with H_2O_2, O_3, CH_3I, and $(CH_3)_2S$: implications for atmospheric Hg cycling. *Atmos. Environ.* **32**, 823-827

Trakhtenberg I. M. and Korshun M. N. [1990] *Mercury and its Compounds in the Environment (Sanitary and Ecological Aspects)*. Vyshcha Shkola, Kiev, 232 p. (In Russian)

Travnikov O. [2001] Hemispheric model of airborne pollutant transport. EMEP/MSC-E Technical Note 8/2001, Meteorological Synthesizing Centre - East, Moscow, Russia

US EPA [1997] Mercury Study Report to Congress. Vol. III, Fate and Transport of Mercury in the Environment. US-EPA-452/R-97003

Vinogradov A. P. [1957] *Geochemistry of rare and diffused elements in soils*. AS of USSR, Moscow, 237 p. (in Russian)

Vong R. J., Baker B. M., Brechtel F. J., Collier R. T., Harris J. M., Kowalski A. S., McDonald N. C., and McInnes L. M. [1997] Ionic and trace element composition of cloud water collected on the Olympic peninsula of Washington State. *Atmos. Environ*. **31**, 1991-2001

Wang Y. J. et al. [1998] Global simulation of tropospheric O_3-NO_x-hydrocarbon chemistry 2: Model evaluation and global ozone budget. *J. Geophys. Res*. **103**, 10727-10755

Williston S. H. [1968] Mercury in the atmosphere. *J. Geophys. Res.* **71**(22), 7051-7057

Wallschläger D., Kock H. H., Schroeder W. H., Lindberg S. E., Ebinghaus R., Wilken R.-D. [2000] Mechanism and significance of mercury volatilization from contaminated floodplains of the Germany river Elbe. *Atmos. Environ.* **34**, 3745-3755

Wängberg I., Shcmolke S.R., Ebinghaus R., Munthe J., Schager P., and Iverfeldt A. [1999] Estimates of the air-sea exchange of gaseous mercury in the southern Baltic Sea, summer and winter 1997-1998. In: Mercury as a Global Pollutant. 5th International Conference, May 23-28, 1999, Rio de Janeiro, Brazil. Book of abstracts, p. 133

Xiao Z. F., Munthe J., Schroeder W. H., and Lindqvist O. [1991] Vertical fluxes of volatile mercury over the soil and lake surfaces in Sweden. *Tellus* **43**(B3), 267-279

Xiao Z. F., Munthe J., Strömberg D., and Lindqvist O. [1994] Photocemical Behavior of Inorganic Mercury Compounds in Aqueous Solution. In: Watras C. J. and Huckabee J. W. (Eds.) Mercury Pollutiom: Integration and Synthesis. Lewis Publishers, Boca Raton, 581-592

Xu X., Yang X., Miller D. R., Helble J. J., and Carley R. J. [1999] Formulation of bi-directional atmosphere-surface exchanges of elemental mercury. *Atmos. Environ.* **33**, 4345-4355

Yanenko N. N. [1971] *The method of fractional steps. The solution of problems of mathematical physics in several variables*. Springer-Verlag, New York. 160 p.

Yin Yu., Allen H. E., Huang C. P., Sparks D. L., and Sanders P. F. [1997] Kinetics of mercury (II)

adsorption and desorption on soil. *ES&T* **31**(2), 496-503

Zhang H. and Lindberg S.E. [1999] Processes influencing the emission of mercury from soils: a conceptual model. *J. Geophys. Res*. **104**(D17), 21889-21896

Zhang H., Lindberg S. E., Marsik F. J., and Keeler G. J. [2001] Mercury air/surface exchange kinetics of background soils of the Tahquamenon River watershed in the Michigan upper peninsula. *WASP* **126**, 151-169